PNL-8500 Pt. 4
UC-408

Pacific Northwest Laboratory Annual Report for 1992 to the DOE Office of Energy Research

Part 4 Physical Sciences

L. H. Toburen and members of
the Physical and Technological
Programs Staff

April 1993

Prepared for
the U.S. Department of Energy
under Contract DE-AC06-76RLO 1830

Pacific Northwest Laboratory
Richland, Washington 99352

Preface

This 1992 Annual Report from Pacific Northwest Laboratory (PNL) to the U.S. Department of Energy (DOE) describes research in health and environmental issues, conducted during fiscal year 1992. This year the report consists of four parts, each in a separate volume.

The four parts of the report are oriented to particular segments of the PNL program, describing research performed for the DOE Office of Health and Environmental Research in the Office of Energy Research. In some instances, the volumes report on research funded by other DOE components or by other governmental entities under interagency agreements. Each part consists of project reports authored by scientists from several PNL research departments, reflecting the multidisciplinary nature of the research effort.

The parts of the 1992 Annual Report are:

Part 1: Biomedical Sciences		
Program Manager:	J. F. Park	J. F. Park, Report Coordinator S. A. Kreml, Editor
Part 2: Environmental Sciences		
Program Manager:	R. E. Wildung	D. A. Perez, Editor
Part 3: Atmospheric Sciences		
Program Manager:	W. R. Barchet	L. K. Grove, Editor
Part 4: Physical Sciences		
Program Manager:	L. H. Toburen	L. H. Toburen, Report Coordinator W. C. Cosby, Editor

Activities of the scientists whose work is described in this annual report are broader in scope than the articles indicate. PNL staff have responded to numerous requests from DOE during the year for planning, for service on various task groups, and for special assistance.

Credit for this annual report goes to the many scientists who performed the research and wrote the individual project reports, to the program managers who directed the research and coordinated the technical progress reports, to the editors who edited the individual project reports and assembled the four parts, and to Ray Baalman, editor in chief, who directed the total effort.

T. S. Tenforde
Health and Environmental Research Program

Previous reports in this series:

Annual Report for:

1951	HW-25021, HW-25709
1952	HW-27814, HW-28636
1953	HW-30437, HW-30464
1954	HW-30306, HW-33128, HW-35905, HW-35917
1955	HW-39558, HW-41315, HW-41500
1956	HW-47500
1957	HW-53500
1958	HW-59500
1959	HW-63824, HW-65500
1960	HW-69500, HW-70050
1961	HW-72500, HW-73337
1962	HW-76000, HW-77609
1963	HW-80500, HW-81746
1964	BNWL-122
1965	BNWL-280, BNWL 235, Vol. 1-4; BNWL-361
1966	BNWL-480, Vol. 1; BNWL-481, Vol. 2, Pt. 1-4
1967	BNWL-714, Vol. 1; BNWL-715, Vol. 2, Pt. 1-4
1968	BNWL-1050, Vol. 1;, Pt. 1-2; BNWL-1051, Vol. 2, Pt. 1-3
1969	BNWL-1306, Vol. 1;, Pt. 1-2; BNWL-1307, Vol. 2, Pt. 1-3
1970	BNWL-1550, Vol, 1;, Pt. 1-2; BNWL-1551, Vol. 2, Pt. 1-2
1971	BNWL-1650, Vol. 1:, Pt. 1-2; BNWL-1651, Vol. 2, Pt. 1-2
1972	BNWL-1750, Vol. 1;, Pt. 1-2; BNWL-1751, Vol. 2, Pt. 1-2
1973	BNWL-1850, Pt. 1-4
1974	BNWL-1950, Pt. 1-4
1975	BNWL-2000, Pt. 1-4
1976	BNWL-2100, Pt. 1-5
1977	PNL-2500, Pt. 1-5
1978	PNL-2850, Pt. 1-5
1979	PNL-3300, Pt. 1-5
1980	PNL-3700, Pt. 1-5
1981	PNL-4100, Pt. 1-5
1982	PNL-4600, Pt. 1-5
1983	PNL-5000, Pt. 1-5
1984	PNL-5500, Pt. 1-5
1985	PNL-5750, Pt. 1-5
1986	PNL-6100, Pt. 1-5
1987	PNL-6500, Pt. 1-5
1988	PNL-6800, Pt. 1-5
1989	PNL-7200, Pt. 1-5
1990	PNL-7600, Pt. 1-5
1991	PNL-8000, Pt. 4

Foreword

Part 4 of the Pacific Northwest Laboratory Annual Report for 1992 to the DOE Office of Energy Research includes those programs funded under the title "Physical and Technological Research." The Field Task Program Studies reported in this document are grouped by budget category and each Field Task proposal/agreement is introduced by an abstract that describes the projects reported in that section. These reports only briefly indicate progress made during 1992. The reader should contact the principal investigators named or examine the publications cited for more details.

Contents

Figures

Dosimetry Research

Measurement Science

Radiological and Chemical Physics

Tables

Dosimetry Research

Chernobyl Database Management

This project has developed and continued to maintain an information system that provides researchers with data and resource materials related to the Chernobyl nuclear accident of April 1986. The information system represents the official United States repository for Chernobyl data and includes a collection of documents, a database of bibliographic references, and a collection of radiological measurements records. Several major deliverables of the Chernobyl Database project were provided in FY 1992. Publication and distribution of the initial releases of the Chernobyl Bibliographic Search System (*ChernoLit*™[a]) were completed, a hard-copy of the Chernobyl bibliography was published and distributed, presentations were made at technical meetings, and contact with researchers involved in Chernobyl-related research was either established or reestablished.

Chernobyl Database

R. A. Kennedy, R. L. Hill, J. A. Mahaffey, S. K. Smith, and F. Carr, Jr.

We have identified nine tasks which, collectively, provide successful collection, management, and distribution of information associated with the Chernobyl Database project. These tasks include 1) evaluating informational needs of scientists involved in Chernobyl research, 2) assessing the effectiveness of the research tools and services provided by this project, 3) maintaining existing communication links with investigators involved in Chernobyl-related research studies or in data collection efforts, 4) establishing new contacts with other researchers involved in Chernobyl-related studies or those who may have radiological measurement data or documents that can be contributed to the Chernobyl Information System, 5) continuing to assemble data and documents related to the accident into readily accessible and easy-to-use formats, 6) processing the information for incorporation into a physical library collection, a bibliographic database, or a series of radiological measurements databases, 7) responding to requests for data assimilated into the information system, 8) generating, maintaining, distributing, and updating research tools developed for this project, and 9) preparing and presenting scientific papers and/or posters to notify researchers of tools and services provided by this project. Previous accomplishments have emphasized establishing communication with researchers and providing a mechanism through which reference and measurement data could be solicited and incorporated into the information system. During FY 1991-1992, the emphasis was on generating and distributing software products that make the information system (and data contained within) easier to use and more accessible to the researchers. During FY 1992, substantial progress was made in organizing and expanding the physical collection of materials and the bibliographic database.

ChernoLit™[a]

During FY 1992, we updated and reviewed the *ChernoLit*™ software and user's manual. The *ChernoLit*™ software package was released in March 1992. *ChernoLit*™, an easy-to-use software package with capabilities to search the bibliographic data, provides bibliographic data and abstracts in a usable format for research studies relating to the Chernobyl accident. The software package was distributed to 30 domestic and 45 foreign contacts who had provided source material for the information system. *ChernoLit*™ is an IBM-compatible, personal-computer-based computer software package that consists of the database of bibliographic references and a graphical user interface with mouse and printer support. The database contains 4500 references, including abstracts.

(a) *ChernoLit*™ is a trademark of Battelle Memorial Institute.

Also during FY 1992, Battelle Memorial Institute (BMI), in cooperation with the technology transfer initiative within DOE, approved business and marketing plans for commercializing the *ChernoLit*™ software package. BMI established a budget using corporate funds to cover the costs of commercialization. The "shrink wrapped" package was made available to the public through Battelle Development Corporation at a cost of $395 (U.S./Canada)/ $500 (International). *ChernoLit*™ is being direct marketed internationally to commercial and university prospects using BMI resources.

ChernoDat

We continued work on preparing the *ChernoDat* Radiological Measurements Information System (a software package that provides access to radiological measurements collected by PNL subsequent to the Chernobyl accident) during FY 1992. Additional features were added to the user interface, additional data sets were incorporated, and a draft user's manual was prepared. Data in *ChernoDat* are organized into a series of satellite databases containing the data in their original record formats, with a central database that stores all data in a standardized record format. *ChernoDat* allows the user to browse, query, and export the radiological data from both the central and satellite databases. *ChernoDat* is an IBM-compatible, personal-computer-based computer software package that consists of a graphical user interface with mouse and printer support and has more than 50,000 records in the central database.

Interaction with Researchers

We made a concerted effort during FY 1992 to reestablish existing communication links and establish new contacts with individuals who, through their involvement in Chernobyl-related research studies, may have access to reference and measurement data that could be incorporated into the various databases of the Chernobyl Information System. Eighty-five letters were written to recipients of the *ChernoLit*™ software informing them that a poster on the Chernobyl Database Project would be presented at the IRPA8 meeting. The letter included information on how to obtain a copy of the printed bibliography and a request for materials to be added to the repository's physical collection of references. At the IRPA8 meeting, meetings with several individuals were held to discuss items of interest to this project. Letters and documents were also received in response to our request for materials.

A printed bibliography of the 4500 references included in the bibliographic database, complete with author index, was published and distributed during 1992. This bibliography is an update of the printed bibliography prepared and distributed by this project in 1989.

Organization and Expansion of the Information System

During FY 1992, we made efforts to organize and expand the physical collection of reference materials and radiological measurement data associated with the Chernobyl accident. To properly maintain the physical collection, the bibliographic database was modified and expanded to serve as the key to the physical collection. This key information can then be transported to future versions of *ChernoLit*™ allowing users to determine which references are available in the physical collection. The organization and filing of the physical collection to correspond with the numbering scheme used in *ChernoLit*™ was completed during FY 1992. Software utilities were written to incorporate additional information concerning document acquisition into *ChernoLit*™. The bibliographic database was also updated with data downloaded from the *Energy Science and Technology* database.

Biological Effectiveness of Radon Alpha Particles

Radiation exposures due to radon in indoor air result in only one or two alpha particles to a typical lung cell. The consequences of these exposures, relative to the effects of the large numbers of electron tracks required to produce the same dose, are a major concern in establishing exposure limits for radon. Determining these effects is complicated by the fact that normal experimental techniques result is a Poisson distribution of the number of tracks through the individual cells making up the experimental population. Since, at the dose of interest, the mean number of tracks per cell is very small the relative variance is so large that the results of such experiments do not adequately test theories about the consequences of exposure. An accelerator based single-particle irradiation facility, which will irradiate large populations of cells with specific numbers of charged particles, is being tested. Techniques for plating cells and positioning them relative to the beam have been developed. Tests of the collimator and shutter mechanism, using radiachromic film and etched tracks in plastic show that the beam can be collimated to spot sizes less than 5 μm across, and that exposures can be limited to single particles. Remaining problems, primarily with the tuning of the accelerator for each experiment, are being resolved.

Single-Particle Irradiation of Mammalian Cells

L. A. Braby and J. M. Nelson

Testing and refinement of the single particle irradiation system described last year (Braby 1992) has continued. This system utilizes a thin plastic scintillator and a photomultiplier to detect each particle as it passes through the target cell. A piezoelectric crystal is used to move a shutter approximately 40 μm to shut off the beam, and the irradiation is controlled by a personal computer. The position of each cell is determined with the aid of a phase contrast microscope with reflected light optics, an image intensifier, video camera, and an image processing system. The cells to be irradiated, which are allowed to attach to the 1.5 μm thick bottom of special petri dishes, are positioned relative to the charged particle beam using the coordinate information from the image processing system. Several unexpected complications, that had not been detected in preliminary tests of components of the irradiation system were identified during preliminary cell irradiation experiments.

One of the critical issues in irradiating populations of cells, one at a time, is the efficiency of finding and positioning the cells. This depends on the clarity of the video image as well as the speed of the positioning system and the control software. Reflected light imaging is necessary in most microbeam applications in order to eliminate optical components between the target and the radiation source. However, since living cells are nearly transparent, small variations in the light reflected by the background can overwhelm the image and make it difficult or even impossible to distinguish the cells. We have found that careful selection of the background material, which is usually the vacuum system exit window, can prevent serious delays in locating the cells. Aluminized mylar can not be used because the aluminum breaks up into small patches when the mylar is stretched by the vacuum, and cells can not be seen against the resulting alternately black and then reflective backgrounds. Even transparent mylar reflects enough light that the concave surface that is produced when it is used as the vacuum window produces an out-of-focus virtual image of the light source. Careful adjustment of the microscope illumination system can reduce the difference in background brightness so that cells can be seen over the entire video field.

We also discovered that the mylar bottoms of the petri dishes change characteristics when cells and tissue culture media are added. When dry, the film is tight, and moving the dish a few micrometers or more causes each point on the film to move in the same way.

However, when exposed to tissue culture medium for a two hours, the film loses tension and begins to stick to the surface it is resting on. When the motion needed to position a cell over the collimator is calculated from the video image, the actual position will often differ by more than 10 μm. The software controlling the irradiation process has been modified so that the actual position of the cell can be observed, and small corrections can be made before each irradiation. This increases the irradiation time slightly, but is essential to proper operation.

Determining the exact position where the charged particle beam intersects the plane of the petri dish bottom presents a challenge since the microscope optics and video imaging systems are not sensitive enough to detect the light produced by individual charged particle tracks in a thin plastic scintillator. Zinc sulphide produces more light, but the individual crystals are large, and light scattering prevents resolving the beam spot when it is less than about 10 μm in diameter. Our initial procedure involved locating the beam position with the help of ZnS when the beam size was large, then extrapolating to the final beam position when the collimator is adjusted. However, this procedure includes some uncertainty due to the nonuniform optical properties of ZnS screens.

An improved procedure, using radiachromic film, was developed to eliminate this uncertainty. Radiachromic film contains a dye, which changes color on irradiation, in solution in a plastic film. Although this material is relatively insensitive (it requires a dose on the order of a Mrad to produce a clearly visible spot), it is homogeneous on the micrometer scale, and small beam spots can be measured accurately. Figure 1 shows the radiachromic film image of an 8-μm square beam spot photographed with a transmitted light microscope. With the improvements which have been made in the background for cell imaging, the exposed spot can now be identified using reflected light with the cell positioning microscope and image processor. Although the reflected light image shows many surface imperfections, it is relatively easy to determine the position of the beam spot with one pixel, that is 1 μm, accuracy.

Preliminary experiments with the microbeam collimator, before the cell positioning system was installed, were conducted with plastic etched track detectors in order to determine the effectiveness of the single particle detection system and the shutter mechanism. Single tracks were specified at 25 μm intervals. The mechanical mount used to position the track etch material was not ridged enough to accurately position the dish after each 25 μm move, but the results clearly showed tracks spaced at the specified interval, indicating that the collimator and shutter were working properly. Recent experiments indicate that this positive result may have been uncharacteristic of the typical operating characteristics of the accelerator. Using the ZnS screen to evaluate the beam, and starting with the collimator apertures set for a large beam spot, it has generally been possible to adjust the accelerator focus and steering elements to produce a beam which can be trimmed down to a 5-μm square spot as indicated by the radiachromic film. But the necessary adjustments involve setting lens voltages to a fraction of a percent of their full scale values, and the changes which bring a badly misaligned beam into alignment can not be detected on the analog readouts of our accelerator console. Furthermore, the lens and steering power supplies are unregulated, and drift with time. Thus, even though the beam is well aligned at the beginning of an experiment, it often drifts out of alignment before a significant number of cells can be irradiated. This shifts the position of the beam spot relative to the image processing coordinate system, and also adds a large component of scattered beam which falls outside the collimator dimensions.

The current collimator design, which was developed to provide spot size flexibility and relatively rapid adjustment, is particularly sensitive to the effects of scatter and misalignment because the final aperture is 60 mm from the

target. Angular changes of less than one minute thus translate into 10 μm positioning errors. An alternative collimator design, which places a fixed size aperture in contact with the plastic scintillator, will eliminate the problem of the beam position drifting, but will make it much more difficult to change the beam size. This alternative design will utilize an adjustable aperture 60 mm before the final one, so that the final aperture is used only to stop particles scattered from the edges of the first one. A source of laser drilled holes to make the final aperture has been located, and a system for accurately positioning them on the beam line is being assembled.

Reference

Braby, L. A. 1992. "Single-Particle Irradiation system." In *Physical Sciences, Part 4, of Pacific Northwest Laboratory Annual Report for 1991 to the DOE Office of Energy Research*, PNL-8000. Pacific Northwest Laboratory, Richland, Washington.

Cell Growth Rates in Individual Colonies

L. A. Braby and J. M. Nelson

When individual cells have been irradiated by single charged particles, the biological effects include changes in the growth rate of that cell and its progeny, a probability that some of the progeny will be unable to grow and divide, and production of cells with abnormal characteristics. Each of these is likely to be both an effect of DNA damage and a factor in accurately measuring other effects such as mutation and transformation. In order to measure these effects on the progeny of individual irradiated cells, we have developed a system for following the growth of a large number of individual cells. A conventional inverted microscope fitted with a motorized stage and a video camera is used. Video images are digitized and stored on large capacity computer disk drives. Software controls the position of the stage so that each cell location is recorded at a specified interval, and the images can be viewed as time lapse sequences for a large number of different locations on a tissue culture dish.

Initial experiments with this system have been directed toward characterizing the growth of control and x-ray irradiated cells. This provides a base line for comparing single particle irradiation effects, and provides a data base for evaluating systems for scoring growth characteristics.

Even in an unirradiated population of well adapted cells such as CHO, much variation in the growth of individual clones occurs. Figure 1 shows cell number as a function of time after plating for cells collected mechanically from an exponentially growing CHO population. Generally the progeny of a single cell retain a significant amount of synchrony for three or more divisions, but the mean time between divisions varies substantially from one clone to another. This is particularly true in the first two divisions after replating, but this variation naturally makes a large difference in the size of the clone at later times. Also, even among those cells which were chosen for their healthy appearance a few hours after plating, there is a significant incidence of individual cells at the second of higher generation failing to divide further. This constitutes a significant background in studies of delayed lethal mutation.

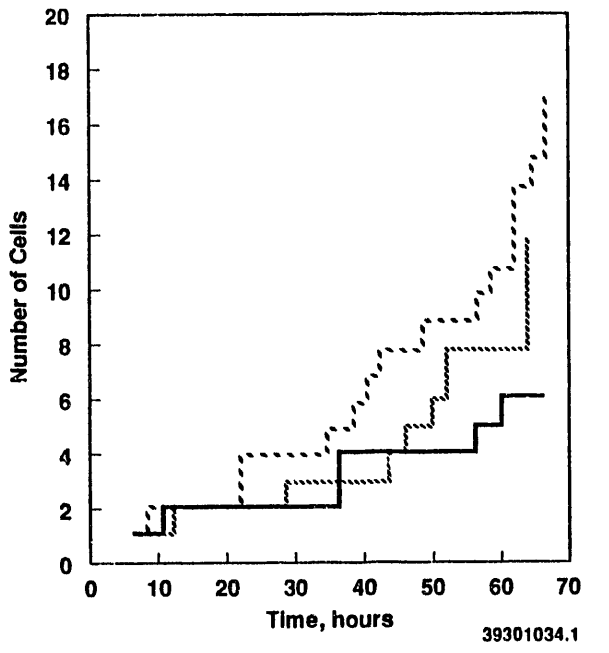

FIGURE 1. The Number of Cells in Each of Three Different Unirradiated CHO Cell Clones as a Function of Time After Plating

Figure 2 shows a typical family tree for an unirradiated CHO cell selected from an exponentially growing population. The divisions are plotted at the time when two daughter cells were first detected in place of the single cell from the previous generation. This experiment was recorded at 2 h intervals, so the division points can be marked as much as 2 h late, but the mean times between divisions (except for the first one, where the starting time is unknown) will be accurate when averaged over a large number of examples. There is also a characteristic of cell behavior which will increase the apparent variance in the division time. Generally both daughter cells attach to the substrate soon after division, but occasionally they will remain one on top of the other, or side by side without flattening, for several hours. Often when this happens, it is impossible to determine when division occurred, and one division time may be recorded as longer than normal while the next one will be recorded as shorter.

All of the data about cell growth within a clone is included in a tree such as Figure 2. Representations such as Figure 1, and various averages such as the mean time between divisions, can all be obtained from Figure 2, or the data on which it is based. However, it is time consuming to record and analyze data in this form. Software to expedite this data collection process is being developed.

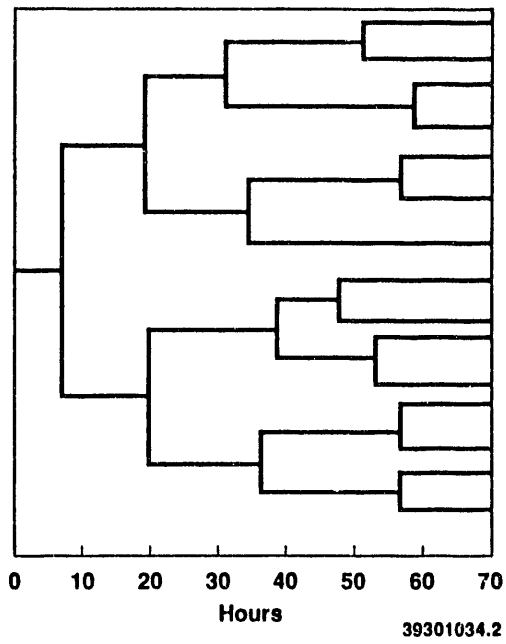

FIGURE 2. The Division Pattern of the Largest Clone from Figure 1. Division points are plotted at the time the division was first detected. A high degree of synchrony is maintained in the clone for the duration of this 64 h experiment.

Measurement Science

Lasers in Analytical Chemistry

Historically, the research conducted under this project has focused on development of a highly selective and extremely sensitive analytical methodology that is generally applicable to determinations of heavy metals and rare isotopes. This effort has culminated in the technique of continuous-wave double resonance ionization mass spectrometry, or cw-DRIMS (Bushaw 1989). The concept utilizes two, sequential, resonant optical excitation steps to populate a chosen high Rydberg state of the analyte atom of interest; this state population is subsequently photoionized and the resultant atomic ions are detected by conventional mass spectrometry methods. Selectivity is achieved through both optical bound-bound transitions by exploiting physical properties unique to the excited states of the analyte atom such as isotope shifts and hyperfine structure splittings. Sensitivity can be limited by spontaneous decay of excited state populations and by the efficiency of the photoionization process. Identification of optimum analytical schemes therefore requires detailed knowledge of the structural and dynamical properties of atomic excited states. Knowledge of factors that can influence the ion production efficiency, such as the location of Cooper minima, that is zeroes in the photoionization cross section, is also needed. While criteria for selection of favorable atomic bound-bound transitions have been elucidated, the dynamics of the photoionization event remain poorly characterized.

Over the past two years, the emphasis of this research project has been directed to systematic investigations of the structural and dynamical properties of selected small molecules, and to studies of photoionization dynamics through photoelectron angular distribution measurements. The principal objectives of these endeavors are (*i*) to examine the potential of cw-DRIMS type techniques for analytical applications to molecules, and (*ii*) to obtain a more comprehensive understanding of the photoionization process thereby contributing to improved sensitivity and reliability in all photoionization based analytical methods.

The potential rewards resulting from these developments in laser based measurement science are vast indeed. Applications relevant to current and future health and environmental concerns include contributions to chemical speciation of environmental contaminants; to identification and quantification of atmospheric constituents; to definition of the mechanisms of formation and destruction of reactive intermediates within the atmosphere; to design of synthetic enzymes for immobilization and treatment of hazardous wastes; and to elucidation of structure-function relationships associated with newly discovered enzymatic processes within the brain.

The cw-DRIMS methodology has been applied to detection of the radionuclide strontium-90 which is a significant health risk and environmental contaminant generated in nuclear power and weapons cycles. Prior studies have demonstrated attogram detection limits while current investigations have focused on investigations of isotope shifts for improved analytical selectivity.

Ultrahigh Resolution Studies of Molecular Structure and Dynamics

R. J. Miller and J. E. Murphy[a]

The excited states of molecules typically lie at higher energies than those of heavy atoms, and molecular transition probabilities tend to be significantly smaller than those of atoms. The existence of vibrational and rotational degrees of freedom, the occurrence of more diverse decay mechanisms, and the general propensity for interactions between electronic states combine to complicate studies of molecules over those of atoms. Basic questions therefore arise. Can ultrahigh resolution cw lasers be applied successfully to molecular multiphoton excitation schemes and to molecular multiple resonance sequences? Can ultrahigh resolution studies decipher the richness of molecular phenomena? Initial investigations of the molecule nitric oxide (NO) have been undertaken to address these basic questions.

Two-Photon Spectroscopy of *A* $^2\Sigma^+$ NO

Two-photon fluorescence excitation spectroscopy has been used to probe the $(3ss)A\ ^2S^+$ Rydberg state of nitric oxide. All experiments have been conducted in a static cell and Doppler-free resolution has been achieved employing counterpropagating beams obtained with a spherical retroreflector.

Fine structure and hyperfine structure splittings have been resolved within six rotational branches of the $A\ ^2S^+(u'=1,\ N'=3)\leftarrow X\ ^2P(u''=0)$ two-photon band of $^{14}N^{16}O$ (Miller 1989a). Figure 1 portrays a typical spectrum of the $R_{11}(J''=2.5)$ branch illustrating all eight of the allowed $\Delta F = 0, \pm 1, \pm 2$ transitions. The effective cross section for two-photon excitation of this branch is estimated from experimental observables to be 1×10^{-44} $cm^{-1}\cdot s$. A zero-field spin Hamiltonian appropriate for Hund's case (b_{bJ}) coupling has been used to extract the fine structure and hyperfine structure parameters of the *A* state.

The parameters characterizing the magnetic hyperfine structure interactions yield detailed structural information specific to the spin distribution and orbital motion of the unpaired electron; the nuclear electric quadrupole moment describes electrostatic interactions involving all charged particles within the molecule. The theoretical spectrum depicted in Figure 1 was generated using these *A* state parameters in conjunction with observed ground state splittings. Signal amplitudes are weighted to Clebsch-Gordon coefficients calculated for two-photon excitation with $\Delta m_F = 0$. Line shapes reflect experimental Voigt profiles: laser jitter (2 MHz) and transit broadening (7.6 MHz) contribute to the Gaussian component, while the natural linewidth (0.8 MHz), pressure broadening (1 MHz), and a residual width (1.6 MHz) attributed to a non-Gaussian beam waist contribute to the Lorentzian component.

In preparation for the ultrahigh resolution, double resonance investigations discussed below, it has proven necessary to catalogue a large number of the two-photon rotational transitions comprising the $A\leftarrow X(1,0)$ band of NO. Energies of 351 transitions have been observed. Figure 2 illustrates the two-photon fluorescence excitation spectrum of the

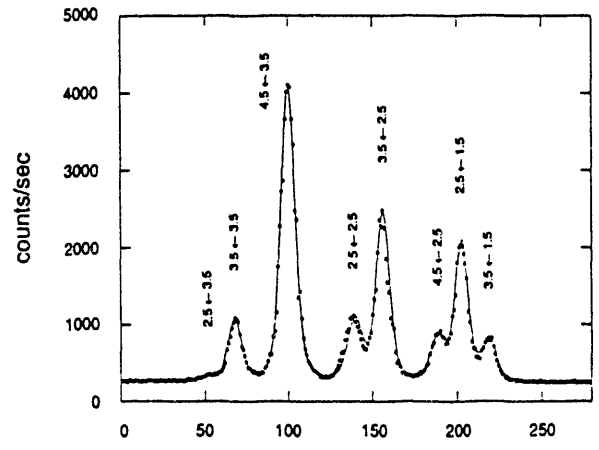

FIGURE 1. Fluorescence Excitation Spectrum Resulting from Two-Photon Pumping of the $R_{11}(J''=2.5)$ Rotational Branch of $(3s\sigma)A\ ^2\Sigma+(v'=1,\ N'=3)\leftarrow X^2\Pi(v''=0)\ ^{14}N^{16}O$

(a) NORCUS Postdoctoral Research Associate.

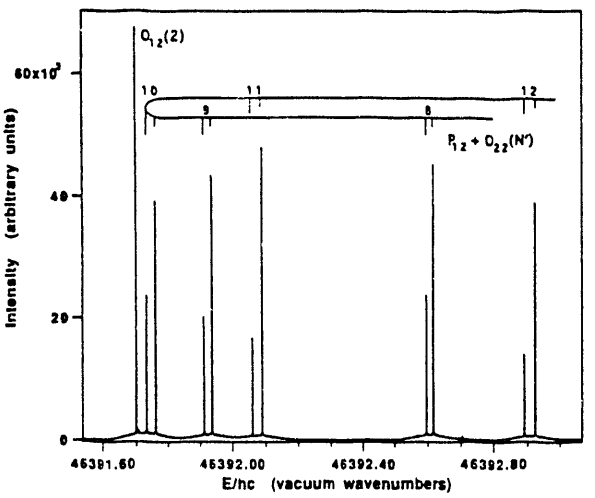

FIGURE 2. Doppler-Free, Two-Photon Fluorescence Excitation Spectrum of the $P_{12}+O_{22}$ Bandhead Region Within A←X(1,0) NO

typically congested P_{12} + O_{22} bandhead in the region of 46,392 cm^{-1} that is observed under the Doppler-free conditions of these experiments. These data have been analyzed via diagonalization of effective Hamiltonian matrices to obtain molecular parameters that retain maximum mechanical and magnetic significance and which are therefore useful for construction of reliable Rydberg-Klein-Rees potentials and for direct comparison to *ab initio* theoretical predictions (Zare 1973). The results of this study have been accepted for publication in *The Journal of Molecular Spectroscopy*.

Double Resonance Spectroscopy of High Rydberg States

Ultrahigh resolution, (2 + 1′) double resonance laser induced fluorescence dip spectroscopy has been used to determine the term energies and natural linewidths of individual rovibronic levels of the (4*pp*)K $^2P(u=2)$ and the (3*dd*)F $^2D(u=3)$ Rydberg states of NO (Miller 1990). The complexities of the structures and of the dynamics of states in this energy region (Miller 1989b) provide a stringent test of the utility of cw laser sources in investigations of highly excited molecular electronic states. Once again, experiments were conducted in a static cell; in this case, Doppler-free resolution was obtained using velocity selection techniques.

A plot of the reduced term energies as a function of total angular momentum exclusive of spin N (Figure 3) clearly manifests the complexity of the molecular structure. The crossings of the $K(u=2)$ and $F(u=3)$ potential curves reveal local perturbations involving both the *e* and *f* symmetry components of the rovibronic levels. These interactions are quite weak, with magnitudes & 1 cm^{-1}. The overall structure of the $K(u=2)$ state is particularly interesting. The spin-orbit splitting observed at low N results predominantly from coupling to the B $^2P(u=29)$ valence state. With increasing nuclear rotation, **S**-uncoupling and **L**-uncoupling (Lefebrve-Brion 1986) occur completing a rapid transition from Hund's case (*a*) to case (*b*) to case (*d*).

Figure 4 illustrates the marked variation of the natural linewidths as a function of N, thus providing further evidence for the existence of complex multistate interactions. These natural linewidths, which correspond to state lifetimes of the order of hundreds of picoseconds, are thought to be determined by predissociative decay to ground state nitrogen and oxygen atoms (Miller 1989b). It is noteworthy that,

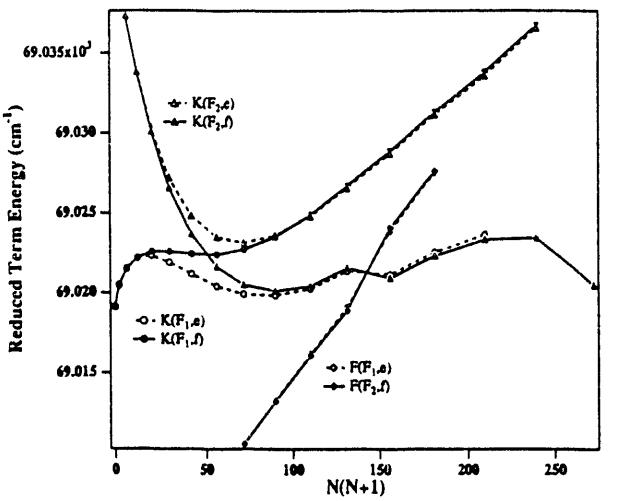

FIGURE 3. Reduced Term Energies as a Function of Total Angular Momentum Exclusive of Spin N for Rovibronic Levels of the (4*pπ*)$K^2\Pi(v=2)$ and (3*dδ*)$F2_\Delta(v=3)$ Rydberg States of $^{14}N^{16}O$

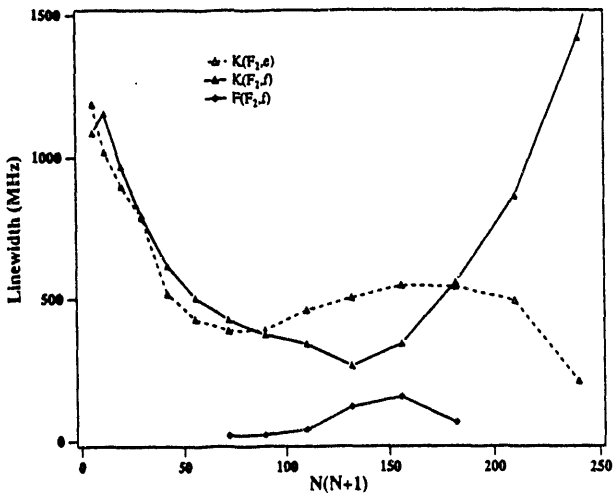

FIGURE 4. Natural Linewidths as a Function of Total Angular Momentum Exclusive of Spin N for Rovibronic Levels of the F_2 Spin Component of the $(4p\pi)K^2\Pi(v=2)$ and $(3d\delta)F2_\Delta(v=3)$ Rydberg States of $^{14}N^{16}O$

compared to unperturbed F state lifetimes (Hart 1987), the weak $K(u=2) \sim F(u=3)$ interaction reduces the F state lifetimes by as much as a factor of 30!

The results summarized above establish the utility of ultrahigh resolution cw lasers in studies of molecules. Both multiphoton excitation schemes and multiple resonance sequences can be exploited to advantage, and the information content of such investigations is clearly sufficient to decipher the rich phenomena of molecular structure and dynamics. Knowledge of term energies serves to identify those states that can provide maximum selectivity in applications of measurement science. Knowledge of the mechanisms and rates of spontaneous decay processes serves to identify those states that can provide maximum sensitivity in applications of measurement science.

Circular Dichroism in Hyperfine State Resolved Photoelectron Angular Distributions

R. J. Miller and R. G. Tonkyn

Experimental and theoretical investigations of the circular dichroism of angular distributions (CDAD) in photoelectron spectra (Dubs 1985a) are being used to probe photoionization phenomena from single, completely specified hyperfine quantum states. These studies are being pursued in collaboration with Dr. Robert Compton of Oak Ridge National Laboratory and Professor Vincent McKoy of The California Institute of Technology. In the CDAD experiment, a chosen intermediate state is prepared by absorption of linearly polarized light thus creating a condition of finite angular momentum alignment. The aligned state is then probed by measuring the difference in the photoelectron angular distributions obtained with left- and right-handed circularly polarized light. For one-photon excitations, the CDAD intensity is given by (Dubs 1988)

$$I^{CDAD}(\theta) = \frac{1}{2} A_2 \beta_2 \sin(2\theta) \qquad (1)$$

where θ defines the angular relationship between the photoelectron detector and the electric field vector of the linearly polarized photon. The quadrupole moment of the alignment A_2 fully characterizes the anisotropy of the resonant intermediate state. The β_2 term contains all possible information about the dynamics of the photoionization event (Dubs 1988). In the case of atoms, β_2 depends explicitly upon the radial matrix elements describing elimination of the competing electron partial waves and upon the phase shift between the $\ell+1$ and $\ell+1$ ionization channels (Dubs 1985b).

To extract the photoionization dynamics from experimentally observed CDAD spectra, it is necessary to have accurate knowledge of the angular momentum alignment. Internal, bound state phenomena can, however, alter or destroy an initially prepared angular momentum alignment (Greene 1982). Hyperfine interactions, for example, induce dynamical mixing of degenerate states leading to loss of alignment. This process is easily visualized. The nuclear spin angular momentum vector $\vec{I}$ couples to the angular momentum vector $\vec{J}$ to yield the total angular momentum vector $\vec{F}$. Classically, $\vec{I}$ and $\vec{J}$ precess about $\vec{F}$ thereby changing the projection of $\vec{J}$ onto the axis of quantization that defines M_J thus destroying the alignment defined within the $|J,M_J\rangle$

representation. For an idealized two-level system, the rate of this precession, and therefore the rate of hyperfine induced disalignment is determined by the magnitude of the hyperfine splitting. In real, many-level systems, the exact consequences of this mixing are difficult to predict.

Such disalignment phenomena can be expected to occur whenever a coherent superposition of states is prepared as will typically be possible under pulsed laser excitation. The resultant loss of alignment will affect CDAD measurements (Cuéllar 1991) and may even adversely influence the reliability of certain isotope ratio measurement techniques. Note however that in the absence of external fields, $|F,M_F\rangle$ defines a pure eigenstate of the system such that alignment prepared within the $|F,M_F\rangle$ representation will not decay via internal dynamical processes. The corresponding alignment parameter A_2 can be calculated exactly therefore allowing $\bar{\bar{\beta}}_2$ to be extracted from experimental observations and compared directly to the predictions of *ab initio* theories of photoionization. CDAD studies as a function of the energy of the ionizing photon also provide a probe that is sensitive to the location of Cooper minima in the photoionization cross section (Rudolph 1990). Hyperfine resolved CDAD achieved through use of ultrahigh resolution cw lasers is thus the preferred method for investigations of photoionization dynamics.

Hyperfine state resolved CDAD spectra have been measured for the following three bound-bound transitions in atomic cesium: $7p\ ^2P_{3/2}(F'=3,4,5)\leftarrow 6s\ ^2S_{1/2}(F''=4)$. Photoionization has been accomplished using 514 nm light, and the resultant photoelectrons have been detected using a spherical sector electrostatic energy analyzer. The inherent angular resolution of the instrumentation is approximately $\pm 2°$.

Figure 5 illustrates a representative CDAD spectrum for the $F'=5\leftarrow F''=4$ transition. Table I summarizes the existing experimental CDAD amplitudes and compares them to calculated quadrupole moments of the alignment for each transition studied. Given the near degeneracy of the F' states, it is plausible to assume

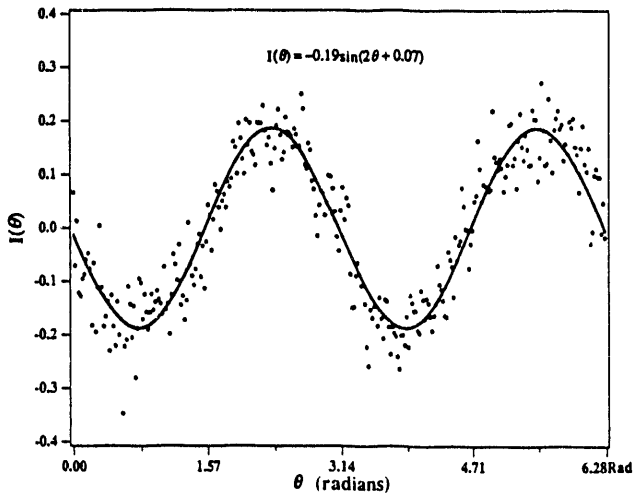

FIGURE 5. Hyperfine State Resolved CDAD Spectrum Observed for the $7p\ ^2P_{3/2}(F'=5)\leftarrow 6s\ ^2S_{1/2}\ (F''=4)$ Transition of Atomic Cesium

TABLE 1. Experimental CDAD Amplitudes and Theoretical Alignment Parameters A_2 for Hyperfine State Resolved Transitions Within the $7p\ ^2P_{3/2}\leftarrow 6s\ ^2S_{1/2}$ Manifold of Cesium

Transition ($F'\leftarrow F''$)	Experimental CDAD Amplitude	Calculated A_2
5←4	−0.18 ± 0.02	−0.109
4←4	−0.07 ± 0.01	+0.292
3←4	+0.03 ± 0.02	−0.178

that $\bar{\bar{\beta}}_2$ should be independent of F'. This assumption leads to the conclusion that the observed CDAD amplitudes and phases (±) should scale directly with the alignment parameters. Inspection of Table I clearly indicates that this is in fact not the case. A thorough search for possible systematic experimental errors has been conducted with great care. The experimental results are found to be highly reproducible and independent of cesium beam density. Saturation effects in both optical transitions have been examined. The purities of the light polarizations have been scrutinized. Potential artifacts associated with stray electromagnetic fields have been explored. To date, there is no evidence to indicate the existence of any such systematic errors in the experimental measurements. Thus, suspicion grows that the photoionization

dynamics of even relatively simple atoms may prove to be more complex and more subtle than currently believed. *Ab initio* studies of these dynamics are in progress: it is fully anticipated that the results of these theoretical investigations will provide insight into the physical significance of the experimental studies reported above.

Acknowledgment: Technical assistance provided by B. A. Bushaw is gratefully acknowledged.

Strontium Isotope Shifts

B. A. Bushaw

Detailed measurements of stable strontium isotope shifts in a wide range of upper level Rydberg states within the accessible $5sns\ ^1S_0$, $5snd\ ^1D_2$, and $5snd\ ^3D_2$ manifolds have been performed. Emphasis has been placed on the even, stable isotopes because a precise knowledge of the systematic trends in the changes of the shifts for ^{84}Sr, ^{86}Sr, and ^{88}Sr will contribute to the development and understanding of predictive models for ^{90}Sr isotope shifts. Transition isotope shifts for isotopes without nuclear spin are conventionally described by Eq. 2 (Heilig 1974):

$$\Delta\nu_{ij}(AA') = \nu_{ij}\left[\frac{m_e}{m_p}\right] + C_{ij}\left[\frac{A'-A}{AA'}\right] + F_{ij}\delta\langle r^2\rangle^{AA'} \quad (2)$$

where the first term is the normal mass shift (NMS) arising from the difference in the finite nuclear masses of the isotopes A and A' for a transition at frequency ν_{ij}. The second term is the specific mass shift (SMS) that arises from recoil of the ion core on exchange of one of its electrons with the optically active electron. While the SMS has the same functional form as the NMS, the exchange coefficient C_{ij} is very difficult to evaluate theoretically. Accurate experimental determinations of C_{ij} provide tests of developing theories and the validity of the wavefunctions used in these calculations. The third term is the field shift (FS), or nuclear volume shift that arises from the finite volume of the nucleus. The screening constant F_{ij} includes the product of the Fermi contact potential and the change in the electron density at the nucleus in the transition between states i and j, while $\delta\langle r^2\rangle^{AA'}$ is the change in the mean charge square radii of the nuclei of the two isotopes. Determinations of FS provide information for nuclear conformation models. More fundamental information can be obtained if this description is reformulated in terms of *level* shifts (Eq. 3):

$$\Delta\nu_{ij}(AA') = NMS + (C_i - C_j)\left(\frac{A'-A}{AA'}\right) + (F_i - F_j)\delta\langle r^2\rangle^{AA'} \quad (3)$$

where the NMS remains unchanged, but the SMS and FS are decomposed into the differences in these effects in the two specific atomic levels involved in the transition. In the treatment of experimental data it is convenient to subtract out the easily calculated NMS, leaving the residual isotope shift (RIS). The resulting RIS's that have been measured for the ^{84}Sr–^{88}Sr isotope pair in the $5sns\ ^1S_0$, $5snd\ ^1D_2$, and $5snd\ ^3D_2$ Rydberg series are shown in Figure 6, and a similar set of data have been obtained for the ^{86}Sr–^{88}Sr isotope pair. It can be seen that at a sufficiently high principal quantum number, where the excited electron no longer has any probability of penetrating the nucleus or interacting with the core electrons, all three series converge to the same RIS value,

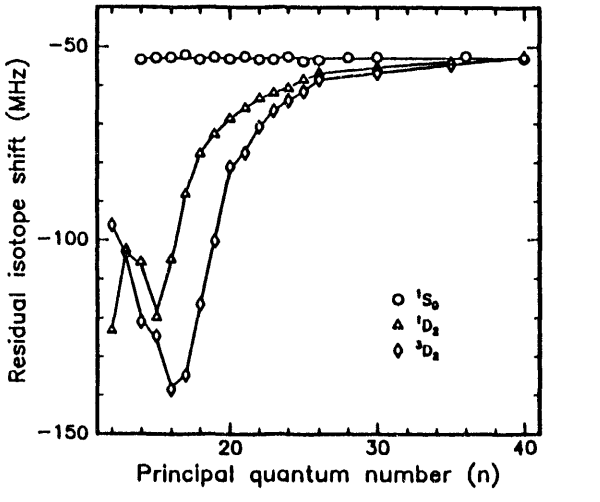

FIGURE 6. Residual Isotope Shifts for ^{84}Sr with Respect to ^{88}Sr in the $5sns\ ^1S_0$, $5snd\ ^1D_2$, and $5snd\ ^3D_2$ Rydberg Series

which is purely the level RIS of the ground state. Analysis of the data for the members of the $5sns\ ^1S_0$ series, which show no change throughout the region studied, has yielded ground state level shift values for ^{84}Sr and ^{86}Sr (with respect to ^{88}Sr) of −54.89 ± 0.10 Mhz and −20.85 ± 0.18 MHz, respectively. Also, the fact that no change in the RIS is observed throughout the $^1S_0$ series indicates that the deviations observed in lower lying members of the $^{1,3}D_2$ series must arise purely from the excited state SMS. Normalizing for the *(A'-A)/AA'* factor has yielded the Rydberg level specific mass shift constants which, for the two isotope pairs studied, agree to within experimental uncertainty throughout the $^{1,3}D_2$ series.

References

Bushaw, B. A. 1989. "High-Resolution Laser-Induced Ionization Spectroscopy." *Prog. Analyt. Spectrosc.* 12:247.

Cuéllar, L. E., C. S. Feigerle, H. S. Carman, Jr., and R. N. Compton. 1991. "Circular Dichroism in Photoelectron Angular Distributions for the $7P_{3/2}$ Level of Cesium." *Phys. Rev. A* 43:6437.

Dubs, R. L., S. N. Dixit, and V. McKoy. 1985a. "Circular Dichroism in Photoelectron Angular Distributions from Oriented Linear Molecules." *Phys. Rev. Letters* 54:1249.

Dubs, R. L., S. N. Dixit, and V. McKoy. 1985b. "Circular Dichroism in Photoelectron Angular Distributions from Absorbed Atoms." *Phys. Rev. B* 32:8389.

Dubs, R. L., V. McKoy, and S. N. Dixit. 1988. "Atomic and Molecular Alignment from Photoelectron Angular Distributions in $(n+1)$ Resonantly Enhanced Multiphoton Ionization." *J. Chem. Phys.* 88:968.

Greene, C. H., and R. N. Zare. 1982. "Photofragment Alignment and Orientation." *Ann. Rev. Phys. Chem.* 33:119.

Hart, D. J., and J. W. Hepburn. 1987. "Vacuum Ultraviolet Laser Spectroscopy: Radiative Lifetimes of Interacting ^2D States of NO." *J. Chem. Phys.* 86:1733.

Heilig, K., and A. Steudel. 1974. *Atom. and Nucl. Data Tables* 14:613.

Lefebrve-Brion, H., and R. W. Field. 1986. *Perturbations in the Spectra of Diatomic Molecules*. Academic Press-Orlando.

Miller, R. J., and B. A. Bushaw. 1990. "Continuous Wave-Continuous Wave Molecular Double Resonance Spectroscopy: Lifetimes and Term Energies of Individual Rovibronic Levels of the $(4pp)K\ ^2P(u=2)$ Rydberg State of Nitric Oxide." *J. Chem. Phys.* 92:3245.

Miller, R. J., W. L. Glab, and B. A. Bushaw. 1989a. "Two-Photon Spectroscopy at Ultra-High Resolution: Fine Structure and Hyperfine Structure of the $(3ss)A\ ^2S^+(u=1,\ N=3)$ Rydberg State of NO." *J. Chem. Phys.* 91:3277.

Miller, R. J., L. Li, Y. Wang, W. A. Chupka, and S. D. Colson. 1989b. "Multiphoton Ionization Studies of NO: Spontaneous Decay Channels in the $(4pp)K\ ^2P(u=2)$ Rydberg State." *J. Chem. Phys.* 90:754.

Rudolph, H., R. L. Dubs, and V. McKoy. 1990. "Cooper Minima and Circular Dichroism in Photoelectron Angular Distributions." *J. Chem. Phys.* 93:7513.

Zare, R. N., A. L. Schmeltekopf, W. J. Harrop, and D. L. Albritton. 1973. "A Direct Approach for the Reduction of Diatomic Spectra to Molecular Constants for the Construction of RKR Potentials." *J. Mol. Spectrosc.* 46:37.

Capillary Zone Electrophoresis

The analysis of environmental, hazardous mixed waste or biological mixtures is best addressed by combined separation-mass spectrometry techniques. Developing these improved analytical methods depends upon the speed, selectivity, and efficiency of the separation combined with the sensitivity and flexibility of mass spectrometric analysis methods. This program is developing methods that are widely applicable to nonvolatile or highly polar compounds that are interactable with more conventional methods such as gas chromatography-mass spectrometry. Currently, new methods based upon capillary electrophoresis-mass spectrometry (CE-MS) are being investigated. The goal of this research is to develop ultrasensitive CE-MS methods applicable at the attomole level for environmental and health-related problems.

Development of Capillary Electrophoresis-Mass Spectrometry for DNA Adduct Research

R. D. Smith, H. R. Udseth, C. J. Barinaga, B. E. Winger, C. G. Edmonds, and J. A. Loo

The history of analytical advances in mass spectrometry (MS) has highlighted the special importance of combining separation methods having high selectivity and resolving power in conjunction with the high sensitivity and specificity of mass spectrometric detection. "Real world" samples are invariably mixtures and are often very complex. Any useful analytical methods must accommodate contributions from the sample matrix, interfering substances, etc. Thus, the dynamic combination of capillary electrophoresis (CE), a separation method of high efficiency, speed, and flexibility, with electrospray ionization (ESI)-MS is particularly advantageous.

The on-line combination of capillary zone electrophoresis (CZE), one form of CE, with ESI-MS (Olivares et al. 1987; Smith et al. 1988b) was developed at PNL. Subsequently, a liquid sheath-electrode interface was developed from which the solvent composition and flow rate of the electrosprayed liquid could be controlled independently of the CZE buffer (which is desirable since high-percentage aqueous and high-ionic strength buffers that are useful in CZE are not well tolerated by ESI) (Smith et al. 1988a). The interface provides greatly improved interface stability and performance and is adaptable to other forms of CE. Because CE relies on analyte charge in solution, and the ESI process is nearly universal for charged species, the CE/ESI-MS combination is highly complementary. Thus, the CZE/MS approach offers previously unobtainable separation efficiencies (for the combination with MS) as well as detection limits that can greatly surpass existing methods (Edmonds et al. 1989; Loo et al. 1989a, 1989b; Smith et al. 1989; Smith et al. 1990a, 1990b; Smith et al. 1991).

One reason for the current interest in CE-MS techniques is for identifying and analyzing DNA adducts. This is an important but formidable analytical challenge due to the extremely low concentrations at environmental levels of exposure. Ideally, we desire not only the ability to detect "known" compounds, but to determine the structure of unknown DNA adducts with sample sizes far too small to be addressed by other analytical methods. This provides the essential tool in order to understand the origin of health effects upon exposure at the molecular level. These desires lead to our interest in CE, ESI-MS, and ESI-MS/MS. In fact, it can be argued that the CE-MS/MS combination obtained using the ESI interface should provide a near-ideal analytical approach for DNA adducts.

To realize the full potential of this new analytical marriage, several problems remain to be addressed:

- The utilization and transmission of ESI-produced ions must be increased. Currently, ESI losses in the interface and

during transmission reduce potential sensitivity by 10^4 (Smith et al. 1990b).

- High-resolution separations utilizing an analyte enrichment scheme are required to both deal with the complexity of "real" samples and to obtain sufficient sensitivity with the small volumes utilized in CE.

- Improved MS and MS/MS sensitivity, resolution, and mass measurement accuracy are necessary to enhance detection and allow interpretation of mass spectra containing multiply-charged molecules.

In the last year, we have developed a new "microspray" ESI interface which has provided a large gain in sensitivity. Figure 1 shows a CE-MS separation of a simple pentapeptide mixture, demonstrating the attomole-level sensitivity obtainable with the "microspray" dance. We have also explored new methods for enhancing the sensitivity of ESI-MS when combined with CE separations. We have shown that using small diameter capillaries can significantly boost ESI sensitivity by providing a near ideal match of analyte and ESI capabilities. Figure 2 shows reconstructed single ion electropherograms obtained during a CE-MS separation using full scan detection. The separation was conducted in a 5-μm-diameter capillary, and ~600 attomoles of each protein was injected. Mass spectra were obtained from each component with sufficient quality to allow accurate molecular weight determination.

In addition to the above, a new Reduced Elution Speed (RES) concept for CE-MS has been developed and demonstrated. The method is readily implemented by instituting a step change in the CE electric field strength for desired periods of time during a separation. As a result, the *m/z* range can be scanned while a solute elute is increased by a factor proportional to the decrease in CE electric field strength. Under conditions where the quantity

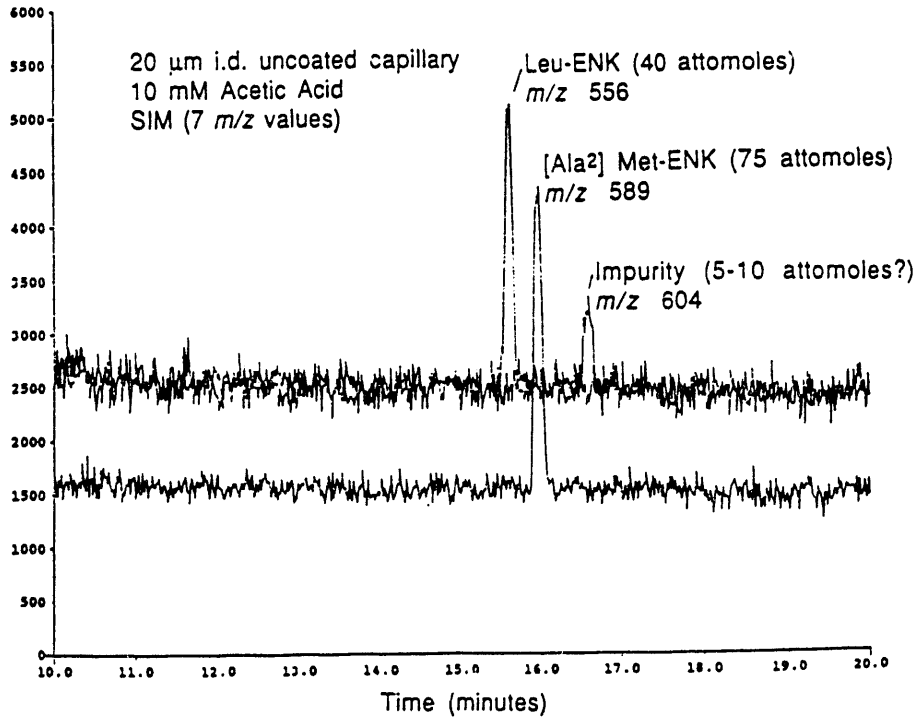

FIGURE 1. Reconstructed Single Ion Electropherograms for Ions Representative of the Three Pentapeptides Separated in a 20-μm Inside Diameter Capillary by CZE

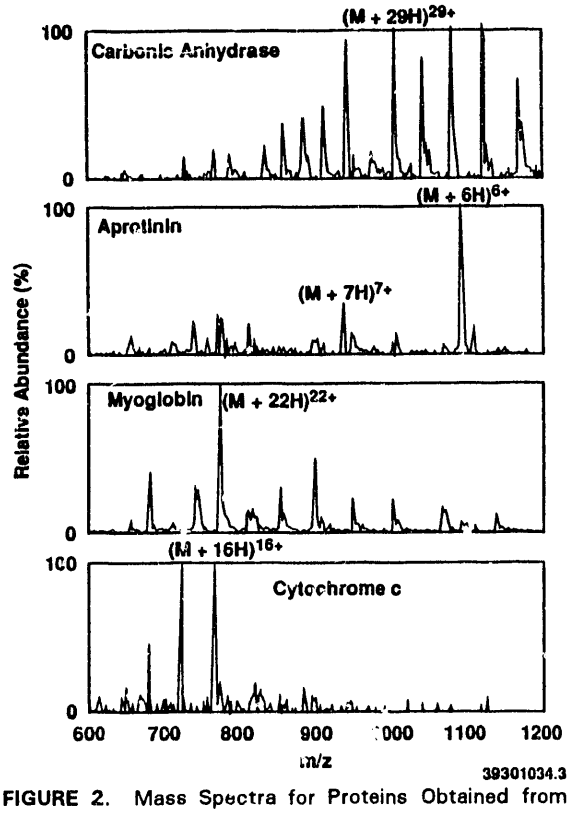

FIGURE 2. Mass Spectra for Proteins Obtained from an Injection of 600 Attomoles of Protein into a 5-μm Capillary for CE-MS Analysis

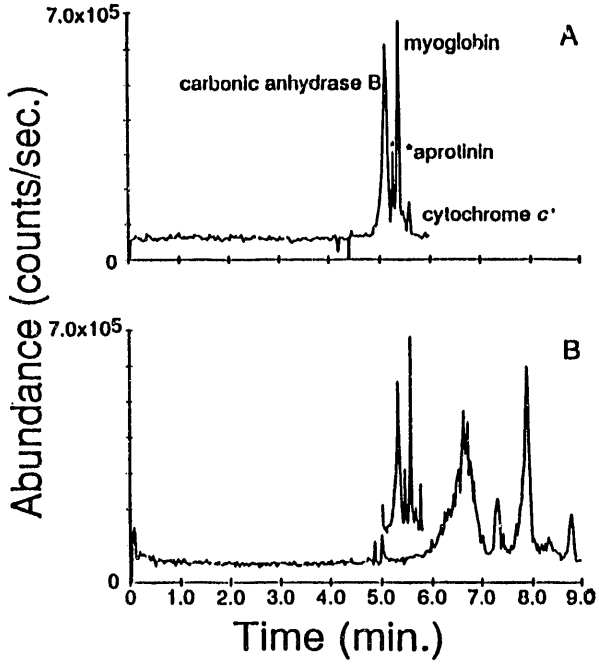

FIGURE 3. Comparison of Constant Field Strength (a) and Reduced Elution Speed (b) CE/ESI-MS Analysis of a Mixture Containing Carbonic Anhydrase, Aprotinin, Myoglobin, and Cytochrome c. The constant field strength CE/ESI-MS analysis was conducted at 300 V/cm. The reduced elution speed CE/ESI-MS analysis was conducted at 300 V/cm until 1 minute prior to elution of the first protein when the electric field strength was reduced to 60 V/cm.

of solute entering the ESI source per unit of time exceeds the current available for ionization of all solute molecules present (i.e., solute "saturates" the electrospray process), we project no substantial decrease in maximum ion intensity when the electric field strength is decreased. Thus, a larger fraction of the analyte will be transferred to the gas phase as ions during RES CE-MS than during constant electric field strength CE-MS. The experiments described below (and other work) have shown this expectation to be correct.

Figure 3a shows the total ion electropherogram for the separation of 60 fmoles (injected) each of carbonic anhydrase B, aprotinin, myoglobin, and cytochrome *c* using a constant electric field strength of 300 V/cm during CE-ESI/MS. In comparison, Figure 3b shows the total ion electropherogram (TIE) for the same mixture where the electric field strength was reduced to 60 V/cm 1 minute prior to migration of the first protein into the ESI source. The insert of Figure 3b shows the same total ion electropherogram after the abscissa has been compressed by a factor of five. The prolonged residence time of solute in the electrospray can be exploited in several ways, including 1) an increase in the *m/z* range scanned, 2) an increase in the number of scans recorded during elution of a given solute, and 3) an enhancement of sensitivity (integrated ion intensity) for a given solute. The method does not increase solute consumption, it allows sensitivities for peptide and protein analyses extending into the low femtomole regime, and it incurs very little loss in ion intensity, particularly important for MS/MS methods and their potential application to peptide sequencing.

During the last year, we have also explored the following methods for probing the primary and higher order structure of biopolymers using ESI-MS and ESI-MS/MS methods:

- Methods for the negative ion ESI of proteins were developed (Loo et al. 1992).

- Charge effects of the activation energy for molecular ion dissociation were determined (Busman et al. 1992).

- Solvent effects on protein structure and ESI spectra were reported (Loo et al. 1991).

- The use of H/D exchange reactions for probing noncovalent protein structure was reported (Winger et al. 1992).

- Methods for using ion-molecule reactions of amines to probe protein structure were developed (Ogorzalek Loo et al. 1992a).

- Investigations of noncovalent associations probed by ESI-MS were reported (Smith et al. 1992).

- New methods for studying gas phase ion-ion reactions involving biomolecules were reported (Ogorzalek Loo et al. 1992b).

During the next year, we intend to develop capillary isotachophoresis (CITP-ESI MS) methods to study DNA adducts (Udseth et al. 1989). The approach will aim at exploiting the recent gains in MS sensitivity, as well as the greater sample volume and analyte focusing properties of CITP. The CITP method will allow larger volumes of sample to be analyzed than possible with conventional CZE. In order to further enhance MS sensitivity, a new orthogonal time of flight mass spectrometer is being developed at PNL. This new instrumental approach will provide near ideal utilization efficiency for electrospray-generated ions. With such instrumentation, we anticipate obtaining sub-attomole detection limits, and the ability to detect DNA adducts (known and unknown) at environmental levels.

References

Busman, M., A. L. Rockwood, and R. D. Smith. 1992. "Activation Energies for Gas Phase Dissociations of Multiply Charged Ions from Electrospray Ionization Mass Spectrometry." *J. Phys. Chem.* 96:2397-2400.

Edmonds, C. G., J. A. Loo, C. J. Barinaga, H. R. Udseth, and R. D. Smith. 1989. "Capillary Electrophoresis-Electrospray Ionization-Mass Spectrometry." *J. Chromatogr.* 474:21-37.

Loo, J. A., H. K. Jones, H. R. Udseth, and R. D. Smith. 1989a. "Capillary Zone Electrophoresis-Mass Spectrometry with Electrospray Ionization of Peptides and Proteins." *J. Microcolumn Sep.* 1:223-229.

Loo, J. A., H. R. Udseth, and R. D. Smith. 1989b. "Peptide and Protein Analysis by Electrospray Ionization Mass Spectrometry and Capillary Zone Electrophoresis-Mass Spectrometry." *Anal. Biochem.* 179:404-412.

Loo, J. A., R. R. Ogorzalek Loo, H. R. Udseth, C. G. Edmonds, and R. D. Smith. 1991. "Solvent-Induced Conformational Changes of Polypeptides Probed by Electrospray Ionization-Mass Spectrometry." *Rapid Commun. Mass Spectrom.* 5:101-105.

Loo, J. A., R. R. Ogorzalek Loo, K. J. Light, C. G. Edmonds, and R. D. Smith. 1992. "Multiply Charged Negative Ions by Electrospray Ionization from Polypeptides and Proteins." *Anal. Chem.* 64:81-88.

Ogorzalek Loo, R. R., J. A. Loo, H. R. Udseth, J. L. Fulton, and R. D. Smith. 1992a. "Protein Structural Effects in Gas Phase Ion-Molecule Reactions with Diethylamine." *Rapid Commun. Mass Spectrom.* 6:159-165.

Ogorzalek Loo et al. 1992b. "A New Approach for the Study of Gas Phase Ion-Ion Reactions Using Electrospray Ionization." *J. Amer. Soc. Mass Spectrom.*, 3, 695-705.

Olivares, J. A., N. T. Nguyen, C. R. Yonker, and R. D. Smith. 1987. "On-Line Mass Spectrometric Detection for Capillary Zone Electrophoresis." *Anal. Chem.* 59:1230-1232.

Smith, R. D., C. J. Barinaga, and H. R. Udseth. 1988a. "Improved Electrospray Ionization Interface for Capillary Zone Electrophoresis-Mass Spectrometry." *Anal. Chem.* 60:1948-1952.

Smith, R. D., J. A. Olivares, N. T. Nguyen, and H. R. Udseth. 1988b. "Capillary Zone Electrophoresis-Mass Spectrometry Using an Electrospray Ionization Interface." *Anal. Chem.* 60:436-441.

Smith, R. D., C. J. Barinaga, and H. R. Udseth. 1989. "Tandem Mass Spectrometry of Highly Charged Cytochrome c Molecular Ions Produced by Electrospray Ionization." *J. Phys. Chem.* 93:5019-5022.

Smith, R. D., S. M. Fields, J. A. Loo, C. J. Barinaga, and H. R. Udseth. 1990a. "Capillary Isotachophoresis with UV and Tandem Mass Spectrometric Detection for Peptides and Proteins." *Electrophoresis* 11:709-717.

Smith, R. D., J. A. Loo, C. G. Edmonds, C. J. Barinaga, and H. R. Udseth. 1990b. "New Developments in Biochemical Mass Spectrometry: Electrospray Ionization." *Anal. Chem.* 62:882-899.

Smith, R. D., H. R. Udseth, C. J. Barinaga, and C. G. Edmonds. 1991. "Instrumentation for High-Performance Capillary Electrophoresis-Mass Spectrometry." *J. Chromatogr.* 559:197 208.

Smith, R. D., K. J. Light-Wahl, B. E. Winger, and J. A. Loo. 1992. "Preservation of Noncovalent Association in Electrospray Ionization Mass Spectrometry: Formation and Dissociation of Multiply Charged Polypeptide and Protein Dimers." *Org. Mass Spectrom.* 27:811 821.

Udseth, H. R., J. A. Loo, and R. D. Smith. 1989. "Capillary Isotachophoresis/Mass Spectrometry." *Anal. Chem.* 61:228.

Winger, B. E., K. J. Light-Wahl, and R. D. Smith. 1992. "Probing Qualitative Conformational Differences of Multiply Protonated Gas-Phase Proteins via H/D Isotopic Exchange with D_2O." *J. Am. Chem. Soc.* 114, 5897-5898.

DNA Sequencing

New approaches to DNA sequencing should improve efficiency, but they will not produce the massive increase in speed and cost reduction that is needed for the Human Genome Program. Several new approaches are being investigated, but no clearly superior technology has yet emerged. This project attempts to speed DNA sequencing greatly by sequentially degrading a single DNA molecular ion in an ion cyclotron resonance (ICR) mass spectrometer. This approach would eliminate the need for the preparation and electrophoretic ordering of mixtures of nested oligonucleotides. If successful, this approach would also make possible important studies of site-specific DNA modifications, adduction, and damage at the single molecule level that are now precluded at the single molecule level. This new approach, termed single molecule analysis by mass spectrometry (SMAMS), will be explored using new ICR instrumentation developed at PNL. Initial studies are being conducted of appropriate ionization methods for large DNA segments and to define ICR performance.

Rapid Sequencing Techniques for DNA

R.D. Smith, C.G. Edmonds, S.A. Hofstadler, J.E. Bruce, and B.E. Winger

ICR-MS of DNA Molecular Ions

Generating oligonucleotide mixtures, separating them by electrophoresis, and reading and verifying them presently constitutes in excess of 80% of the total effort in DNA sequencing. Limitations of these methods arise from the behavior of the enzymes employed for chain extension, the chemistry and spectroscopy of the fluorescently labeled residues, and the resolution and speed of the gel separations. Presently, overall raw sequencing rates of 600 residues per hour with accuracies in the range of 95 to 99% can be achieved. Most new approaches for reducing the cost and time required for these sequencing activities involve automation and/or multiplexing of currently practiced methods. As an example, electrophoresis in gel-filled capillaries, or very thin gel layers, is being investigated as an approach for speeding the electrophoretic separation and facilitating its automation. These approaches should improve efficiency, but still fall short of the massive increase in speed and cost reduction desired for large scale DNA sequencing.

In the search for methods to increase sequencing speed, a number of new approaches are being investigated, but no clearly superior technology has yet emerged. This project is aimed at greatly speeding DNA sequencing by sequentially degrading a single trapped DNA molecular ion. Such methods could have inherently high rates of sequence determination, and could significantly accelerate the overall process of DNA sequence determination by eliminating the preparation and electrophoretic ordering of mixtures of nested oligonucleotides. Successfully developing this approach would not only be relevant to DNA sequencing, but perhaps even more importantly, would make possible important studies of site-specific DNA modifications, adduction and damage, which, presently, are precluded at the single molecule level. New developments in combined ion cyclotron resonance (ICR) mass spectrometry and electrospray ionization (ESI) provide the basis for the formation, isolation, and extended trapping of single highly charged DNA molecular ions with molecular weights well into the mega-dalton range. This new approach, termed single molecule analysis by mass spectrometry (SMAMS), will be explored utilizing new ESI-ICR instrumentation developed at PNL. Figure 1 gives a schematic illustration of the ICR instrumentation. The instrumentation consists of an ESI source interfaced to an external ion injection ICR instrument. Key features of the instrumentation include 1) a dual-stage capillary inlet ESI source; 2) a total of six differential pumping stages that allow for operating an atmospheric pressure ion source and an ultrahigh vacuum analyzer region;

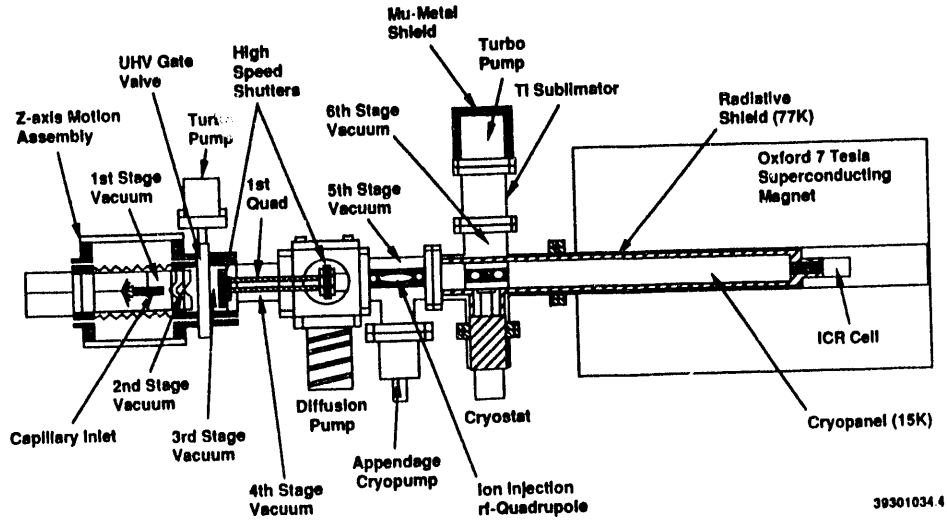

FIGURE 1. Schematic of the Electrospray Ionization - FTICR Instrumentation Developed at PNL

3) solenoid-driven mechanical shutters that block the molecular beam produced by the ESI source; 4) a unique cryobaffle located in the ICR cell region that is capable of pumping speeds for nitrogen in excess of 200,000 L/s; 5) an ultrahigh vacuum (UHV)-compatible pulsed valve used for trapping and cooling the injected ions as well as for collision-induced dissociation and ion-molecule reactions; and 6) a 7 Tesla superconducting magnet with a highly homogeneous magnetic field. With this system, an ESI mass spectra can be obtained for ions trapped in the ICR cell under conditions in which the effects of pressure do not degrade obtainable resolution (i.e., in the 10^{-10} Torr range).

Fourier transform ion cyclotron resonance (FTICR) mass spectrometry has the advantage of producing ultrahigh resolution mass spectra, and can provide ultrahigh precision mass measurements. It has been recently demonstrated that coupling ESI with FTICR can produce high resolution (>400,000) for proteins in excess of 12 kDa molecular weight. One factor that affects the attainable resolution in ICR is the transient lifetime, which is highly dependent upon the pressure in the ICR cell. For larger molecules, a transient lifetime of several seconds is necessary to obtain high resolution. At higher pressures, collisions with background gas can cause a dephasing of the ion packet and a rapid damping of the transient signal, resulting in shorter lifetimes and lower resolution. Therefore, UHV in the analyzer cell is needed to obtain longer transient lifetimes.

Applying ICR-MS to DNA sequencing will require obtaining high resolution and high mass measurement accuracy, developing appropriate ionization methods, and developing chemistry appropriate for sequencing. The high-resolution capability has now been established. Figure 2a gives a mass-to-charge spectrum obtained for bovine cytochrome c (average molecular weight = 12,231) in a 4:1 methanol:water mixture with 5% acetic acid. The charge state distribution ranges from 8+ to 11+; molecular ion charge states differ somewhat from ESI spectra acquired previously with quadrupole instrumentation. This appears to depend upon the trapping conditions used, i.e., an energy analysis inherent in the trapping process. Expanding about the $(M+10H)^{10+}$ ion, one observes the isotopic distribution for the molecular species of a particular charge state illustrated in Figure 2b. The measured mass resolution, $m/\Delta m$, is 111,000 with a full apodization applied to the transient, while the unapodized transient yields a resolution of 204,000.

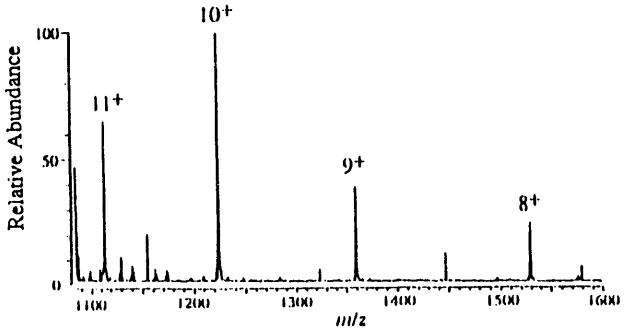

FIGURE 2a. Mass Spectrum for the Protein Cytochrome c Obtained Using FTICR. The spectrum was obtained from a single 200 msec injection and trap sequence.

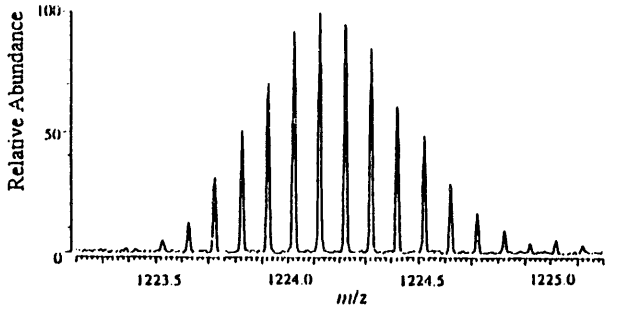

FIGURE 2b. The High Resolution Obtained for One Charge State (the 10+ Molecular Ion) from this Experiment, Demonstrating Resolution of More than 200,000

In conjunction with the instrumentation development, initial studies are being conducted of appropriate ionization methods for large DNA segments. Our current focus is to develop the methods necessary to trap and detect individual ions and to conduct sequential processes to obtain the sequence of extended DNA segments.

Radiological and Chemical Physics

Radiation Dosimetry

The primary goal of the Radiation Dosimetry program is to understand the connections between the physical events produced by ionizing radiation interacting with matter and the biological consequences of those events. These consequences result from complex sequences of reactions involving a variety of initial radiochemical products as well as the products of later chemical reactions and biological responses. However, differences in consequences occur when only the type of charged particle that deposits the energy is changed. This indicates that the spatial and temporal relationships of those initial products profoundly influence the subsequent reactions.

Dosimetry research attempts to provide realistic models of the physical processes and to combine them with information on likely chemical and biological reactions to produce models for response at the cellular level. The models are designed to be testable by experiments at each level of the system. Models of energy deposition along individual charged particle tracks have been used to calculate energy deposition in small volumes and the fraction of the energy deposited by track ends. Volumes a few nanometers in diameter, as well as those a few micrometers in diameter, appear to be directly relevant to the biological damage. Energy deposition in the larger volumes can be measured experimentally and used to test the validity of the calculations. The impact of the difference in energy deposition patterns in solids as compared to vapors is being investigated by calculating the spectrum of electrons ejected by collisions of ions with thin foils, a configuration which can also be measured experimentally.

In order to determine characteristics of the energy deposition patterns of different radiations that are relevant to the biological response, it is necessary to develop and test both phenomenological and mechanistic models that can be related to specific assumptions about the effects of energy deposition patterns and initial chemical products. As models are developed, data from the literature or from specific experiments conducted in the Radiation Biophysics program are used to determine if the model is applicable to a specific biological system. As inappropriate models are rejected, those that remain converge to form an acceptable description of the relevant damage and biological processes. The phenomenological models also can be applied more directly to calculate risk of environmental radiation exposure since they give direct predictions of effects which may be related to changes in the health of an organism. Although the phenominological and mechanistic models often emphasize different properties of the irradiation, it is important to assure that the two types of models are consistent in the areas where they overlap.

Implications of Hit Size Effectiveness in Radiation Protection

L. A. Braby

Evaluating the stochastics of energy deposition in small volumes such as cell nuclei and the biological effectiveness of different types of radiation show that average quantities such as dose and linear energy transfer (LET) are not a good way to describe low dose irradiations. Unfortunately, a consensus has not been reached on an ideal method for describing radiations, a method which would relate directly to biochemical mechanisms. This may be due to the evolving assumption that different aspects of ionization's spatial distribution are related to different types of biological damage. However, one group of phenomenological models based on the correlation between the energy deposited by single events in a spherical volume and the probability that a specific effect will be produced have been particularly successful (Varma et al. 1985). Models of this sort have been proposed by a number of different authors (Zaider and Brenner; 1985, Morstin et al. 1989), under a variety of different names, but will be referred to as "hit size effectiveness". In these

models, the energy deposition is generally expressed as lineal energy, y, in a 1-μm diameter volume.

It has been suggested that radiation protection should be formulated in terms of the fluence of charged particles rather than the dose, since at the doses of concern in radiation protection, the number of charged particle events per cell is generally small, and the variations from cell to cell may be responsible for much of the difference in the effect of different radiations. However, fluence alone is clearly an insufficient description of the radiation. The spectrum of the fluence as a function of some property of the radiation is required. Given the lack of a single property of radiation which can be related to all biological damage, and considering the success of hit size effectiveness functions for predicting effects at low doses, it seems appropriate to investigate the consequences of basing radiation protection on fluence as a function of lineal energy in 1-μm diameter sites.

First, it should be pointed out that converting to a fluence based system does not, in any way, change the amount of biological data available for estimating the biological effect of an irradiation. Decisions will still have to be made based on the same limited, and slowly growing, pool of data on the biological effects of different radiations and different exposure conditions. Furthermore, a change to a fluence based system does not automatically solve the problems of defining quantities which are both unambiguous and measurable. What the change would do is make the definitions that would be used in radiation protection consistent with the physical processes occurring at the relevant exposure levels. In other fields, such as radiation therapy, the exposure conditions are such that average quantities such as dose are consistent with the actual processes, and there is no need to change. Thus, fluence based risk estimation should be considered an addition to the list of techniques for characterizing an irradiation, rather than a replacement for conventional dosimetry.

For the purpose of risk evaluation, the important feature of a radiation field is the interaction of charged particles with sensitive biological cells. Thus, the natural tendency is to specify the radiation in terms of the fluence of directly ionizing particles in the tissue of concern. An alternative is to specify the radiation in terms of the incident fluence of directly and indirectly ionizing particles. Advantages and disadvantages exist in both of these approaches. Most radiation detection systems actually measure directly ionizing particles, but it is generally difficult to make the measurement in the tissue of interest. If, on the other hand, we specify risk in terms of the incident fluence, we have an uncertainty due to the differences in secondary particle distributions which will be produced in different irradiation geometries. Furthermore, it is difficult to measure the spectrum of some indirectly ionizing particles, especially when they are part of a mixture of radiations. However, if the lineal energy is specified as the variable, in order to make the correlation with hit size effectiveness, then the depth in tissue-like material (the detector wall thickness) as well as the site diameter must be specified. Thus, some compromise must be made. Specification of directly ionizing fluence seems to be preferable, in part because it can be calculated from the incident fluence if that is known, and it can be approached by relatively simple measurement techniques.

The average risk, R, which is the quantity which should be controlled by limiting radiation exposure, can be defined as $R = kr$. This is done to separate the two major areas where judgment is required to evaluate and apply the experimental data. The relative risk, r, is defined by

$$\bar{r} = \int_0^\infty n(y) y q(y) dy \qquad (1)$$

where y is the lineal energy, and q(y) is the specific quality function so that yq(y) is the hit size effectiveness function. The hit size effectiveness function will be determined from experiments, and possibly epidemiological data, for effect as a function of y. In general, a different function q(y) may emerge for each experimental system and endpoint. Thus, judgement is required to determine one

function which is representative of all endpoints of concern for radiation protection. This function will make it possible to calculate r for any irradiation where f(y) can be determined. The constant of proportionality, k, can be evaluated utilizing the data for human exposures to low LET radiations. Since nearly all of this data is for x and γ ray exposures (BEIR 1989), the first step is to calculate f(y) for these radiations. This can be done with good reliability when the radiation is well characterized in the conventional way (x-ray voltage, filtration, half-value layer, field size, irradiation geometry for backscatter calculation etc.). For each epidemiological situation where the average risk, R, and the relative risk, r, can be evaluated, an estimate of k can be determined. These estimates of k may differ from one study to another, and they may change as additional cases are reported. Judgement is again required to chose a representative value for k.

Thus, judgement must be exercised twice, in choosing a representative function q(y) which is satisfactory for all endpoints, and in selecting an appropriate value for k in order to assign an average risk, $R = kr$, to an occupational exposure. These are exactly the same judgment based decisions which have to be made in the present dose based radiation protection system. The quality factor has to be based on an acceptable representative function for relative biological effectiveness (RBE) as a function of LET. This takes into account the magnitude of the effect for different endpoints. Then, an acceptable dose equivalent has to be determined based on the risk observed in different epidemiological studies.

A change to a fluence based radiation protection system does not materially affect the data available for use in evaluating risk, nor does it necessarily result in any change in the radiation exposures which are judged to be acceptable. What it does do is change the emphasis in evaluating radiation exposures from "the effects of average energy depositions" to "the average effects of random energy depositions."

This change in emphasis will provide a much more realistic framework for evaluating dose rate effects and the interaction of radiation with other hazards in the workplace.

Track Ends

W. E. Wilson, L. A. Braby, and J. Song[a]

Researchers have speculated that the presumed high density of ionization and energy deposition at the end of secondary electron tracks, a so called "track end", may constitute a significant contribution of radiation of high relative biological effectiveness (RBE) character. In an attempt to investigate this speculation, we have simulated low energy electron tracks and are analyzing their energy and ionization depositions. Monoenergetic electrons of 0.5, 1, 2, 5, 7.5, and 10 keV have been simulated using Monte Carlo methods, and the number of track ends and the fraction of energy deposited by them and their secondaries per primary have been determined.

For each primary electron energy, the stochastics of the energy deposition were analyzed as a function of two energy parameters defined as thresholds. One energy threshold, E_t, defines the fraction of absorbed energy appearing as the presumed high linear energy transfer (LET) radiation in the track end; as the electron slows prior to degrading to E_t, all energy depositions are considered to be of low LET. The second energy parameter, E_b, defines a "branch track;" that is, a secondary electron generated with energy greater than E_b is assumed to be a separate low LET track entity until it degrades in energy to less than E_t, then becoming a track end. Thus, the number of track ends is one greater than the number of branch tracks.

Figure 1 shows the average number of branch-tracks per primary produced by primary electrons of 1 to 10 keV as a function of the threshold energy, E_b, defining a branch track. Generally, less than one branch-track is produced on average by each primary electron. Only for 10 keV primaries and a branch-track threshold of 300 eV or less does the frequency

(a) Visiting scientist, Institute of Biophysics, Chinese Academy of Sciences, Beijing, China.

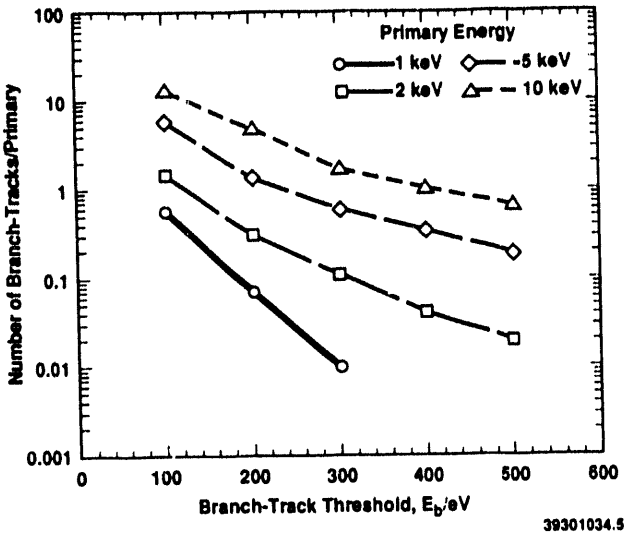

FIGURE 1. Number of Branch Tracks Produced by Low Energy Electrons as a Function of Threshold Energy, E_b. A secondary electron is considered a separate track entity, a branch track, if its initial energy exceeds E_b.

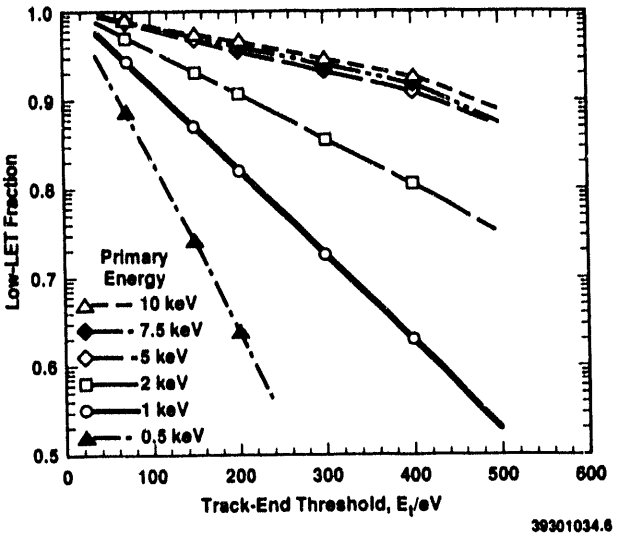

FIGURE 2. Fraction of Energy Deposited as Low-LET Radiation as a Function of Track-End Threshold, E_t. A track end is presumed to be high-LET radiation and distinguished from the low-LET portion of the fast electron track by the energy threshold E_t.

get much above one per track. These results indicate that electrons of 10 keV or less produce very few branch-tracks and thus few track-ends.

The fraction of energy deposited as low LET, that is, outside of track-ends, is shown in Figure 2 for the case E_b = 500 eV. The fraction is a linear function of track-end threshold, E_t. Furthermore, for those primary energies for which there is no significant number of branch-tracks, the slope of the function is essentially $1/E_0$, where E_0 is the primary electron energy; this is to be expected because if there are no branch-tracks, then the fraction of energy deposited "not in track-ends", F_{lo}, is simply given by

$$F_{lo}=(E_0-E_t)/E_0=1-E_t/E_0 \qquad (2)$$

With sufficient primary energy to produce a small number of branch tracks, F_{lo} remains large, at around 90%.

One can conclude that for electrons of energy $E_0 <= 10$ keV, less than 10% of the energy deposition appears as "track-ends." Instead, the energy deposition is mostly clustered along the meandering path of the primary electron.

References

Committee on Biological Effects of Ionizing Radiation (BEIR). 1989. "Effects of Ionizing Radiation," BEIR V report. National Academy of Sciences/National Research Council. National Academy Press, Washington DC.

Morstin, K., V. P. Bond, and J. W. Baum. 1989. "Probabilistic Approach to Obtaining Hit-Size Effectiveness Functions Which Relate Microdosimetry and Radiobiology." *Radiat Res.* 120, 383-402.

Varma, M. N., V. P. Bond, and G. Matthews. 1985. "Hit-Size Effectiveness Theory Applied to High Doses of Low LET Radiation for Pink Mutations in Tradescantia." *Radiat. Prot. Dos.* 13:307-309.

Zaider, M., and D. J. Brenner. 1985. "On the Microdosimetric Definition of Quality Factors." *Radiat. Res.* 103, 302-316.

Radiation Physics

The chemical and biological response to energy deposition by ionizing radiation is largely determined by the initial spatial and temporal pattern of excitation and ionization produced in the absorbing medium. These patterns are established through producing and slowing secondary electrons that define the structure of charged particle tracks. Studies in radiation physics focus on experimental and theoretical investigation of differential cross sections for secondary electron production by charged particles, with emphasis on charged particle energies and species representative of neutron-induced recoils in tissue and radon alpha particles. These studies provide quantitative information and insight into the processes of energy deposition by high-LET radiation. Mathematical models of energy degradation and transport are developed using these data to describe the initial pattern of energy deposition in representative biological media. Emphasis in the Monte Carlo modelling effort is on understanding the role of the heterogeneous nature of the cellular environment in the energy transport process.

Recent experimental studies have focused on differential cross sections for ionization by ions that possess bound electrons and on electron production and transport in foil targets following passage of fast protons. Theoretical work has also been continued, in collaboration with other investigators, to better understand the role of bound projectile electrons in collisional ionization of atomic and molecular targets. The results of our studies of electron production by charged particles are combined with literature data for Monte Carlo-based energy transport studies that focus on understanding the systematics of local energy deposition in molecular, cellular, and heterogeneous condensed phase systems. Knowledge of energy deposition processes and models of energy transport contributes to the ability to extrapolate observe biological effects as a function of dose, dose rate, and radiation quality.

Cross Sections for Partially Stripped Ion Impact

R. D. DuBois

Heavy ions traversing matter lose energy and slow due to coulomb interactions with bound electrons of the media. When the projectile velocity decreases to roughly that of the electrons in the media, target electrons can be captured into bound states of the projectile ion, thus reducing the net projectile charge. In subsequent collisions, additional electrons may be captured or those already captured may be ionized. Thus the projectile charge is a dynamically changing variable along the path of the ion. In stopping power studies, this phenomenon has led to the concept of an "average effective" ion charge for describing the average characteristics of energy loss as ions traverse matter. However, energy deposition is a stochastic process which means that Monte Carlo based track structure models must treat the energy loss "event-by-event." For these purposes, the concept of an average effective charge is inadequate because the amount of energy deposited depends on the charge and energy of the projectile ion for each event.

Thus, to provide an understanding of energy deposition by dressed particles, our latest research efforts have concentrated on studying electron emission as electrons are systematically added to a bare ion. During the past year, we have focussed on two aspects of this subject. We are primarily interested in how ionization cross sections scale as a function of the electron emission angle, the ejected electron energy, projectile velocity, charge and type. In addition, we have investigated the processes of energy deposition by neutral projectiles.

Scaling of Differential Ionization Cross Sections

R. D. DuBois, O. Jagutzke,[a] and R. Herrmann[a]

Electrons bound to a bare projectile ion tend to partially screen the nuclear charge z. For very distant interactions, the screening is rather effective, and, according to the Born approximation (McGuire et al. 1981), the cross sections are expected to scale according to the square of the net charge, i.e., as $(z - N)^2$, where N is the number of bound electrons. For interactions occurring within the orbitals of the bound electrons, the screening is negligible, and hence the cross sections should scale as z^2. The possibility also exists that the bound projectile electrons can directly interact with the target electrons; these interactions should scale as N. Where both the projectile nucleus-target electron and projectile electron-target electron interactions are important, an incoherent sum of their probabilities is required, i.e., the electron emission should scale according to $(z^2 + N)$.

Thus with respect to a bare nucleus, target ionization produced by a projectile possessing N bound electrons is expected to scale as Z_{eff}^2 where Z_{eff} ranges in value from z-N for distant collisions to z for close collisions or to $(z^2 + N)^{1/2}$ for situations where projectile electron-target electron interactions are also important. This concept has been formulated for total target ionization cross sections. We are investigating whether it can be applied to differential electron emission cross sections as well.

Using data previously collected in our laboratory for 0.5 MeV/u boron, carbon, oxygen and fluorine ions colliding with a helium target, we have determined Z_{eff} as a function of laboratory emission angle, Θ, and ejected electron energy, ϵ. Specifically,

$$Z_{eff}(\epsilon,\Theta) = [5\ DDCS(P^{q+})/DDCS(B^{5+})]^{1/2}. \quad (1)$$

Here DDCS(P^{q+}) represents the doubly differential cross section for electron emission induced by a projectile P with net charge +q. These data are compared to cross sections obtained for fully stripped boron in order to determine $Z_{eff}(\epsilon,\Theta)$. Note that a helium target was chosen in order to minimize multiple electron emission or inner shell ionization probabilities that might influence our interpretation of Z_{eff}.

Our values of Z_{eff} for oxygen ion impact are shown in Figure 1. In order to more conveniently compare results obtained for different angles of emission or impact velocity, Z_{eff} is plotted versus the emitted electron velocity in units of the incoming projectile velocity divided by cos(Θ), where the cos(Θ) term is added so that the binary encounter position occurs precisely at 2, independent of emission angle. In this way, scaling for "close collisions" but for different angles of electron emission can be compared more easily.

The data demonstrate that for small ejected electron velocities Z_{eff} is on the order of, and increases with, the net projectile charge, q, whereas for the fastest electron velocities, Z_{eff}

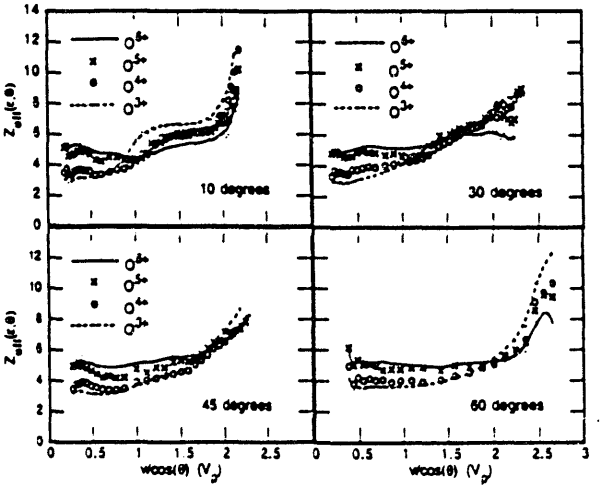

FIGURE 1. The Effective Charges for 0.5 MeV/u Oxygen Ions Interacting with a Helium Target as a Function of Electron Emission Velocity and Angle. The emission velocities are in units of the projectile velocity (V_p) divided by cosΘ in order to place the binary encounter peak at V = 2 for all angles.

(a) Institute for Nuclear Physics, The J. W. Goethe University of Frankfurt, Germany.

decreases as the net charge increases. This decrease for high-energy electron emission arises because binary collisions, which are important in this region, are related to target electrons elastically scattering off the incoming projectile. As the charge of the incoming projectile increases, the large-angle elastic scattering cross sections (in the projectile frame) decrease. This means that the small angle (lab frame) binary encounter contributions decrease as the net charge increases (Schultz and Olson 1991). Another interesting feature is that Z_{eff} for very fast electrons emitted in collisions involving partially stripped projectile impact can exceed z, the bare nuclear charge. In fact, the data demonstrate that they also can exceed $(z^2 + N)^{1/2}$.

In Figures 2 and 3, the behavior of Z_{eff} is investigated for distant and close collisions respectively. It was assumed that distant collisions lead primarily to the emission of slow electrons, e.g., scaled electron velocities <0.5, and close collisions are responsible for the emission of fast electrons, e.g., scaled velocities ≈ 2. For distant collisions, Z_{eff} scales rather nicely with the net projectile charge--independent of the projectiles tested (Figure 2) and of emission angle (Figure 1).

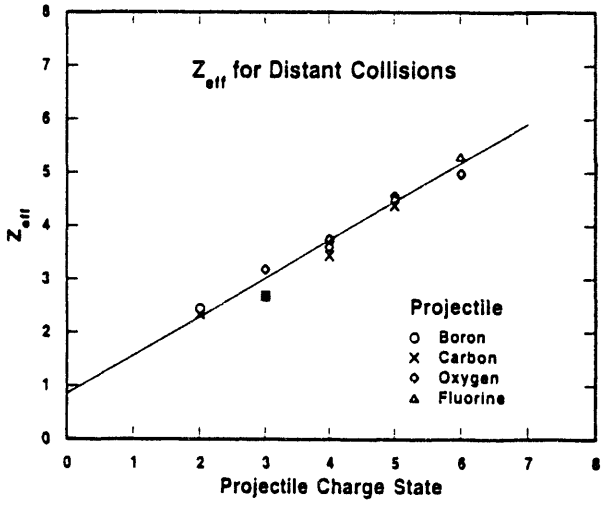

FIGURE 2. The Effective Charges Obtained for Distant Collisions, i.e., for Low Energy Electron Emission, for 0.5 MeV/u Ions Impacting on Helium

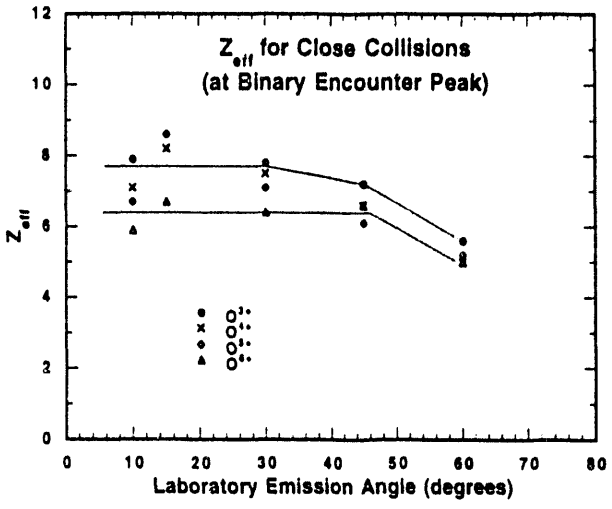

FIGURE 3. The Effective Charges for 0.5 MeV/u Oxygen Ions Impacting on Helium as a Function of Emission Angle. The charges were determined at the binary encounter peak (V = 2 in Figure 1).

Since low-energy electron emission is the dominant contributor to the total emission cross section, this independence of ejected electron cross sections on angle of emission and projectile type is why an average effective projectile charge may be successful when applied to stopping power measurements.

For close collisions, Figure 3 again indicates that Z_{eff} increases as the net projectile charge decreases. It also demonstrates that Z_{eff} is rather constant for smaller angles of emission, but decreases for larger angles of emission. As a preliminary explanation, we attribute this decrease to the fact that the binary peak (hard collision) intensity is rapidly decreasing with respect to the soft collision intensity as the angle of emission increases. Thus the decrease in Z_{eff} may indicate that the high-energy electron emission at 60° results primarily from distant interactions and that close binary collisions are playing a negligible role in producing high-energy electrons. Additional studies will indicate whether this assumption is correct.

Data for carbon ions colliding with helium were also collected at lower impact energies (25 to 150 keV/amu). Some of these data are shown

in Figure 4. This time Z_{eff} is plotted against the scaled ejected electron energies. Except for charge state 4, a nearly constant Z_{eff} is found in the 1 to 30 eV range. For higher electron energies, Z_{eff} increases to values on the order of, or slightly larger than, the nuclear charge of 6. A brief comparison of the data for 500 keV/amu and 150 keV/amu carbon impact indicates that Z_{eff} does not strongly depend on the impact energy. Data for additional energies and angles need to be evaluated to investigate this further.

Ionization by Neutral Projectiles

R. D. DuBois and S. T. Manson[a]

Researchers often assume that because no long-range coulomb forces exist, neutral projectiles produce little or no target ionization. Thus energy deposition models ignore projectile ions once they become neutralized. However, previous studies in our laboratory (DuBois and Köver 1989) have shown that total ionization cross sections for neutral hydrogen impact can be comparable to those resulting from proton impact. Also, collaborative studies (Heil et al. 1992) have shown that the differential electron emission cross sections resulting from fast H and He impact are non-negligible in magnitude.

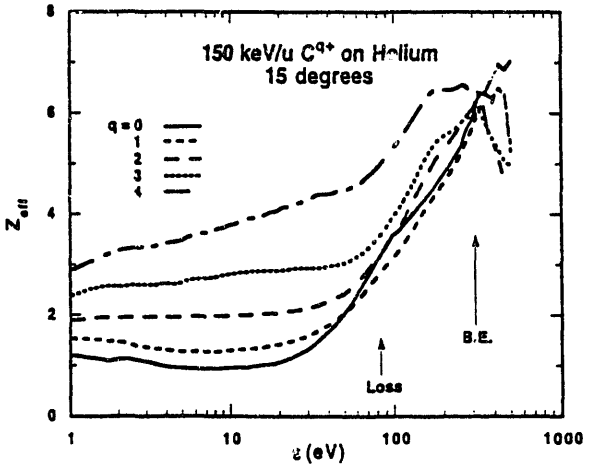

FIGURE 4. The Effective Charges for 0.15 MeV/u Carbon Ions Impacting on Helium as a Function of Electron Emission Energy. The data are for 15° laboratory electron emission angles.

In order to understand how neutral projectiles induce target ionization, a collaborative effort with S. T. Manson, Georgia State University, Atlanta, Georgia, has investigated the first Born approximation for collisions involving dressed ions. For fast collisions involving dressed particles, the dominant process is simple target (or projectile) ionization, i.e., ionization of one of the collision partners with the configuration of the other remaining unchanged. This process results from a first-order interaction between the electron that is ejected and the nucleus of the collision partner, which we designate as the e-n process. However, first order interactions between target electrons and projectile electrons, which lead to ionization-excitation of the collision partners, can also be important.

For example, for fast neutral particles with N electrons in a single occupied electron subshell, e.g., H and He projectiles, the doubly differential cross section (DDCS) for ionizing a target via the e-n process is given by the following equation (Manson and DuBois 1992):

$$\sigma(\epsilon)_{e-n} = \int A(\epsilon,K)\ [|Z - N\,F(K)\,|^2]dK. \quad (2)$$

The DDCS for the projectile electron-target electron process, i.e., for ionizing the target and simultaneously exciting the incident particle, is given approximately by the following equation (Manson and DuBois 1992):

$$\sigma(\epsilon)_{e-e} = \int A(\epsilon,K)\ [N - N\,|F(K)|^2]dK. \quad (3)$$

In this formulation, all information about the target is contained in $A(\epsilon,K)$, where the term in brackets contains information about screening the incident particle's nuclear charge by its bound electrons, ϵ is the energy of the ejected target electron, $\hbar K$ is the momentum transfer, and F(K) is the single electron form factor for the initial state of the projectile, $|\ i\ >$. F(K) is given by

(a) Department of Physics and Astronomy, Georgia State University, Atlanta, Georgia.

$$F(K) = \langle i \mid e^{iKr} \mid i \rangle. \quad (4)$$

By definition, | F(K) | is bounded by 1 and 0 as K -> 0 and ∞, respectively. This corresponds to low- and high-energy electron emission, i.e., to large and small impact parameter collisions.

In evaluating the relative importance of the e-n and the e-e interactions, note that the major difference between $\sigma(\epsilon)_{e\text{-}n}$ and $\sigma(\epsilon)_{e\text{-}e}$ is due to the terms in brackets, which we refer to as $[]_{e\text{-}n}$ and $[]_{e\text{-}e}$ respectively. For neutral projectiles, Z = N, and $\sigma(\epsilon)_{e\text{-}n}$ is proportional to [| N - N F(K) | ^{2}] while $\sigma(\epsilon)_{e\text{-}e}$ is unchanged. Hence, the first Born formulation predicts that for distant collisions involving target ionization by neutral projectiles, the e-e interactions will dominate the electron emission cross section. This is because distant collisions mean that F -> 1 and hence $[]_{e\text{-}e}/[]_{e\text{-}n}$ -> ∞. Since low-energy electron emission is the major contributor to the total target ionization cross section, e-e interactions also dominate the total ionization cross sections. Experiments are in progress to confirm these predictions and to identify exactly where, and how important, these electron-electron processes are.

References

DuBois, R. D., and A. Köver. 1989. "Single and Double Ionization of Helium by Hydrogen-Atom Impact." *Phys. Rev. A* 40:3605.

Heil, O., R. D. DuBois, R. Maies, M. Kuzel, and K-O Groeneveld. "Ionization in Fast-Neutral-Particle-Atom Collisions: H and He Atoms Impacting on He." 1992. *Phys. Rev. A* 45:2850.

McGuire, J. H., N. Stolterfoht, and P. R. Simony. 1981. "Screening and Antiscreening by Projectile Electrons in High-Velocity Atomic Collisions." *Phys. Rev. A* 24:97.

Manson, S. T., and R. D. DuBois. 1992. "Multielectron Transitions Resulting from Interactions Between Target and Projectile Electrons in Ionizing Collisions." *Phys. Rev. A* R6773-6.

Schultz, D. R., and R. E. Olson. 1991. "Binary Peak Enhancement and Structure in Partially Stripped Ion-Atom Collisions." *J. Phys. B* 24:3409.

Secondary Electron Emission from Thin Foils

C. Dexler[a] and R. D. DuBois

In order to provide experimental information about electron production and transport in condensed phase media, a year ago we assembled and tested an apparatus for investigating proton-induced electron emission from thin carbon foils. Briefly, it consists of a pulsed proton beam interacting with a thin carbon foil positioned perpendicular to the beam direction. Electrons ejected from the foil are energy analyzed using time-of-flight (TOF) techniques. The TOF spectrometer can be rotated in order to investigate electrons emitted between 15 and 165° with respect to the proton beam direction. Preliminary data were reported in this publication last year.

During the past year, additional studies were undertaken. These studies indicated that contamination of the foil surface by adsorbed molecules from the residual gases inside the vacuum chamber constitute a more serious problem than originally anticipated. As an example, Figure 1 shows the differential electron yield (electrons/proton/solid angle) measured at 135° for 2 MeV proton impact. The various curves were accumulated in succession as gas molecules slowly adhered to the surface. Although we had no direct means of verifying the initial surface conditions, we assume that the foil was free of adsorbed gases initially since we baked the foil at 200 to 300°C for 24 hours and then immediately (within a few seconds) begin our measurements of the electron emission. As Figure 1 indicates, over a period of time the low-energy electron yield increases dramatically, and also the maximum of the distribution moves to

(a) GSF-Institute für Strahlenschutz, Neuherberg, Germany.

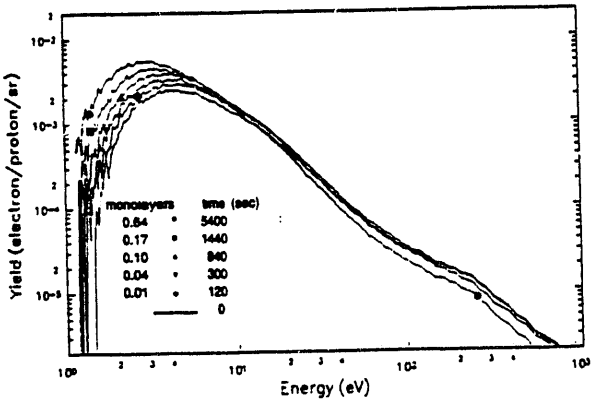

FIGURE 1. The Electron Yield (electron/proton) for 135° Electron Emission from a Thin (5 $\mu g/cm^2$) Carbon Foil Resulting from 2 MeV Proton Impact. The yields demonstrate how surface contaminants influence the yield.

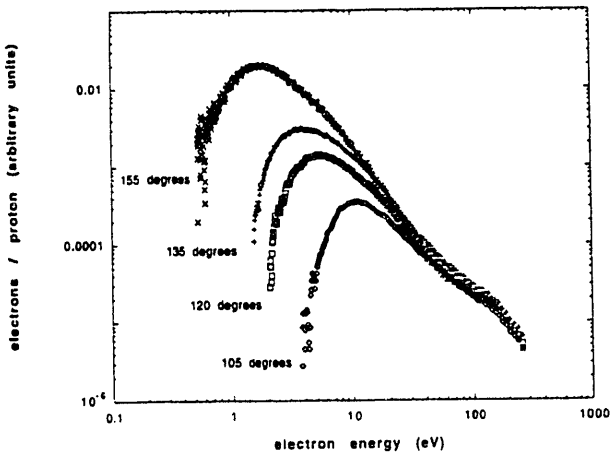

FIGURE 2. The Electron Yield as a Function of Emission Angle for 1 MeV Proton Impact on a 5 $\mu g/cm^2$ Carbon Foil

lower electron energies. Also note that the high-energy electron yield decreases over a period of time.

The increase in yield of low-energy electrons is attributed to gas molecules, primarily O_2, being adsorbed on the surface. Using the measured chamber pressure, 2 x 10^{-9} Torr in this case, and assuming that all oxygen molecules striking the surface adhere to it, the number of monolayers of oxygen on the surface were calculated and is indicated in the figure. Clearly, surface contamination exceeding a fraction of a percent of a monolayer is unacceptable for reliable yield measurements. With present vacuum limitations, we are limited in the time that a "clean" surface can be investigated to approximately 1 minute. A low-energy ion sputtering gun has been purchased in order to more easily and consistently produce a clean surface for investigation. Also, efforts are in progress to improve the chamber vacuum and thus to extend the time available for analysis before surface contamination becomes a problem.

In spite of our limitations in maintaining a clean surface, we were able to acquire some information about the differential electron yields as a function of angle of emission. These are shown in Figure 2. We find that electrons emitted more parallel to the foil surface have dramatically smaller yields, particularly for lower emission energies, than do electrons emitted more perpendicular to the surface. One possible explanation for this is due to the image charge formed within the foil.

A Stochastic Model of Ion Track Structure[a]

W. E. Wilson and H. G. Paretzke[b]

Experts in the field generally accept that the initial spatial distribution of energy depositions is a crucial factor determining the relative biological effectiveness of high linear energy transfer (LET) radiations. The initial spatial pattern provides the starting conditions for the subsequent biochemical processes leading to radiation damage. For this reason, the microscopic dosimetry of heavy ion tracks has been a subject of considerable experimental and theoretical interest for two decades. Much of the theoretical modeling effort (Chunxiang, Dunn, and Katz 1985) has focused on the *average* radial dosimetry, ignoring the stochastic effects inherent in producing and transporting energy by secondary electrons (delta-rays).

(a) A poster presented at the 11th Microdosimetry Symposium, Gatlinbutg, TN, 12-18 September 1992, accepted for publication in Radiation Protection Dosimetry.

(b) GSF-Institut für Strahlenschutz, D-8042, Neuherberg, FRG.

These effects can become quite significant for nanometer-sized targets. The following examples illustrate how numerical evaluation of the model can provide an estimate of straggling and delta-ray transport effects in nanodosimetry problems.

Ion track structure can be simulated by Monte Carlo methods and the results used to calculate energy deposition distributions around the ion path, but efforts are generally limited to bare ions owing to a dearth of suitable heavy-ion cross sections. We have performed extensive computer calculations of proton track structures using the detailed-histories Monte Carlo code MOCA14 to obtain the probability density functions (PDF) for ions passing through (Wilson, Metting, and Paretzke 1988; Wilson and Paretzke 1988) and near the region of interest[a,b] and described the results with empirical analytic functions for convenient application.

Because energetic delta-rays are infrequently produced by MeV protons, enhanced scoring methods were required, especially for radial distances near the maximum delta-ray range. To achieve acceptable statistical accuracy, scoring was done at multiple positions for each track. Logarithmically distributed bin widths were used in scoring the energy and ionization density distributions for each site in order to cover a wide dynamic range in parameter values with a minimum computer-memory requirement. Site diameters for which results were computed were 2 to 100 nanometers for ion energies of 0.3 to 20 MeV. The empirical fitting of the simulated PDFs to arrive at the phenomenological model is described in detail in the symposium proceedings[c] and therefore is not repeated here.

The stochastic ion track model predicts the PDF in ionization number or alternatively, in energy imparted as a function of radial distance from the ion path. One can numerically integrate the model PDFs over radial distance to obtain a prediction of the PDF for a broad beam of monoenergetic ions. The results for 1-MeV protons for the site sizes of 2 to 100 nanometers are shown in Figure 1. The integration in this instance converged very rapidly beyond four site radii. For the larger site sizes, the calculated probability density distributions exhibit the expected increase at small values of energy imparted arising from delta-ray effects (ICRU 1983). This effect has been observed experimentally, but for larger sites.

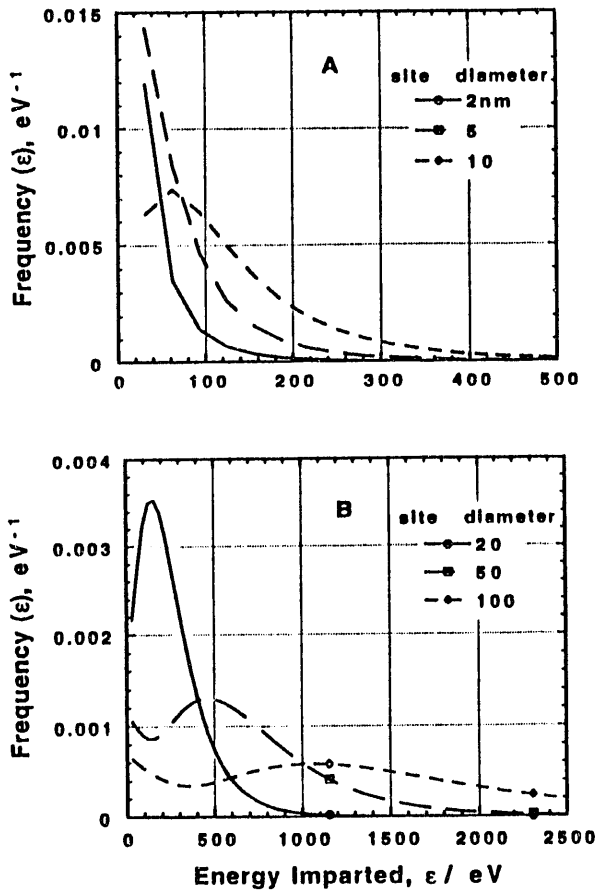

FIGURE 1. Model Calculations of the Probability Density in Energy Imparted for a Uniform Broad Beam of 1-MeV Protons Irradiating Sites of 2 to 100 Nanometers Diameter

(a) W. E. Wilson. "On the Stochastics of the Ion Penumbro" (submitted for publication).

(b) W. E. Wilson and H. G. Paretzke. "Microdosimetric Aspects of 0.3 to 20-Mev Proton Tracks: II Touchers" (in preparation).

(c) W. E. Wilson and H. G. Paretzke. "A Stochastic Model of Ion Track Structure." *Radiat. Prot. Dosim.* (accepted for publication).

Alternatively, one can integrate the model PDFs over ionization number to obtain the probability for an ionizing event as a function of radial distance. This was done, again for 1-MeV protons, and the results are shown in Figure 2. Except for the 2-nanometer site, the probability is 1, that is, a certainty, that the site will experience an ionization by a crosser. At a radial distance equal to the site radius, the probability drops abruptly and then monotonically decreases until near the maximum delta-ray range. For the 2-nanometer site, the probability for an ionization by a crosser is less than 1 simply because the dimension of the site is comparable with the mean-free-path for ionization by 1-MeV protons, and thus the proton may pass through such a small site without producing ionization within it.

References

Chunxiang, Z., D. E. Dunn, and R. Katz. 1985. "Radial Distribution of Dose and Cross Sections for the Inactivation of Dry Enzymes and Viruses." *Radiat. Prot. Dosim. 13:215-218.*

International Commission on Radiation Units (ICRU). 1983. "Microdosimetry," Report 36. Washington, DC.

Wilson, W. E., and H. G. Paretzke. 1988. "An Analytic Model for Ionization Distributions Produced in Nanometer Volumes by Recoil Protons." *Radiat. Prot. Dosim.* 23:45-47.

Wilson, W. E., N. F. Metting, and H. G. Paretzke. 1988. "Microdosimetric Aspects of 0.3 - 20-MeV Proton Tracks: I. Crossers." *Radiat. Prot. Dosim.* 115:389-402.

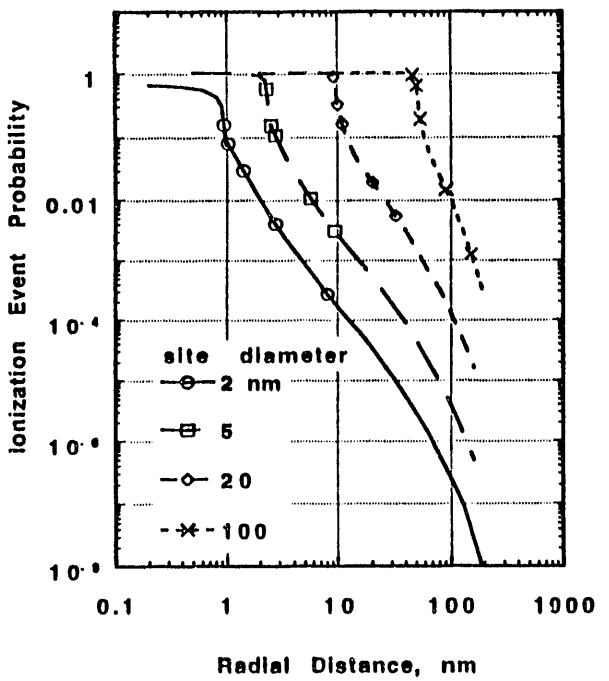

FIGURE 2. Ionization-Event Probability for 1-MeV Protons Passing at Various Distances Through or Near Simulated Absorbers of 2 to 100 Nanometers Diameter. The probability becomes very small at the range of the maximum energy delta ray.

The Stochastics of the Positive Ion Penumbra[a]

W. E. Wilson

It is generally accepted that the initial spatial distribution of energy depositions is a crucial factor determining the relative biological effectiveness of high linear energy transfer (LET) radiations. The initial spatial pattern provides the starting conditions for the subsequent biochemical processes leading to radiation damage. For this reason, the microscopic dosimetry of heavy ion tracks has been a subject of considerable experimental and theoretical interest for two decades. The experimental studies fall into two general categories, those that focus on average dosimetry quantities and those that measure stochastic properties as a function of radial distance from the path of the ion. The experimental work has inspired an extensive theoretical modeling effort focused primarily on the *average* radial dosimetry (Waligorski et al. 1986). Ion track structure can be simulated by Monte Carlo methods and the results used to calculate energy deposition distributions around the ion path (Waligorski et al. 1986; Wilson 1988), but efforts are limited to bare ions owing to a dearth of suitable heavy-ion cross sections.

(a) A paper describing this work by this title was submitted for publication.

That a statistical treatment of the ion penumbra is ultimately required is evident when one considers the cross sections for producing energetic secondary electrons (Wilson et al. 1984; Miller, et al. 1987); it is a simple matter to estimate the mean-free path for inelastic collisions producing energetic delta rays. Consider,

$$1/\lambda_\Delta = n\int_\Delta^{w_{max}} \sigma(w)dw \qquad (1)$$

where $\sigma(w)$ is the single differential cross section for ejecting ionization electrons of energy between w and w + dw (Wilson et al. 1984; Miller et al. 1987), w_{max} is the kinematic maximum energy that an ion can transfer to the electron, and n is the number of target molecules per unit volume. λ_Δ is then the mean free path for producing secondary electrons with energy, $w \geq \Delta$. This quantity was calculated for 1-MeV protons in unit density water vapor, and the result is shown in Figure 1. From this, one can conclude that the mean free path for producing secondary electrons of 500 eV or greater (short tracks) is about 200 nm (0.2 microns), and for 200 eV and greater (blobs plus short tracks), it is about 65 nm in unit density tissue. The effect of this is depicted by the example in Figure 2 of a Monte Carlo simulation of a segment of a 1 MeV proton track. Two energetic delta rays (short tracks) are shown, one of almost 1 keV in energy, the other slightly over 500 eV; their separation is nominally 250 nm, much longer than their combined ranges. The short tracks in this example do not overlap, so averaging their energy deposition does not tell the whole story. A complete model of the ion penumbra should allow for the stochastic nature of the *individual* delta rays.

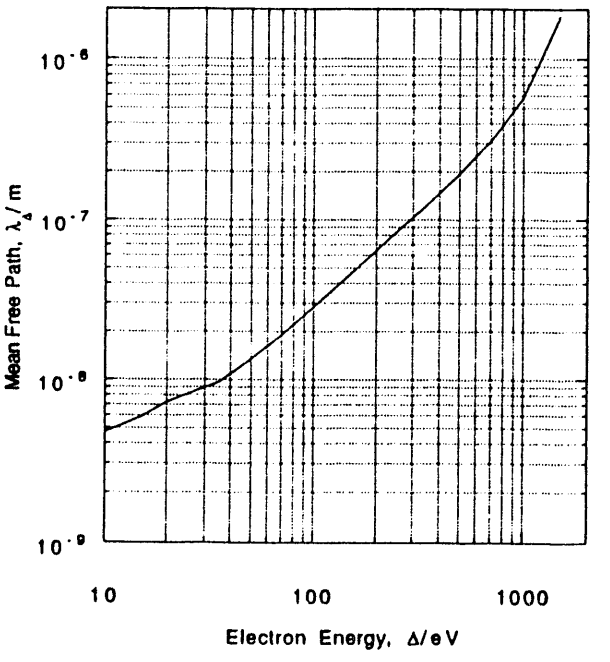

FIGURE 1. Mean-Free-Path, λ_Δ, for the Production by 1-MeV Protons of Delta-Rays Having Energy Equal to or Greater Than Δ. The mean-free-path was obtained by numerically integrating the single differential cross section for secondary electron production (3,4).

This work extends our previous Monte Carlo calculations of proton track structure (Wilson et al. 1988), for 1-Mev protons whose paths pass outside the region of interest and therefore deposit energy only by delta ray transport; such events have been referred to as "touchers" (ICRU 1983; Harder and Blohm 1984). Since energetic delta-rays are produced infrequently, and they are therefore relatively far apart, the probability that a site will experience any energy deposition at all is most often quite small. In this study, normalization of differential frequency distributions is on a unit fluence or per track basis except where specifically noted otherwise. The absolute probability for a proton to deposit energy via

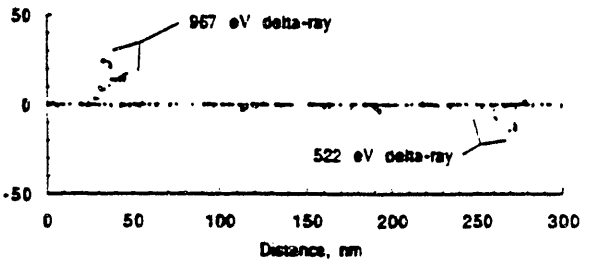

FIGURE 2. Segment of Simulated 1-MeV Proton Track. Two delta-ray short tracks are shown, one of 967 eV and another of 522 eV energy, separated by approximately 250 nanometers. The mean-free-path for production of short tracks by 1 MeV protons is about 200 nanometers. The interaction transfer points are projected onto the plane of the figure.

delta-rays is determined directly from the output of the simulation and is called the delta-ray event probability (DEP). The radial-distance dependence of the DEP is a primary topic of this study. Secondly, the density distributions for energy imparted and for ionization number and their moments are presented.

The ion track simulation method was described previously (Wilson et al. 1988). The detailed history Monte Carlo code MOCA15 simulated the delta-ray field around proton tracks that were restricted to pass outside the absorber region of interest.

Since very energetic delta-rays are produced infrequently, and the DEP is small, enhanced scoring methods were required, especially at radial distances near the maximum delta-ray range. To achieve acceptable efficiencies, scoring was done at multiple positions for each track. Rings of sites were defined at several radii and individually scored; distributions obtained for positionally equivalent members of the ensemble were then combined. In this way, more information was obtained from each track. Logarithmically distributed bin widths were used in scoring the energy and ionization density distributions for each site in order to cover a wide dynamic range in parameter values with a minimum computer-memory requirement. Single-event distributions for energy imparted and ionization number were computed for radial distances until the absolute probability for any deposition fell to less than about 10^{-5}. Site diameters for which results were computed were 2 to 100 nanometers for an ion energy of 1 MeV. Statistical sample sizes typically were 10^5 to 10^6 tracks depending on site size.

The probability that a site experiences any energy deposition at all due to delta-ray transport is very small. It was found that the probability is proportional to the solid angle subtended by the site at its point of closest approach. The functional dependence of the conditional frequency density distributions in energy imparted and in ionization number is approximately exponential, and their first and second moments were found to be largely independent of radial distance.

These results provide an explanation for why the average dose about an ion track varies as the inverse square of the radial distance from the ion path. Energy deposited at a distance from the ion path is produced, by and large, by a single delta-ray. Therefore, the fluence will behave geometrically as if from a point source rather than from a line source. Given that the delta-ray arrives at the site and interacts, the average deposition (first moment) is constant, so no additional radial-distance dependence is introduced. The average dose is proportional to the quotient of two quantities, one is the probability that some energy is deposited, which varies as $1/r^2$, the other is the (conditional) average energy deposited, which is independent of radial distance.

References

Harder D., and R. Blohm. 1984. "Microdosimetric Characterization of Photon and Electron Radiations." *Radiat. Prot. Dosim.* 9:171-174.

International Commission on Radiation Units and Measurements (ICRU). 1983. Report 36. Washington, D.C.

Miller, J. H., W. E. Wilson, S. T. Manson, and M. E. Rudd. 1987. "Differential Cross Sections for Ionization of Water Vapor by High-Velocity Vare Ions and Electrons." *J. Chem. Phys.* 86:157-162.

Waligorski, M.P.R., R. N. Hamm, and R. Katz. 1986. "The Radial Distribution of Dose Around the Path of a Heavy Ion in Liquid Water." *Nucl. Tracks Radiat. Meas.* 11:309-319.

Wilson, W. E., N. F. Metting, and H. G. Paretzke. 1988. "Microdosimetric Aspects of 0.3- 20-MeV Proton Tracks: I. Crossers." *Radiat. Res.* 115:389-402.

Wilson, W. E., J. H. Miller, and L. H. Toburen. 1988. "Differential Cross Sections for Ionization of Methane, Ammonia, and Water Vapor by High Velocity Ions." *J. Chem. Phys.* 80:5631-5638.

Radiation Biophysics Program

The Radiation Biophysics Project provides experimental radiobiological data to test currently evolving theoretical models of the molecular and cellular effects developing in the Radiation dosimetry and Modeling Cellular Effects programs. These studies address predictions of mechanistic mathematical models that relate endpoints such as damage produced at the molecular level, structural alterations of DNA, mutation, transformation, cell inactivation, and the kinetics of damage production and removal to their initiating physical energy-deposition events. Experiments are designed specifically to provide information on radiation response in areas where modeling studies suggest such measurements will have the greatest impact to facilitate distinguishing between different basic concepts of damage production and expression in macromolecules. Plasmid and genomic DNA are irradiated under specific conditions of dose, dose rate, and radiation quality. The damage produced is then identified, quantified, and evaluated to determine the relative sensitivity of the DNA molecule, of specific DNA sequences, and of macromolecular structures to formation of that damage. Data so derived provides information relating lesion formation, distribution, and type to the structure of the target DNA molecule.

Studies of initial damage and the effects of biological processing of that damage are studied in carefully defined cultured mammalian cells, irradiated under controlled conditions and allowed different opportunities for damage alteration or removal. These studies provide a means of evaluating the cellular mechanisms upon which cellular-effects models are based. A variety of techniques provides the detail and precision required to distinguish between mechanisms predicted by different cellular-effects models. Experimental data is integrated into improved biophysical and biochemical models, and this helps focus attention on new or alternative mechanisms to be tested.

Plasmid Structure and Spontaneous Strand Separation

J. M. Nelson, E. W. Fleck, J. H. Miller, and M. Hristova

Although the initial physical interaction and deposition of energy are entirely random, the distribution of biologically important lesions, e.g., single- and double-strand breaks with the subsequent loss of genetic material, is certainly not. Double-strand breakage of the DNA molecule, with the concurrent rearrangement, substitution, or deletion of information, appears to be the most significant radiation induced lesion associated with cellular radiation effects.

DNA plasmids are covalently bound circular molecules of naked DNA having defined primary and higher-order structures. They are particularly useful for studying the induction of strand breaks (in particular, the first single-strand break) because they are not associated with stabilizing proteins as is genomic DNA, and their structural alteration can be relatively easily identified.

We previously demonstrated a positive correlation between negative supercoiling and the susceptibility of pristine plasmid DNA to the induction of its first single-strand break by ionizing radiation (Miller et al. 1991). We then attempted to determine if the site of this breakage was dependent on the molecular architecture, and if it was most likely to occur in a region of the molecule particularly rich in adenine (A) and thymidine (T) bases, where transient strand separation is most likely.

Since single-stranded DNA has been shown to be more fragile than double-stranded DNA, we hypothesized that the position of this first break in a pristine supercoiled molecule might coincide with that region most susceptible to spontaneous transition from duplex to single-strandedness. Transient disruptions of base pairing in plasmid DNA would be associated

with the torsional stress of negative supercoiling, and consequently, we would expect that increased superhelicity would increase the probability of denaturation within the AT-rich sequences. Therefore, if open states are involved in the increased sensitivity to radiation induced strand scission observed in underwound plasmids, then at least part of this increase should be due to nonrandom breakage at the AT-rich regions.

Theory also predicted that the probability of denaturation will increase with temperature and decrease with the ionic strength of the buffer in which the molecules are irradiated. Last year we investigated this hypothesis by assessing nonrandom break induction in the pIBI-30 plasmid, and our early findings indicated that preferential breakage does indeed occur at the most probable site, as hypothesized. In these preliminary experiments, plasmid preparations were irradiated with doses of X-rays sufficient to produce only about one single-strand break per molecule, and although they showed that scission occurred first within an AT-rich region, they could not affirm a correlation between the enhanced probability of strand scission and strand separation within this region.

Using Mung-bean nuclease and five different restriction enzymes, we have now demonstrated that spontaneous single-strandedness occurs naturally in the AT-rich region identified from theoretical determinations based on primary structure, between bp 2000 to 2050. Under optimum conditions, Mung-bean nuclease cuts only one of the two strands of DNA within single-strand or denatured regions. The location of these nicked single-stranded regions is then determined by cutting the nicked plasmid at a specific location with a restriction enzyme which recognizes a unique site on the molecule. We used five different restriction enzymes which uniquely cut the pIBI-30 plasmid at distinctly different sites: EcoR1 @ 276, Hind3 @ 336, Dra3 @ 772, Xmn1 @ 1313, and Sca1 @1432. Each of these should produce fragments of specific lengths if the nuclease nicked the molecule at only one site (or within a single region). As can be seen in Table 1, the lengths of the fragments observed were virtually identical to the lengths predicted for nicking within the AT-rich region around bp 2000.

Mung-bean nuclease has been shown to cut only one of the two DNA strands. In our first experiments we then cut the second strand with another nuclease that cuts only RNA and single-stranded DNA. In the course of these experiments, we learned that Mung-bean nuclease will cut both strands, given sufficient time and under slightly more aggressive digestion conditions. Thereafter, the second nuclease digestion was not done.

These experiments have shown us that the native supercoiled plasmid is naturally single stranded, at least part of the time, and at a location which corresponds precisely with that location where we observed enhanced radiation-induced strand scission (Nelson et al. 1992). Experiments in which plasmid DNA is subjected to Southern-blotting methods coupled with ^{32}P end-labelling procedures are underway, but results of these experiments have not yet corroborated the earlier studies.

Our experiments will continue, as there still remains the question of whether the single-strand region is simply a denatured region or one of the single-strand portions of a cruciform structure.

References

Miller, J. H., J. M. Nelson, M. Ye, C. E. Swenberg, J. M. Speicher, and C. J. Benham. 1991. "Negative Supercoiling Increases the Sensitivity of Plasmid DNA to Single-Strand Break Induction by X-rays." *Int. J. Radiat. Biol.* 59(4):941-949.

Nelson, J. M. 1992. "Base Composition and the Probability of Radiation Strand Scission." In *Pacific Northwest Laboratory Annual Report for 1991 to the DOE Office of Energy Research, Radiation Biophysics*. PNL-8000, Part 4. Pacific Northwest Laboratory, Richland, Washington.

TABLE 1. Predicted and Observed Fragment Sizes from Mung-bean Nuclease Treated pIBI 30 DNA. Size determinations were made from band positions after separation by gel electrophoresis of pIBI 30 DNA digested first with Mung-bean nuclease and then with one of the restriction enzymes listed in the first column.

Restriction Enzyme	Recognition Site in pIBI 30	Predicted Fragment Size[a]	Observed Fragment Size
Hind III	336	1689 (1664-1714) 1237 (1212-1262)	1725 and 1700 1160 and 1100
Dra III	772	1253 (1228-1278) 1673 (1648-1698)	1250 and 1300 1675 and 1550
Xmn I	1313	2214 (2189-2239) 712 (687-737)	2060 700 and 775
Sca I	1432	2333 (2308-2358) 593 (568-618)	~2300 ~550 and ~600
EcoR I	266	1759 (1734-1784) 1167 (1142-1192)	~1700 and ~1800 ~1100 and ~1200

(a) The fragments in parentheses represent sizes based on Mung-bean nuclease cut sites at the limits of the predicted single-stranded region.

Isolation and Radiation Sensitivity of DNA-Synthesis-Deficient CHO Double Mutants

B. S. Jacobson

Double mutants of Chinese hamster ovary (CHO) cells deficient in both the hypoxanthine guanine phosphoribosyl transferase (HPRT) gene and the thymidine kinase (TK) gene have been isolated in order to investigate their radiation response. These mutants are unable to recycle either guanine or thymine through the "salvage pathway" of DNA synthesis, but are resistant to guanine and thymidine analogues which prevent growth in normal cells. The salvage pathway could play a role in repairing radiation damage.

In order to obtain such mutants, it was necessary to have a culture of cells which are mutant at either locus, yet functionally heterozygous or hemizygous at the other. Three CHO cell lines that meet this requirement were obtained from the University of Texas Cancer Center in Smithville. The parent strain of this group is hemizygous or heterozygous at three salvage loci (specifically, APRT, HPRT, and TK). In addition, we have received fully functional HPRT and TK mutants derived from this strain. The substrain, designated AT3-2bu, is homozygous for TK deficiency; that designated AT3-2tg is HPRT-deficient.

Using the method previously used here, we obtained no naturally occurring HPRT-TK double mutants from the homozygous TK-deficient culture out of 300,000 cells plated. However, by challenging the cells with trifluorothymidine (TFT), 75 apparent double mutants, by the criterion of TFT resistance, were obtained from 300,000 HPRT-deficient cells. Four single-colony isolates from this group of double mutants were successfully tested for stability prior to investigating their radiation response. All of the double mutants grow more slowly than either the original parent AT3-2 cells or the HPRT single mutant from which the double mutants were isolated.

Irradiations were performed using single doses of 250 kV x rays, given at 1.0 Gy/min. Ten-percent survival doses for these three lines were 5.2 Gy, 5.0 Gy, and 4.6 Gy, respectively. The small differences are not considered significant. Apparently, the double mutants respond in a normal fashion to single radiation doses, despite their slower growth and reduced plating efficiency. Experiments are under way

to obtain data for split doses by measuring split-dose repair parameters. Studies with ultraviolet-light irradiations are also planned.

Modeling Cell Effects

This project contributes to the understanding of health risks from exposure to ionizing radiation through studies of interactions of swiftly moving ions and electrons with the genetic material of mammalian cells. Two general types of interaction can be distinguished: 1) direct action in which the electric field of charged particles slowing down in the cell produces excitations and ionizations in critical macromolecular structures (DNA, nucleosomes, chromatin fiber, etc.) and 2) indirect action in which energy deposited in the aqueous cellular medium produces free radicals that diffuse to macromolecular structures and induce chemical changes.

Ionization cross sections that are differential in the energy of secondary electrons are needed for analyzing the direct effect of radiation on cellular genetic structures because the amount of energy imparted to the ejected electron plays an important role in determining the nature of direct damage. Most ionizations produce low-energy secondary electrons that geminately recombine with the sibling hole or become trapped very close to it. More energetic secondary electrons can migrate a considerable distance before they are trapped and thereby transmit the biological effects of ionization away from the initial sites of energy deposition. Work in FY-1992 on secondary-electron energy spectra included extending our semiempirical model to systems with more than one electronic shell and formulating a model of DNA ionization that allows for dielectric screening by the solvent. Research on the indirect mode of radiation-induced DNA damage focused on conformational changes resulting from hydroxyl-radical attack on DNA bases.

Semiempirical Model of Differential Ionization Cross Sections for Multishell Atoms and Molecules.

J. Miller, C. Stigers,[a] *and S. Manson*[b]

The energy spectrum of secondary electrons plays a key role in determining the effects on the stopping medium of energy absorbed from ionizing radiation. Hence, accurate differential ionization cross sections are useful in several areas of applied science including plasma physics, atmospheric studies, and radiation therapy. Cross-section data over a broad range of projectile velocities are needed over the full spectrum of secondary electron energies. This need is rarely satisfied by experimental measurements alone; therefore, both *ab initio* quantum calculations and semiempirical models of differential ionization cross sections continue to make contributions to this field.

Work on this project has emphasized semiempirical methods that have the potential for application to both gaseous and condensed absorbing media. The same basic principles of secondary-electron production apply to both types of materials, but application of these principles to condensed matter is more difficult due to the complexity of their electronic structure and the limited amount of experimental data on secondary-electron energy spectra in liquids and solids. Our semiempirical approach uses experimental photoionization cross sections and cross sections for ionization by charged particles that are integrated over the emission characteristics (energy and angle) of secondary electrons to predict cross sections differential in the energy of secondary electrons for ionization by fast electrons and positive ions.

The basic rationale behind our model is as follows:

(a) NORCUS student appointee under the Science and Engineering Research Semester (SERS) program.
(b) Department of Physics and Astronomy, Georgia State University, Atlanta, Georgia.

1. Photoionization cross sections contain the information needed to predict the shape of the energy spectrum at low secondary-electron energies where quantum effects predominate.

2. Classical binary-encounter theory is able to predict with reasonable accuracy the shape of the spectrum at high secondary-electron energies from a knowledge of the number of electrons in each shell and their binding energy.

3. The analytic form of the model forces these two limiting cases to merge smoothly at intermediate secondary-electron energies.

4. Fitting the area under the resulting energy spectrum to experimental total ionization cross sections provides the proper normalization for single differential cross sections (SDCS).

Results obtained for electron-impact ionization of helium by this procedure (Miller and Manson 1991) were encouraging, but most practical applications will involve more complex atomic and molecular species with more than one electronic shell.

Although experiments at cyclotron light sources are expected to increase the database of photoionization cross sections, obtaining shell-specific (i.e., partial) photoionization cross sections is currently a major impediment in applications of our model of secondary-electron energy spectra to multi-shell systems. Data for neon, an exceptionally well-studied case, are presented in Figure 1. The 2p shell predominates for photon energies below 200 eV. The 2s component of valence-shell photoionization gradually increases relative to the 2p component, but does not greatly exceed the 2p component below the K-shell absorbtion edge. This behavior makes neon effectively a two-level system with ejection of 2p electrons always dominating ionization of the valence shell. These results contrast sharply with the isoelectronic water molecule where valence-shell ionization is shared about equally by four subshells.

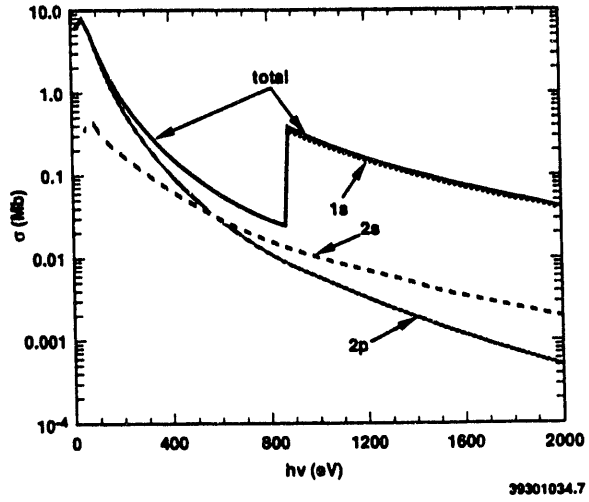

FIGURE 1. Shell-Specific Photoionization Cross Sections for Neon. The abscissa is the photon energy in electron volts and ordinate is the cross section in megabarns.

Figure 2 shows a fit of the model to integrated cross sections for ionization of neon by electron impact. The main purpose for fitting these data is to obtimize for parameters b and C that are used to calculate SDCS, but it also suggests the best value of the integrated ionization cross section where experimental results

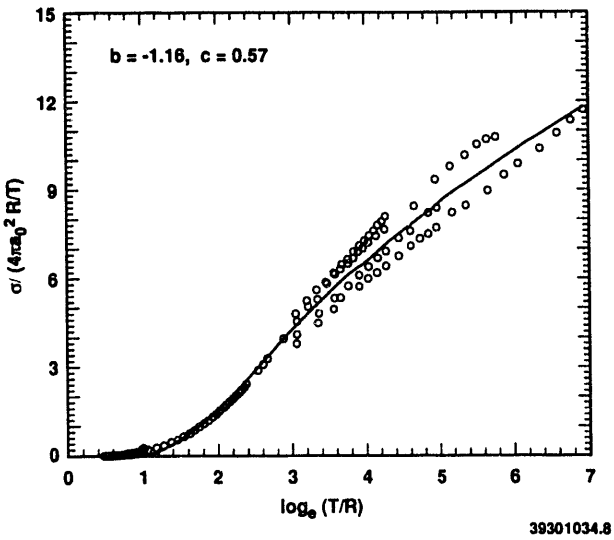

FIGURE 2. Nonlinear Least-Squares Fit of Model to Experimental Electron-Impact Ionization Cross Sections. The abscissa is the natural logarithm of the primary electron energy divided by the Rydberg energy (13.6 eV). The ordinate is the product of the cross section and the primary electron energy scaled by a convenient unit of area ($4\pi a_0^2$ = 3.52 Å^2) and the Rydberg.

exhibit considerable scatter. The model systematically underestimates the integrated ionization cross section for primary electrons with energy less than about 5 Rydbergs. This points to a limitation of the model which does not include mechanisms of ionization that predominate when the velocity of the projectile is comparable to or less than the average velocity of valence electrons in the target.

Figure 3 shows SDCS for ejection of electrons from neon by 500-eV primary electrons that is predicted by the model when parameters b and C are chosen to optimize agreement with the integrated cross section data. Agreement between our model and the measurements by Grissom et al. (1972) of the cross section for ejection of very low-energy secondary electrons is excellent. The data of Opal et al. (1971), which covers a broad range of secondary-electron energies, were obtained by integrating double differential ionization cross sections over emission angles. The limited number of angles sampled probably affects the accuracy of these data and may be partially responsible for the deviation from the model predictions. These results for neon show that

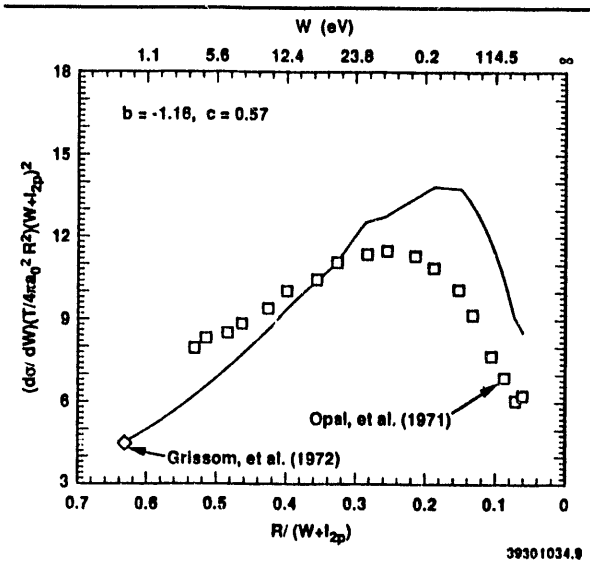

FIGURE 3. Comparison of Model Predictions and Experimental Data. The lower abscissa is the Rydberg divided by the energy lost by the primary electron when a secondary electron is ejected from the 2p shell. The corresponding secondary-electron energy is shown on the upper abscissa. The ordinate is the differential ionization cross section scaled by the Rutherford cross section for ionization of the 2p shell.

our semiempirical method can be used to calculate SDCS for atomic species with more than one electronic shell. Further testing on molecular species and condensed matter are in progress.

References

Grissom, J. T., R. N. Compton, and W. R. Garrett. 1972. "Slow Electrons from Electron-Impact Ionization of He, Ne, and Ar." *Phys. Rev. A 6:977.*

Miller, J. H., and S. T. Manson. 1991. "Relativistic Model of Secondary-Electron Spectra in Electron Impact Ionization. *Phys. Rev. A 44:4321-4327.*

Opal, C. B., W. K. Peterson, and E. C. Beaty. 1971. "Measurements of Secondary-Electron Spectra Produced by Electron Impact Ionization of a Number of Simple Gases." *J. Chem. Phys.* 55:4100-4106.

Ionization of DNA in Solution

J. Miller and R. Ritchie[a]

Energy transfer between a charged particle in a radiation field and DNA in solution is illustrated schematically in Figure 1. We can think of the DNA macromolecule as a collection of atomic centers bound together by a combination of covalent, electrostatic, and hydrogen bonds. Most of the energy in the radiation field is absorbed by the aqueous medium that surrounds the macromolecule, producing numerous reactive species that can diffuse to the DNA and induce chemical modifications. However, within cells, the average diffusion distance of free radicals, which play the major role in mediating the indirect mode of DNA damage, is only a few nanometers because the medium contains a high concentration of small molecules that rapidly scavenge the radiation-induced species. Under these conditions, direct interaction between the electrons bound

(a) Health and Safety Division, Oak Ridge National Laboratory, Oak Ridge, Tennessee.

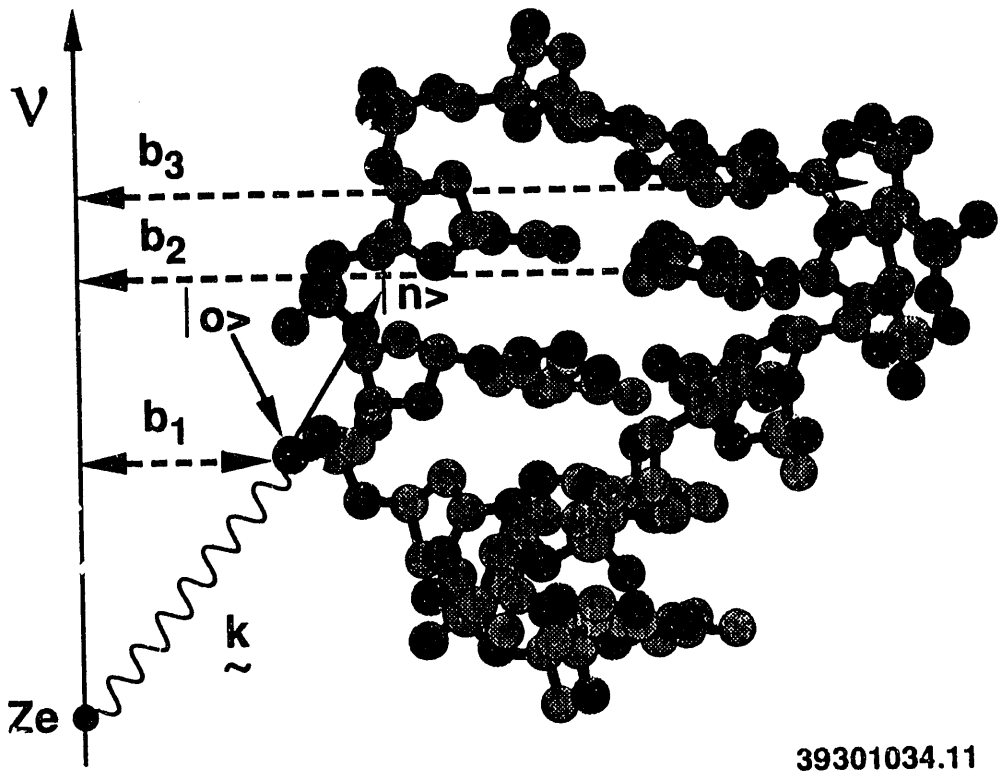

FIGURE 1. Schematic of Ionization of DNA by a Particle with Charge Ze and Velocity v. Broken arrows denote the impact parameter for collision with a phosphate group, a base, and a sugar moiety. Solid arrows denote excitation of an electron from its ground state to an excited state. Wave denotes transfer of momentum **k** to atomic center with impact parameter b_1.

to the atomic centers of DNA and charged particles in the radiation field cannot be neglected as a potential mode of damage induction.

Usually the velocity of particles that make up the radiation field is greater than the average velocity of loosely bound electrons on the atomic centers. When this is the case, the cross section for exciting an electron from its ground state $|0\rangle$ to a more energetic orbital $|n\rangle$ is proportional to the square of the product of the effective charge on the projectile and the inelastic form factor of the target $\langle n|\exp(i\mathbf{k}\cdot\mathbf{r})|0\rangle$, where **k** is the momentum transfer in the collision and **r** is the position of an active electron in the initial and final states. If $|n\rangle$ is localized on the same atomic center as $|0\rangle$, this process is called a discrete excitation, but if $|n\rangle$ is highly delocalized, the electron in this state is characterized as "quasi-free" and the collision process is called ionization.

Electrons bound to the small molecules that make up the aqueous medium will screen the electrons on the atomic centers of DNA from the nuclear charge (Ze) of the projectile. In the linear response theory that is valid for high-velocity projectiles, this effect can be included by replacing Ze by Ze/ϵ, where ϵ is the frequency- and momentum-dependent dielectric function of the aqueous medium. Integration over the range of momentum transfers allowed in the collision by conservation of energy and momentum gives the cross section for exciting an electron in DNA from state $|0\rangle$ with energy E_o to state $|n\rangle$ with energy E_n with concurrent energy loss by the projectile of

$\hbar\omega = E_n - E_o$, where $\hbar$ is Plank's constant divided by 2π and ω is the frequency of dielectric response by the medium that is most effective in screening DNA from the electronic excitation.

Figure 2 illustrates the effect of dielectric screening on the differential energy loss cross section. The dielectric response function of pure water (Ritchie et al. 1989) was used, but the density (d) of the medium was varied to show the effect of different levels of screening. The main effect of dielectric screening is to reduce the cross section for small energy transfers. The slight enhancement of large energy transfers can be interpreted as the result of collective modes of electronic polarization created in water by passage of the charged particle that are absorbed by DNA.

The quantum theory of energy transfer outlined above and used to calculate the results shown in Figure 2 does not resolve the dependence of energy-transfer probabilities on the impact parameter, the perpendicular distance between the particle trajectory, and the scattering center. However, this classical collision variable plays an important role in our intuitive understanding of the energy transfer process. For example, small energy transfers are generally associated with glancing collisions in which the impact parameter is large and the momentum transfer is small; hence, the finding that dielectric screening affects small energy transfers more than large ones is intuitively reasonable.

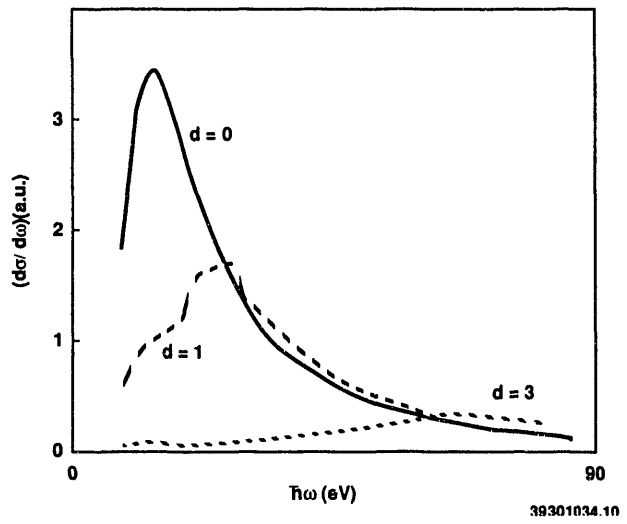

FIGURE 2. Effect of Dielectric Screening by Aqueous Medium on the Differential Cross Section for Energy Transfer to DNA. The abscissa is the energy transfer and electron volts, and the ordinate is the differential cross section in atomic units. The spectrum labeled d = 0 is the unscreened gas-phase result, and the curves labeled d = 1 and d = 3 show results at normal liquid-water density and three times this density, respectively.

A quantitative relationship between energy transfer and impact parameter is useful in semiclassical track-structure simulations by Monte Carlo techniques. In these computer models of radiation-induced DNA damage, case histories of particles making up the radiation field are generated by simulating a series of classical collision events with probability distributions determined from experiments or quantum calculations. The dependence of energy transfer probabilities on impact parameter is particularly important in analyzing these case histories for biologically relevant damage induction.

Ward (1985) has proposed that locally multiply damaged sites (LMDS) are the critical lesions in radiation biology. Our schmatic diagram of charged-particle interaction with DNA (Figure 1) illustrates how the impact-parameter dependence of energy-transfer probabilities affects the production of LMDS by multiple ionizations in DNA. Impact parameters b_1, b_2, and b_3 denote the distances from the trajectory of a charged particle to a DNA phosphate group, base, and sugar moiety, respectively. At the present stage of our model development, each energy-transfer event is assumed to be an independent collision with strict conservation of energy. The probability of any pair of events is the product of the probability for each separate energy transfer. Interesting geometric effects may arise even in this simple linear theory of LMDS. For example, a pair of ionizations in opposite strands of the double helix leading to a double strand break might

involve a collision with impact parameter b_1 followed by a collision with impact parameter b_2 or b_3. Since the probability of energy transfer decreases rapidly with impact parameter, this combination should be less likely than a pair of ionizations in the same strand because at least one of the impact parameters must be large in the interstrand case.

A mathematical expression for the impact-parameter dependence of energy-transfer probabilities can be easily derived in the limit of small momentum transfers where the recoil of the charged particle can be neglected in the conservation of energy. In this case, it is useful to resolve the momentum transfer into components parallel (ρ) and perpendicular (κ) to the particle velocity **v** since, by conservation of energy, $\rho = \hbar\omega/v$. Furthermore, since the impact parameter (b) and the perpendicular component of momentum transfer are canonical dynamic variables, the dependence of the energy transfer probability on b is related to its dependence on κ by Fourier transfers. Arguments of this type lead to the expression

$$P_n = \left(\frac{Ze}{\pi\hbar v}\right)^2 \left| \int \frac{d^2\kappa}{\kappa^2} \exp(i\boldsymbol{\kappa}\cdot\mathbf{b}) \langle n | e^{i\mathbf{k}\cdot\mathbf{r}} | 0 \rangle \left(\frac{1}{\epsilon_{k,\omega}} \right) \right|^2 \quad (1)$$

for the probability to transfer energy $\hbar\omega$ to DNA by the passage of a charged particle at impact parameter b. Methods to evaluate Equation (1) and to extend it beyond the small-momentum transfer limit are being developed.

References

Ritchie, R. H., R. N. Hamm, J. E. Turner, H. A. Wright, J. C. Ashley, and G. J. Basbas. 1989. "Physical Aspects of Charged Particle Track Structure." *Nuclear Tracks and Radiation Measurements 16:141-155.*

Ward, J. F.. 1985. "Biochemistry of DNA Lesions." *Radiat. Res. 104:S103-S111.*

Perturbations of DNA Conformation by Thymine Glycol and Dihydrothymine

J. Miller, K. Miaskiewicz,[a] and R. Osman[b]

Both thymine glycol (Tg) and dihydrothymine (dhT) are modifications of the thymine (T) base caused by free-radical attack that leads to saturation of the C5-C6 double bond. In Tg, saturation results from adding OH groups to the C5 and C6 positions of T, and in dhT it is due to adding H atoms at these positions. The biological consequences of these base lesions are remarkably different. DNA replication in vitro is blocked in most cases by the presence of Tg, while under similar conditions, dhT is only a weak inhibitor of DNA synthesis. The presence of dhT does not affect the survival of transfecting phage DNA, but Tg efficiently inactivates phage DNA. The repair enzyme complex UvrABC is able to recognize and incise DNA containing Tg, but DNA containing dhT is not a substrate for this enzyme. In work that is partially supported by Laboratory Directed Research and Development (LDRD) funds, we are investigating the structural basis for these differences which suggest that Tg is a bulky DNA lesion, but dhT is not.

Insight into the mechanism for the different biological effects of Tg and dhT has been found from *ab initio* quantum calculations of the relative stability of stereoisomers of the lesions. Each of the four stereoisomers of Tg (trans-5R,6R; trans-5S,6S; cis-5S,6R; and cis-5R,6S) can exist in two conformations that differ in the orientation of the substituents on C5 and C6 relative to the pyrimidine ring. By reflection symmetry, these eight conformations of Tg can be grouped into four pairs of enantiomers that we have labeled 5eq-6eq,

(a) NORCUS postdoctoral appointee.
(b) Department of Physiology and Biophysics, Mount Sinai School of Medicine, New York.

5eq-6ax, 5ax-6eq, and 5ax-6ax according to the approximately equatorial (eq) or axial (ax) orientation of the hydroxyl groups at C5 and C6. Similarly, the two unique stereoisomers of dhT can be labeled 5eq and 5ax according to the orientation of the H substituent at the asymmetric C5 carbon.

The dipole moment of hydroxyl groups can interact strongly with dipole moments within T when they add to C5 or C6 in the equatorial orientation. The interaction that results from adding to C5 lowers the electronic energy, while the interaction resulting from adding equatorial OH to C6 raises the electronic energy. This effect is illustrated in Figure 1 which compares the conformation of the most stable (5eq-6ax) and least stable (5ax-6eq) isomers of Tg, which differ in energy by about 9 kcal/mol. Isomer 5eq-6eq has both the favorable and unfavorable dipole-dipole interaction, while isomer 5ax-6ax has neither; hence, their energies lie between the most and least stable isomers shown in Figure 1. Adding hydrogen to the C5 or C6 positions of T does not induce a large dipole moment; hence the two stereoisomers of dhT have similar electronic energies.

The slightly greater stability of the 5ax isomer of dhT (0.5 kcal/mol including solvation) should be enhanced in DNA because its C5 methyl group has approximately the same orientation as in T so that it can be incorporated into DNA without major intrastrand steric clashes. In contrast, the 5eq-6ax isomer of Tg, which has an axially oriented methyl group at C5, is favored by about 5 kcal/mol in solution. Since a large energy cost within the modified base is

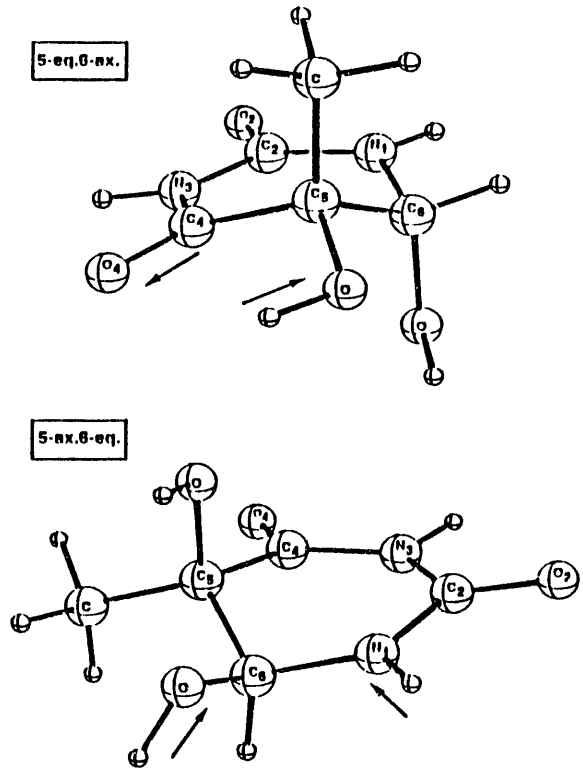

FIGURE 1. Conformation of the Most Stable (5eq-6ax) and Least Stable (5ax-6eq) Stereoisomers of Thymine Glycol. Arrows denote interacting dipole moments.

required for Tg to take on a conformation with its methyl group oriented similar to T, large distortions in DNA structure near this lesion are expected. These speculations about the behavior of the lesions in DNA are currently being tested by molecular dynamics simulations of oligonucleotides containing Tg and dhT.

Publications and Presentations

Presentations

Braby, L. A. 1992. "Introduction to Biophysical Models of Radiation Damage." (INVITED PRESENTATION) Presented at the 11th Symposium on Microdosimetry, Gatlinburg, Tennessee.

Braby, L. A., G. D. Badhwar, T. J. Conroy, D. C. Elergy, and L. W. Brackenbush. 1992. "Automated System for Measuring Dose and Radiation Quality as a Function of Time." Presented at the 11th Symposium on Microdosimetry, Gatlinburg, Tennessee.

Braby, L. A. 1992. "The Effects of a Single High Energy Charged Particle on an Individual Cell." Presented at the 12th International Conference on the Application of Accelerators in Research & Industry, Denton, Texas.

DuBois, R. D., R. R. Haar, J. A. Tanis, D. Schneider, M. W. Clark, M. H. Prior, and K. Randall. 1992. "Low-Energy Continuum Electrons from O^{8+} + He Collisions." Presented at the American Physical Society Conference, a Division of Atomic, Molecular and Optical Physics, Chicago, Illinois.

DuBois, R. D., C. G. Drexler, and L. H. Toburen. 1992. "Doubly Differential Electron Yields from Thin Carbon Foils." Presented at the American Physical Society Conference, a Division of Atomic, Molecular and Optical Physics, Chicago, Illinois.

DuBois, R. D., L. H. Toburen, and O. Jagutzki. 1992. "Differential Electron Emission in multi-Charged Ion-Atom Collisions: Systematics for Distant and Close Collisions." Presented at the VI International Conference on the Physics of Highly Charged Ions (HCI-92), Manhattan, Kansas.

DuBois, R. D., J. A. Tanis, and A. S. Schlachter. 1992. "Double Ionization of Helium by Intermediate-to-High-Velocity Projectiles." Presented at the American Physical Society Conference, a Division of Atomic, Molecular and Optical Physics, Chicago, Illinois.

DuBois, R. D., and S. T. Manson. 1992. "Electron-Electron Interactions in Fast Neutral-Neutral Collisions." (INVITED PAPER) Presented at the 12th International Conference on the Application of Accelerators in Research & Industry, Denton, Texas.

Edmonds, C. G., A. L. Fuciarelli, and D. L. Springer. 1992. "Electrospray Ionization Mass Spectrometry for Natural and Radiation Induced Modifications in Histone Proteins." Presented at the 40th ASMS Conference on MS and Allied Topics, Washington DC, May 31-June 5, 1992. PNL-SA-20439A.

Edmonds, C. G. 1992. "Electrospray Ionization Mass Spectrometry and Tandem Mass Spectrometry for Biochemical Investigations." Presented at WSU Biochemical Dept., February 3-4, 1992. PNL-SA-20529A.

Edmonds, C. G., D. L. Springer, D. M. Sylvester, S. C. Goheen, and R. J. Bull. 1992. "Characterization of Acrylamind Adducted Hemoglobin and Proteolytically-Derived Peptides Based on Electrospray Ionization Mass Spectrometry." Presented at the 40th ASMS Conference on MS and Allied Topics, Washington DC, May 31-June 5, 1992. PNL-SA-20448A.

Edmonds, C. G., J. A. Loo, R. D. Smith, A. F. Fuciarelli, B. T. Thrall, J. D. Morris, and D. L. Springer. 1992. "Evaluation of Histone Sequence and Modifications by Electrospray Ionization Mass Spectrometry and Tandem Mass Spectrometry." Presented at the Hanford Life Sciences Symposium, Richland, WA, October 10-22, 1992. PNL-SA-20992A.

Edmonds, C. G., J. C. Schwartz, and I. Jardine. 1992. "Peptide Sequencing by Quadrupole Ion Trap Mass Spectrometry." Presented at the 40th ASMS Conference on MS and Allied Topics, Washington DC, May 31-June 5, 1992. PNL-SA-20459A.

Edmonds, C. G., J. A. Loo, R. D. Smith, A. F. Fuciarelli, B. T. Thrall, J. D. Morris, and D. L. Springer. 1992. "Evaluation of Histone Sequence and Modifications by Electrospray Ionization Mass Spectrometry and Tandem Mass Spectrometry." Presented at the Pacific Conference on Chemistry and Spectroscopy, 10/21/92, Foster City, CA. PNL-SA-21013A.

Goodlett, D. R., J. H. Wahl, H. R. Udseth, and R. D. Smith. 1992. "Use of CE/ESI-MS to Investigate Solution ande Gas Phase Protein Conformation." Presented at the 40th ASMS Conference on MS and Allied Topics, Washington DC, May 31-June 5, 1992. PNL-SA-???.

Goodlett, D. R., J. H. Wahl, H. R. Udseth, and R. D. Smith. 1992. "CE/ESI-MS in Small ($<20\ \mu m$) Diameter Capillaries." Presented at the 40th ASMS Conference on MS and Allied Topics, Washington DC, May 31-June 5, 1992. PNL-SA-20440A.

Hill, R. L., R. A. Kennedy, F. Carr, Jr., and J. A. Mahaffey. 1992. "ChernoLit™--Chernobyl Bibliographic Search System," in *New Horizons in Radiation Protection and Shielding: Proceedings of the ANS Topical* Meeting, American Nuclear Society. Paper presented at the ANS Topical Meeting, Pasco, Washington, April 27, 1992.

Kennedy, R. A., J. A. Mahaffey, S. K. Smith, and F. Carr, Jr. 1992. "U.S. Department of Energy Chernobyl Databases," in *Conference Proceedings of IRPA8*. Poster presented by R. L. Hill at the Eighth World Congress of the International Radiation Protection Association, Montreal, Canada, May 18, 1992.

Light-Wahl, K. J., B. E. Winger, J. A. Loo, M. Busman, A. L. Rockwood, and R. D. Smith. 1992. "The Use of Electrospray Ionization Mass Spectrometry and Tandem Mass Spectrometry to Gain Insight into Protein Structure." Presented at the 43rd Pittsburgh Conference & Exposition on Analytical Chemistry and Applied Spectroscopy, March 9-13, 1992, New Orleans, LA. PNL-SA-19984A.

Light-Wahl, K. J., B. E. Winger, A. L. Rockwood, and R. D. Smith. 1992. "Internal Energy Affects on the Solvation and Reactivity of Multiply Charged Ions of Large Biomolecules for Electrospray Ionization Mass Spectrometry and Tandem Mass Spectrometry." Presented at the 40th ASMS Conference on MS and Allied Topics, Washington DC, May 31-June 5, 1992. PNL-SA-20444A.

Loo, J. A., A. L. Fuciarelli, D. L. Springer, C. G. Edmonds, R. R. Ogorzalek Loo, and R. D. Smith. 1992. "Elucidation of Covalent Modifications and Non-Covalent Associations in Proteins by Electrospray Ionization Mass Spectrometry." Presented at the 6th Symposium of the Protein Society, San Diego, CA, July 25-29, 1992. PNL-SA-20845A.

Loo, J. A., C. G. Edmonds, R. R. Ogorzalek Loo, K. J. Light-Wahl, and R. D. Smith. 1992. "Electrospray Ionization and Tandem Mass Spectrometry of Noncovalent Protein Complexes." Presented at the 40th ASMS Conference on MS and Allied Topics, Washington DC, May 31-June 5, 1992. PNL-SA-20443A.

Loo, J. A., and R. D. Smith. 1992. "Tandem Mass Spectrometry of Large Multiply Charged Proteins with Electrospray Ionization." Presented at the 40th ASMS Conference on MS and Allied Topics, Washington DC, May 31-June 5, 1992. PNL-SA-20446A.

Manson, S. T., and R. D. DuBois. 1992. "Dominance of Simultaneous Processes in Energetic H-Atom Ionizing Collisions." Presented at the Division of Atomic, Molecular and Optical Physics Conference of the American Physical Society, Chicago, Illinois.

Miller, R. J. 1992. "High Resolution Studies of Atoms and Small Molecules." Presented at the DOE Workshop on Advanced Laser Technology for Chemical Measurements. PNL-SA-21405, Santa Fe, New Mexico.

Miller, R. J. 1991. "Structure and Dynamics of High Rydberg States of Nitric Oxide." Presented at the Gordon Research Conference on Molecular Electronic Spectroscopy. PNL-SA-19692A, Wolfeboro, New Hampshire.

Miller, J. H. 1992. "Radiation Damage to DNA." Presented at the 14th Werner Brandt Workshop, Oak Ridge, Tennessee.

Miller, R. J. 1991. "High Resolution Studies of Nitric Oxide." Presented at the Institute for Physical Chemistry, University of Basel. PNL-SA-19914A, Basel, Switzerland.

Miller, J. H., K. Miaskiewicz, and R. Osman. 1992. "Structure-Function Studies of Modified DNA: Perturbations of DNA Conformation by Thymine Glycol and Dihydrothymine." Presented at the Mathematics and Molecular Biology Conference on Computational Approaches to Nucleic Acid Structure and Function, Santa Fe, New Mexico.

Miller, R. J. 1991. "High Resolution Studies of Nitric Oxide." Presented at the Institute for Physical and Theoretical Chemistry, Technical University of Munich. PNL-SA-19914A, Munich, Germany.

Miller, R. J. 1991. "Structure and Dynamics of High Rydberg States of Nitric Oxide." Presented at the Twenty First International Symposium on Free Radicals. PNL-SA-19692A, Williamstown, Massachusetts.

Miller, J. H., C. C. Stigers, and S. T. Manson. 1992. "Calculation of Secondary-Electron Energy Spectra for Electron-Impact Ionization of Multishell Atoms." Presented at the American Physical Society 1992 Annual Meeting of the Division of Atomic, Molecular, and Optical Physics, Chicago, Illinois.

Myers, L. S. Jr., C. E. Swenberg, and J. H. Miller. 1992. "Reduction Products Formed by Neutron and Proton Irradiation of Oriented DNA." Presented at Pathways to Radiation Damage in DNA, Oakland University, Rochester, Michigan.

Nelson, J. M. and L. A. Braby. 1992. "Irradiation of Single Cells with Individual High-LET Particles." Presented at the Fifth International Symposium on Neutron Capture Therapy, Columbus, Ohio.

Nelson, J. M., J. H. Miller, M. Ye, and E. W. Fleck. 1992. "Relationship Between Plasmid Structure and Radiation Strand Scission." Presented at the Cell Kinetics Society Meeting, New Orleans, Louisiana.

Nelson, J. M. 1992. "Effect of Supercoiling." (INVITED PAPER) Presented in workshop on *DNA Structure and Radiation Damage* at the 40th Annual Meeting of the Radiation Research Society, Salt Lake City, Utah.

Ogorzalek Loo, R. R., J. A. Loo, H. R. Udseth, and R. D. Smith. 1992. "Applying Ion-Molecule Reactions to Studies of Gas Phase Protein Structure." Presented at the 40th ASMS Conference on MS and Allied Topics, Washington DC, May 31-June 5, 1992. PNL-SA-19128A.

Ogorzalek Loo, R. R., H. R. Udseth, and R. D. Smith. 1992. "Ion-Ion Reactions of Large Cations and Anions Generated by Electrospray Ionization." Presented at the 40th ASMS Conference on MS and Allied Topics, Washington DC, May 31-June 5, 1992. PNL-SA-20438.

Rockwood, A. L., and R. D. Smith. 1992. "How Do Electric Fields Effect Proton Transfer Reactions?" Presented at the 40th ASMS Conference on MS and Allied Topics, Washington DC, May 31-June 5, 1992. PNL-SA-20442A.

Rottmann, L. M., R. Bruch, P. Neill, C. Drexler, R. D. DuBois, and L. H. Toburen. 1992. "Electron Capture by 100- to 1500-keV Ions in Several Atomic and Molecular Targets." Presented at the 1992 Atomic, Molecular and Optical Physics Meeting of the American Physical Society, Chicago, Illinois.

Smith, R. D., D. R. Goodlett, J. H. Wahl, and H. R. Udseth. 1992. "High Performance Capillary Electrophoresis-Mass Spectrometry." Presented at the 43rd Pittsburgh Conference & Exposition on Analytical Chemistry and Applied Spectroscopy, March 9-13, 1992, New Orleans, LA. PNL-SA-20644A.

Smith, R. D., K. J. Light-Wahl, R. R. Ogorzalek Loo, B. E. Winger, J. A. Loo, and A. L. Rockwood. 1992. "Experimental and Theoretical Methods for Probing the Higher Order Structure of Protein Ions in the Gas Phase." Presented at the 40th ASMS Conference on MS and Allied Topics, Washington DC, May 31-June 5, 1992. PNL-SA-20441A.

Smith, R. D., J. A. Loo, H. R. Udseth, A. L. Rockwood, B. E. Winger, R. R. Ogorzalek Loo, and K. J. Light-Wahl. 1992. "New Methods and Instrumentation for the Characterization of Biopolymers Using Electrospray Ionization-Mass Spectrometry." Presented at the BMS Kyoto '92, September 20-24, 1992, Osaka, Japan. PNL-SA-20758A.

Smith, R. D., J. H. Wahl, D. R. Goodlett, H. R. Udseth, and C. J. Barinaga. 1992. "Capillary Electrophoresis-Mass Spectrometry in Peptide Mapping." Presented at ACS Annual Meeting, April 5-9, 1992, San Francisco, CA. PNL-SA-20643A.

Tanis, J. A., R. R. Haar, D. Schneider, M. W. Clark, M. H. Prior, R. D. DuBois, and K. Randall. 1992. "Low-Energy Continuum-Electron Emission at 0^0 From 0^{q+} + He Collisions." Presented at the VI International Conference on the Physics of Highly-Charged Ions (HCI-92), Manhattan, Kansas.

Toburen, L. H. and R. D. DuBois. 1992. "Electron Emission Cross Sections for Collisions of Dressed Ions with Atomic and Molecular Targets." Presented at the 11th Symposium on Microdosimetry, Gatlinburg, Tennessee.

Tonkyn, R. G., and R. J. Miller. 1992. "Circular Dichroism in the Photoelectron Angular Distributions from Selected Hyperfine States of Cesium." Presented at the Gordon Research Conference on Electron Spectroscopy. PNL-SA-21144, Wolfeboro, New Hampshire.

Wahl, J. H., D. R. Goodlett, H. R. Udseth, and R. D. Smith. 1992. "Capillary Electrophoresis-Electrospray Ionization Mass Spectrometry in Small Diameter Capillaries." Presented at the 40th ASMS Conference on MS and Allied Topics, Washington DC, May 31-June 5, 1992. PNL-SA-20440A.

Wahl, J. H., H. R. Udseth, and R. D. Smith. 1992. "Examination of Small-Diameter Coated Columns for High Sensitivity Capillary Electrophoresis-Mass Spectrometry of Proteins." Presented at the 43rd Pittsburgh Conference & Exposition on Analytical Chemistry and Applied Spectroscopy, March 9-13, 1992, New Orleans, LA. PNL-SA-19985A.

Wilson, W. E., and H. G. Paretzke. 1992. "A Stochastic Model of Ion Track Structure." Presented at the 11th Symposium on Microdosimetry, Gatlinburg, Tennessee.

Winger, B. E., K. J. Light-Wahl, and R. D. Smith. 1992. "Ion-Molecule Reactions of Electrosprayed Ions Prior to Expansion into a Quadrupole Mass Spectrometer." Presented at the 43rd Pittsburgh Conference & Exposition on Analytical Chemistry and Applied Spectroscopy, March 9-13, 1992, New Orleans, LA. PNL-SA-19986A.

Winger, B. E., K. J. Light-Wahl, and R. D. Smith. 1992. "Probing Conformational Differences of Multiply Protonated Gas-Phase Protein Ions Using Thermal Energy Hydrogen/Deuterium Exchange Reactions." Presented at the 40th ASMS Conference on MS and Allied Topics, Washington, DC, May 31-June 5, 1992. PNL-SA-20447A.

Winger, B. E., J. A. Loo, H. R. Udseth, A. L. Rockwood, and R. D. Smith. 1992. "The Development of a Novel Electrospray Ionization-Fourier Transform Mass Spectrometer for the Investigation of Large Biomolecules." Presented at the 40th ASMS Conference on MS and Allied Topics, Washington DD, May 31-June 5, 1992. PNL-SA-20445A.

Publications

Berg, H., O. Jagutzki, R. Dörner, R. D. DuBois, C. Kelbch, H. Schmidt-Böcking, J. Ullrich, J. A. Tanis, A. S. Schlachter, L. Blumenfeld, B. d'Etat, S. Hagmann, A. Gonzales, and T. Quinteros. 1992. "Double Ionization of Helium by High-Velocity U^{90+} Ions". *Phys. Rev. A*. 46:5539-5544.

Braby, L. A., and T. L. Morgan. 1992. "Role of DNA Deletion Length in Mutation and Cell Survival." In *Biophysical Modeling of Radiation Effects,* eds. R. H. Chadwick, C. Moschini, and M. N. Varma, pp. 219-226. Adam Hilger; IOP Publishing Ltd, Bristol, England.

Braby, L. A., N. F. Metting, W. E. Wilson, and L. H. Toburen. 1992. "Microdosimetric Measurements of Heavy Ion Tracks." *Adv. Space Res.* 12:23-32.

Braby, L. A., and J. M. Nelson. 1992. "Linear-Quadratic Dose Kinetics or Dose-Dependent Repair/Misrepair." In *Biophysical Modeling of Radiation Effects*, eds. R. H. Chadwick, C. Moschini, and M. N. Varma, pp. 331-334. Adam Hilger; IOP Publishing Ltd, Bristol, England.

Braby, L. A., T. J. Conroy, D. C. Elegy, and L. W. Brackenbush. 1992. "Use of Tissue Equivalent Proportional Counters to Characterize Radiation Quality on the Space Shuttle." Submitted to *New Horizons*.

Braby, L. A. 1991. "Phenomenological Models." In *Physical and Chemical Mechanisms in Molecular Radiation Biology*, eds. W. A. Glass and M. N. Varma, pp. 339-365. Plenum Press, New York.

Braby, L. A. 1992. "Microbeam Studies of the Sensitivity of Structures Within Living Cells." *Scanning Microscopy* 6:167-175.

Busman, M., A. L. Rockwood, and R. D. Smith. 1992. "Activation Energies for Gas Phase Dissociations of Multiply Charged Ions from Electrospray Ionization Mass Spectrometry." *J. Phys. Chem.,* 96, 2397-2400.

Busman, M., A. L. Rockwood, and R. D. Smith. 1992. "Activation Energies for Gas Phase Dissociations of Multiply Charged Ions from Electrospray Ionization Mass Spectrometry." *J. of Phys. Chem.*, 1992, 96, 2397-2400. PNL-SA-20317.

Carr, F., Jr., R. A. Kennedy, and J. A. Mahaffey. 1992. *ChernoLit™--Chernobyl Bibliographic Search System User's Manual.* PNL-7992, Pacific Northwest Laboratory, Richland, Washington.

Clark, M. W., J. A. Tanis, E. M. Bernstein, N. R. Badnell, R. D. DuBois, W. G. Graham, T. J. Morgan, V. L. Plano, A. S. Schlachter, and M. P. Stockli. 1992. "Cross Sections for Resonant Transfer and Excitation in Fe^{q+} + He Collisions." *Phys. Rev. A*. 45:7846-7850.

DuBois, R. D., J. A. Tanis, and A. S. Schlachter. 1992. "Comment on 'Double and Single Ionization of Helium by High-Velocity N^{7+} Ions'." *Phys. Rev. Letters* 68:897.

DuBois, R. D., L. H. Toburen, and O. Jagutzki. 1992. "Differential Electron Emission in Multi-Charged Ion-Atom Collisions: Systematics for Distant and Close Collisions." *American Institute of Physics Conference Proceedings* (in press).

DuBois, R. D., O. Heil, R. Maier, M. Kuzel, and K.-O. Groeneveld. 1992. "Ionization In Fast-Neutral-Particle-Atom Collisions: H and He Atoms Impacting On He." *Phys. Rev. A.* 45:2850-2858.

DuBois, R. D. and S. T. Manson. 1992. "Multi-Electron Transitions Resulting from Interactions Between Target and Projectile Electrons in Ionizing Collisions." In *Phys. Rev. A.* (in press).

DuBois, R. D., and S. T. Manson. 1992. "Electron-Electron Interactions in Fast Neutral-Neutral Collisions." *Nuclear Instruments and Methods* (in press).

DuBois, R. D. 1992. "Ionization in Few Electron Atom-Atom Collisions." Published in *Atomic and Molecular Physics*, eds. E. Cisneros, I. Alvarez, and T. J. Morgan, pp. 96-104. World Scientific, Singapore.

Edmonds, C. G., J. A. Loo, R. R. Ogorzalek Loo, H. R. Udseth, C. J. Barinaga, and R. D. Smith. 1991. "Application of Electrospray Ionization Mass Spectrometry and Tandem Mass Spectrometry in Combination with Capillary Electrophoresis for Biochemical Investigations." *Biochem. Soc. Trans.,* 19, 943-947.

Goodlett, D. R., D. G. Camp, C. C. Hardin, M. Corregan, and R. D. Smith. "Direct Observation of a DNA Quadruplex by Electrospray Ionization-Mass Spectrometry." *Biol. Mass Spectrom.,* in press.

Goodlett, D. R., J. H. Wahl, H. R. Udseth, and R. D. Smith. "Reduced Elution Speed Detection for Capillary Electrophoresis--Mass Spectrometry." Submitted to *J. Microcolumn Sep.*

Kennedy, R. A., J. A. Mahaffey, F. Carr, Jr. 1992. *U.S. Department of Energy Chernobyl Accident Bibliography.* PNL-8080, Pacific Northwest Laboratory, Richland, Washington.

Light-Wahl, J. J., J. A. Loo, C. G. Edmonds, R. D. Smith, H. E. Witkowska, C.H.L. Shackelton, and C.S.C. Wu. "Tandem Mass Spectrometry of Intact Hemoglobin β-Chain Variant Proteins with Electrospray Ionization." *Biol. Mass Spectrom.,* in press.

Light-Wahl, K. J., D. L. Springer, B. E. Winger, C. G. Edmonds, D. G. Camp, B. D. Thrall, and R. D. Smith. "Observation of a Small Oligonucleotide Duplex by Electrospray Ionization-Mass Spectrometry." *J. Am. Chem. Soc.,* in press.

Loo, J. A., C. G Edmonds, and R. D. Smith. "Tandem Mass Spectrometry of Very Large Molecules. II. Dissociation of Multiply Charged Proline-Containing Proteins from Electrospray Ionization." Anal. Chem

Loo, J. A., C. G. Edmonds, H. R. Udseth, R. R. Ogorzalek Loo, and R. D. Smith. "Electrospray Ionization Mass Spectrometry and Tandem Mass Spectrometry of Large Biomolecules." *Experimental Mass Spectrometry,* in press.

Loo, J. A., R. R. Ogorzalek Loo, D. R. Goodlett, R. D. Smith, A. F. Fuciarelli, D. L. Springer, B. D. Thrall,a nd C. G. Edmonds. "Elucidation of Covalent Modifications and Noncovalent Associations in Proteins by Electrospray Ionization Mass Spectrometry." *Techniques in Protein Chemistry III, (Academic Press).*

Loo, J. A., R. R. Ogorzalek Loo, H. R. Udseth, C. G. Edmonds, and R. D. Smith. 1991. "Solvent-Induced Conformational Changes of Polypeptides Probed by Electrospray Ionization-Mass Spectrometry." *Rapid Commun. Mass Spectrom.,* 5, 101-105.

Loo, J. A., R. R. Ogorzalek Loo., K. J. Light, C. G. Edmonds, and R. D. Smith. 1992. "Multiply Charged Negative ions by Electrospray Ionization from Polypeptides and Proteins." *Anal. Chem.,* 64, 81-88.

Miaskiewicz, K., J. H. Miller, and R. Osman. "*Ab Initio* Theoretical Study of the Structures of Thymine Glycol and Dihydrothymine." Submitted to *The Int. J. of Radia. Biol.*

Miller, J. H., D. L. Frasco, C. E. Swenberg, and A. Rupprect. 1992. "Energy Transfer Mechanisms in DNA: Relationship To Energy Deposition in Submicroscopic Volumes." *Radiation Research: A Twentieth-Century Perspective* Vol. II, eds. W. D. Dewey, M. Edington, R. J. M. Fry, E. J. Hall, and G. R. Whitmore, pp. 433-438. Academic Press, Inc., San Diego.

Miller, J. H. 1992. "Radiation Damage to DNA." In *Proceedings of the 14th Werner Brandt Workshop on Charged Particle Penetration Phenomena*, ORNL report, Oak Ridge, Tennessee (in press).

Murphy, J. E., B. A. Bushaw, and R. J. Miller. 1992. "Doppler-Free Two-Photon Fluorescence Excitation Spectroscopy of the $A \leftarrow X(1,0)$ Band of Nitric Oxide: Fine Structure Parameter for the $(3ss)A\ ^2S^+(u=1)$ Rydberg State of $^{14}N^{16}O$." PNL-SA-21438, *The J. of Mol. Spectrosc.* (in press).

Nelson, J. M., J. H. Miller, M. Ye, and E. W. Fleck. "Relationship Between Plasmid Structure and Radiation Strand Scission." *Cell Prolif eration* (in press).

Nelson, J. M., and R. G. Stevens. 1992. "Body Iron Stores May Modify Sensitivity to Occupational Radiation Exposure." *Applied Occup. and Env. Hygiene J.* (in press).

Nelson, J. M., and R. G. Stevens. 1992. "Ferritin Iron Increases Killing of Chinese Hamster Ovary Cells by X Irradiation." *Cell Proliferation* (in press).

Nelson, J. M., and L. A. Braby. 1992. "Irradiation of Single Cells With Individual High-LET Particles." Submitted to Plenum Press.

Ogorzalek Loo, R. R.., H. R. Udseth, and R. D. Smith. 1991. "Evidence of Charge Inversion in the Reaction of Singly Charged Anions with Multiply Charged Macroions." *J. Phys. Chem.*, 95, 6412-6415.

Ogorzalek Loo, R. R., H. R. Udseth, and R. D. Smith. 1992. "A New Approach for the Study of Gas Phase Ion-Ion Reactions using Electrospray Ionization." *J. Amer. Soc. Mass Spectrom.*, 3, 695-705.

Ogorzalek Loo, R. R., J. A. Loo, H. R. Udseth, J. L. Fulton, and R. D. Smith. 1992. "Protein Structural Effects in Gas Phase Ion-Molecule Reactions with Diethylamine." Submitted to *Rapid Commun. Mass Spectrom.*, 6, 159-165.

Rockwood, A. L., M. Busman, and R. D. Smith. 1991. "Thermally Induced Dissociation of Ions in Electrospray Mass Spectrometry." *Rapid Commun. Mass Spectrom.* 5, 582-585.

Rockwood, A. L., M. Busman, and R. D. Smith. 1991. "Coulombic Effects in the Dissociation of Large Highly Charged Ions." *Int. J. Mass Spectrom. Ion Proc.*, 111, 103-129.

Rottmann, L. M., M. Brunch, P. Neill, C. Drexler, R. D. DuBois, and L. H. Toburen. 1992. "Single-Electron Capture by 100- to 1500 keV C^+ Ions in Several Atomic and Molecular Targets." *Phys. Rev. A.* 46:3883-3888.

Schmidt-Böcking, H., U. Ramm, G. Kraft, J. Ullrich, H. Berg, C. Kelbch, R. E. Olson, R. D. DuBois, S. Hagmann, and F. Jiazhen. 1992. "δ-Electron Emission in Fast Heavy Ion Atom Collisions." *Adv. Space Res.* 12:7-15.

Smith, R. D., and H. R. udseth. "Mass Spectrometric Detection for Capillary Electrophoresis." *Capillary Electrophoresis,* ed. N. A. Guzman.

Smith, R. D., K. J. Light-Wahl, B. E. Winger, and J. A. Loo. 1992. "Preservation of Noncovalent Association in Electrospray Ionization-Mass Spectrometry: Formation and Dissociation of Multiply Charged Polypeptide and Protein Dimers." *Org. Mass Spectrom.*, 27, 811-821.

Smith, R. D., H. R. Udseth, J. H. Wahl, and D. R. Goodlett. "Methods in Enzymology: High Resolution Separation Methods of Biological Macromolecules." CE/MS, B. L. Karger and W. S. Hancock, eds., Academic Press, New York, in press.

Smith, R. D., J. A. Loo, and C. G. Edmonds. "The Analysis of Biomolecules by Electrospray Ionization-Mass Spectrometry and Tandem Mass Spectrometry." *Clinical Mass Spectrometry,* Volume 1, D. M. Desiderio, ed., Plenum Press, New York, in press.

Smith, R. D., J. A. Loo, R. R. Ogorzalek Loo, M. Busman, and H. R. Udseth. 1991. "Principles and Practice of Electrospray Ionization-Mass Spectrometry for Large Polypeptides and Proteins." *Mass Spectrom. Rev.,* 10, 359-451.

Smith, R. D., J. A. Loo, C. G. Edmonds, and H. R. Udseth. 1991. "Combined Capillary Electrophoresis and Electrospray Ionization Mass Spectrometry." *Analytical Applications of Spectroscopy II,* A.M.C. Davies and C. S. Creaser, ed., Royal Society of Chemistry, 149-164.

Smith, R. D., B. W. Wright, and C. R. Yonker. 1992. "Supercritical Fluid Chromatography; Current Status and Prognosis." In: *Instrumentation in Analytical Chemistry 1988-1991,* ed. L. Voress, American Chemical Society, 290-298.

Smith, R. D., H. R. Udseth, C. J. Barinaga, and C. G. Edmonds. 1991. "Instrumentation for High-Performance Capillary Electrophoresis-Mass Spectrometry. *J. Chromatogr.,* 559, 197-208.

Tanis, J. A., R. R. Haar, D. Schneider, M. W. Clark, M. H. Prior, R. D. DuBois, and K. Randall. 1992. "Low-Energy Continuum-Electron Emission at 0° From O^{q+} + He Collisions." *American Institute of Physics Conference Proceedings* (in press).

Toburen, L. H., and R. D. DuBois. 1992. "Electron Emission Cross Sections for Collisions of Dressed Ions with Atomic and Molecular Targets." *Radiation Protection Dosimetry* (in press).

Toburen, L. H. 1991. "Atomic and Molecular Physics in the Gas Phase." In *Physical and Chemical Mechanisms in Molecular Radiation Biology*, eds. W. A. Glass and M. N. Varma, pp. 51-97. Plenum Press, New York.

Wahl, J. H., D. R. Goodlett, H. R. Udseth, and R. D. Smith. "Use of Small-Diameter Capillaries for Increasing Peptide and Protein Detection Sensitivity in Capillary Electrophoresis-Mass Spectrometry." Submitted to *Electrophoresis.*

Wahl, J. H. H. R. Udseth, and R. D. Smith. "Capillary Electrophoresis-Mass Spectrometry in Peptide Mapping." *Characterization of Proteins: New Methods in Peptide Mapping*, W. S. Hancock, ed., CRC Press, in press.

Wahl, J. H., D. R. Goodlett, H. R. Udseth, and R. D. Smith. "Attomole Level Capillary Electrophoresis-Mass Spectrometric Protein Analysis Using 5 μm i.d. Capillaries." *Anal. Chem.,* in press.

Wilson, W. E., and H. G. Paretzke. 1992. "A Stochastic Model of Ion Track Structure." *Rad. Pro. Dos.* (in press).

Wilson, W. E. 1992. "The Stochastics of the Positive Ion Penumbra." Submitted to *Radiation Research.*

Winger, B. E., K. J. Light-Wahl, and R. D. Smith. 1992. "Gas Phase Proton Transfer Reactions Involving Multiply Charged Cytochrome c Ions and Water under Thermal Conditions." *J. Amer. Soc. Mass Spectrom.,* 3, 624-630.

Winger, b. E., K. J. Light-Wahl, A. L. Rockwood, and R. D. Smith. 1992. "Probing Qualitative Conformational Differences of multiply Protonated Gas-Phase Proteins via H/D Isotopic Exchange with D_2O." *J. Am. Chem. Soc.*, 114, 5897-5898.

Yee, G. G., J. L. Fulton, and R. D. Smith. 1992. Fourier Transform Infrared Spectroscopy of Molecular Interactions of Heptafluoro-1-butanol in Supercritical Carbon Dioxide and Supercritical Ethane." *J. Phys. Chem.*, 96, 6172-6181.

Distribution

Distribution

OFFSITE

W. R. Albers
EH-12, GTN
Department of Energy
Washington, DC 20545

D. Anderson
ENVIROTEST
1108 NE 200th Street
Seattle, WA 98155-1136

Assistant Secretary
Environment, Safety & Health
EH-1, FORS
Department of Energy
Washington, DC 20545

F. Badgley
13749 NE 41st Street
Seattle, WA 98125

R. E. Baker
8904 Roundleaf Way
Gaithersburg, MD 20879-1630

R. W. Barber
EH-131, GTN
Department of Energy
Washington, DC 20545

N. F. Barr
ER-72, GTN
Department of Energy
Washington, DC 20545

J. R. Beall
ER-72, GTN
Department of Energy
Washington, DC 20545

W. R. Bibb
Energy Programs and Support Division
Department of Energy
P.O. Box 2001
Oak Ridge, TN 38731

R. Borders
Health Protection Division
U.S. Department of Energy
P.O. Box 5400
Albuquerque, NM 87185

L. C. Brazley, Jr.
NE-22, GTN
Department of Energy
Washington, DC 20545

D. J. Brenner
Radiological Research Lab
College of Physicians and Surgeons
Columbia University
630 W. 168th Street
New York, NY 10032

G. Burley
Office of Radiation Programs, ANR-458
Environmental Protection Agency
Washington, DC 20460

W. W. Burr, Chairman
Medical & Health Sciences Division
Oak Ridge Associated Universities
P.O. Box 117
Oak Ridge, TN 37830

L. K. Bustad
College of Veterinary Medicine
Washington State University
Pullman, WA 99164-7010

R. J. Catlin
U.T. Health Science Center-Houston
13307 Queensbury Lane
Houston, TX 77079

A. Chatterjee
Lawrence Berkeley Laboratory
MS 29-100
1 Cyclotron Road
Berkeley, CA 94720

N. Cohen
New York University Medical Center
P.O. Box 817
Tuxedo, NY 10987

Council on Environmental Quality
722 Jackson Place, NW
Washington, DC 20503

The Honorable Gail de Planque
U.S. Nuclear Regulatory Commission
Washington, DC 20555

DOE Office of Scientific and Technical Information (12)

B. H. Fimiani
Battelle, Pacific Northwest Laboratories
Washington Operations
370 L'Enfant Promenade, Suite 900
901 D Street, SW
Washington, DC 20024

M. E. Frazier
Office of Health and Environment
Office of Energy Research
Department of Energy
ER-72, GTN
Germantown, MD 20875

W. R. Garrett
Oak Ridge National Laboratory
P.O. Box 2008
Oak Ridge, TN 37831

T. F. Gesell
Idaho Operations Office
Department of Energy
785 DOE Place
Idaho Falls, ID 83402-4149

R. D. Gilmore, President
Environmental Health Sciences, Inc.
Nine Lake Bellevue Building
Suite 220
Bellevue, WA 98005

G. Goldstein
Office of Epidemiology & Health Sciences, Inc.
Nine Lake Bellevue Building
Suite 220
Bellevue, WA 98005

G. H. Groenewold
Energy and Mineral Research Center
University of North Dakota
Box 8123, University Station
Grand Forks, ND 58202

E. J. Hall
Radiological Research Laboratory
Columbia University
630 West 168th Street
New York, NY 10032

E. J. Hall
Radiological Research Laboratory
Columbia Univeristy
630 West 168th Street
New York, NY 10032

W. Happer
ER-1, FORS
U.S. Department of Energy
Washington, DC 20585

J. W. Healy
51 Grand Canyon Drive
White Rock, NM 87544

R. F. Hirsch
Office of Health and Environment
Office of Energy Research
Department of Energy
ER-72, GTN
Germantown, MD 20875

R. O. Hunter, Jr.
ER-1, FORS
Department of Energy
1000 Independence Avenue, SW
Washington, DC 20545

F. Hutchinson
Department of Molecular Biophysics & Biochemistry
Yale University
260 Whitney Avenue
P.O. Box 6666
New Haven, CT 06511

M. Inokuti
Argonne National Laboratory
9700 South Cass Avenue
Argonne, IL 60439

H. Ishikawa, General Manager
Nuclear Safety Research Association
P.O. Box 1307
Falls Church, VA 22041

A. W. Johnson
San Diego State University
6310 Alvardo Court, Suite 110
San Diego, CA 92120

L. J. Johnson
Idaho National Engineering Lab
IRC MS 2203
P.O. Box 1625
Idaho Falls, ID 83415

G. Y. Jordy, Director
ER-30, GTN
Department of Energy
Washington, DC 20545

B. J. Kelman
Failure Analysis Associates, Inc.
P.O. Box 3015
Menlo Park, CA 94025

G. A. Kolstad
ER-15, GTN
Department of Energy
Washington, DC 20545

R. T. Kratzke
NP-40
Department of Energy
Germantown, MD 20875

Librarian
Colorado State University
Documents Department--The Libraries
Ft. Collins, CO 80523

Librarian
Electric Power Research Institute
3412 Hillview Avenue
P.O. Box 10412
Palo Alto, CA 94303

Librarian
Health Sciences Library, SB-55
University of Washington
Seattle, WA 98195

Librarian
Los Alamos National Laboratory
Report Library, MS P364
P.O. Box 1663
Los Alamos, NM 87545

Librarian
Oregon Regional Primate Research Center
505 NW 185th Avenue
Beaverton, OR 97006

Librarian
Washington State University
Pullman, WA 99164-6510

Library
Serials Department
(#80-170187)
University of Chicago
1100 East 57th Street
Chicago, IL 60637

J. N. Maddox
ER-73, GTN
Department of Energy
Washington, DC 20545

J. R. Maher
ER-65, GTN
Department of Energy
Washington, DC 20545

S. J. Maheras
Idaho National Engineering
Laboratory, EG&G Idaho
P.O. Box 1635
Idaho Falls, ID 83415-2110

C. R. Mandelbaum
ER-32, GTN
Department of Energy
Washington, DC 20545

S. Marks
8024 47th Place West
Mukilteo, WA 98275

H. M. McCammon
ER-75, GTN
Department of Energy
Washington, DC 20545

C. B. Meinhold
President
National Council on Radiation
Protection and Measurements
7910 Woodmont Avenue
Suite 800
Bethesda, MD 20814

C. Miller
P.O. Box 180
Watermill, NY 11976

T. L. Morgan
Department of Radiation
Oncology
Kaiser Permanente Regional
Medical Center
4950 Sunset Blvd
Los Angeles, CA 90027

N. S. Nelson
Office of Radiation Programs,
ANR-461
Environmental Protection
Agency
401 M Street, SW
Washington, DC 20460

W. R. Ney
Executive Director
National Council on Radiation
Protection and Measurements
7910 Woodmont Avenue
Suite 1016
Bethesda, MD 20814

Nuclear Regulatory
Commission
Advisory Committee on Reactor
Safeguards
Washington, DC 20555

M. J. O'Brien
Radiation Safety Office, GS-05
University of Washington
Seattle, WA 98195

L. E. Porter, Associate
Director
Nuclear Radiation Center
Washington State University
Pullman, WA 99164

R. G. Rader
ER-33, GTN
Department of Energy
Washington, DC 20545

D. P. Rall, Director
National Institutes of
Environmental Health
Sciences
P.O. Box 12233
Research Triangle
Park, NC 27709

L. A. Rancitelli
Battelle Memorial Institute
505 King Avenue
Columbus, OH 43201-2693

J. Rasey
Division of Radiation Oncology
University of Washington
Medical School
Seattle, WA 98195

C. R. Richmond
Oak Ridge National Laboratory
4500N, MS-62523
P.O. Box 2008
Oak Ridge, TN 37831-6253

J. S. Robertson
ER-73, GTN
Department of Energy
Washington, DC 20545

S. L. Rose
ER-73, GTN
Department of Energy
Washington, DC 20545

R. D. Rosen, Tech. Librarian
Environmental Measurements
Laboratory
Department of Energy
376 Hudson Street
New York, NY 10014

L. Sagan
Electric Power Research
Institute
3412 Hillview Avenue
P.O. Box 10412
Palo Alto, CA 94304

R. A. Scarano
Mill Licensing Section
Nuclear Regulatory Commission
Washington, DC 20545

M. Schulman
ER-70, GTN
Department of Energy
Washington, DC 20545

R. Shikiar
Battelle - Seattle
4000 NE 41st Street
Seattle, WA 98105

H. P. Silverman
Beckman Instruments
2500 Harbor Blvd.
Fullerotn, CA 92634

W. K. Sinclair, President
National Council on Radiation Protection and Measurements
7910 Woodmont Avenue
Suite 800
Bethesda, MD 20814

J. N. Stannard
17441 Plaza Animado #132
San Diego, CA 92128

E. T. Still
Kerr-McGee Corporation
P.O. Box 25861
Oklahoma City, OK 73125

J. Stroman
Library
Department of Energy/NIPER
P.O. Box 2128
Bartlesville, OK 74005

M. Tanaka
Physics Library
510A
Brookhaven National Laboratory
Upton, NY 11973

Technical Information Service
Savannah River Laboratory
Room 773A
E. E. duPont de Nemours & Company
Aiken, SC 29801

R. G. Thomas
Argonne National Laboratory
Environment Research
Building 203
9700 S. Cass Avenue
Argonne IL 60439

L. H. Toburen (15)
National Academy of Sciences
2101 Constitution Avenue, NW
Washington, DC 20418

P. W. Todd
Department of Chemistry
University of Colorado
Boulder, CO 80303

E. J. Vallario
15228 Red Clover Drive
Rockville, MD 20853

M. N. Varma
ER-74
Department of Energy
Washington, DC 20545

G. J. Vodapivc
DOE - Schenectady Naval Reactors Office
P.O. Box 1069
Schenectady, NY 12301

G. L. Voelz
Los Alamos National Laboratory
MS-K404
P.O. Box 1663
Los Alamos, NM 87545

B. W. Wachholz
Radiation Effects Branch
National Cancer Institute
EPN, Room 530
8000 Rockville Pike
Bethesda, MD 20892

R. A. Walters
Assistant to the Associate Director
Los Alamos National Laboratory
MS-A114
P.O. Box 1663
Los Alamos, NM 87545

W. W. Weyzen
Electric Power Research Institute
3412 Hillview Avenue
P.O. Box 10412
Palo Alto, CA 94303

F. J. Wobber
Department of Energy
14 Goshen Court
Gaithersburg, MD 20879-4403

R. W. Wood
PTRD, OHER
ER-74, GTN
Department of Energy
Washington, DC 20545

D. Woodall, Manager
Physics Group
EG&G Idaho, INEL
P.O. Box 1625
Idaho Falls, ID 83415

Zhu Zhixian
Laboratory for Energy-Related Health Research
University of California
Davis, CA 95616

FOREIGN

G. E. Adams, Director
Medical Research Council
Radiobiology Unit
Harwell, Didcot
Oxon OX11 ORD
ENGLAND

D. C. Aumann
Institut für Physikalische Chemie
Universität Bonn
Abt. Nuklearchemie
Wegelerstraë 12
5300 Bonn 1
GERMANY

M. R. Balakrishnan, Head
Library & Information Services
Bhabda Atomic Research Centre
Bombay - 400 085
INDIA

G. W. Barendsen
Laboratory for Radiobiology
AMC, FO 212
Meibergdreef 9
1105 AZ Amsterdam
THE NETHERLANDS

A. M. Beau, Librarian
Département de Protection Sanitaire
Commissariat á l'Énergie Atomique
BP No. 6
F-92265 Fontenay-aux-Roses
FRANCE

G. Bengtsson, Director-General
Statens Stralskyddsinstitut
Box 60204
S-104 01 Stockholm
SWEDEN

D. J. Beninson
Gerencía de Protección Radiológica y Seguridad
Comisión Nacional de Energía Atómica
Avenida del Libertador 8250
2° Piso Of. 2330
1429 Buenos Aires
ARGENTINA

J. Booz
KFA Jülich Institut für Medezin
Kernsforschungsanlage Jülich
Postfach 1913
D-5170 Jülich
GERMANY

M. J. Bulman, Librarian
Medical Research Council
Radiobiology Unit
Harwell, Didcot
Oxon OX11 ORD
ENGLAND

Cao Shu-Yuan, Deputy Head
Laboratory of Radiation Medicine
North China Institute of Radiation Protection
P.O. Box 120
Tai-yuan, Shan-Xi
THE PEOPLE'S REPUBLIC OF CHINA

M. Carpentier
Commission of the European Communities
200 rue de la Loi
J-70 6/16
B-1049 Brussels
BELGIUM

Chen Xing-An
Laboratory of Industrial Hygiene
Ministry of Public Health
2 Xinkang Street
Deshengmenwai, Beijing
THE PEOPLE'S REPUBLIC OF CHINA

R. Clarke
National Radiological Protection Board
Harwell, Didcot
Oxon OX11 ORQ
ENGLAND

Commission of the European Communities
DG XII - Library SDM8 R1
200 rue de la Loi
B-1049 Brussels
BELGIUM

Deng Zhicheng
North China Institute of Radiation Protection
Tai-yuan, Shan-Xi
THE PEOPLE'S REPUBLIC OF CHINA

Director
Commissariat á l'Énergie Atomique
Centre d'Etudes Nucléaires
Fontenay-aux-Roses (Seine)
FRANCE

Director
Commonwealth Scientific and Industrial Research Organization
Aspendal, Victoria
AUSTRALIA

Director
Laboratorio di Radiobiologia Animale
Centro di Studi Nucleari Della Casaccia
Comitate Nazionale per l'Energia Nucleare
Casella Postale 2400
I-00100 Roma
ITALY

D. Djuric
Institute of Occupational and Radiological Health
11000 Beograd
Deligradoka 29
YUGOSLAVIA

L. Feinendegen, Director
Institut für Medezin
Kernsforschungsanlage Jülich
Postfach 1913
D-5170 Jülich
GERMANY

A. Geertsema
Sasol Technology (Pty), Ltd.
P.O. Box 1
Sasolburg 9570
REPUBLIC OF SOUTH AFRICA

J. A. B. Gibson
Radiation Dosimetry Department
AEA Environment & Energy
Harwell Laboratory
Didcot
Oxon OX11 ORA
ENGLAND

D. Goodhead
Medical Research Council
Radiobiology Unit
Harwell, Didcot
Oxon OX11 ORD
ENGLAND

A. R. Gopal-Ayengar
73-Mysore Colony
Mahul Road, Chembur
Bombay-400 074
INDIA

G. F. Gualdrini
ENEA
8 Viale Ercolani
I-40138 Bologna
ITALY

J. L. Head
Department of Nuclear Science & Technology
Royal Naval College Greenwich
London SE 109NN
ENGLAND

T. Jaakkola
University of Helsinki
Department of Radiochemistry
Unioninkatu 35, 00170
Helsinki 17
FINLAND

Jiang Shengjie, Standing Vice President
Chinese Nuclear Society
P.O. Box 2125
Beijing
THE PEOPLE'S REPUBLIC OF CHINA

K. E. Lennart Johansson
National Defense Research Institute
FOA 45 1
S-901-82 Umeå
SWEDEN

A. M. Kellerer
Institut für Strahlenkunde
GSF
Ingelstädter Landstr. 1
D-8042 Neuherberg b.
München
GERMANY

H.-J. Klimisch
BASF Aktiengesellschaft
Abteilung Toxikologie, Z470
D-6700 Ludwigshafen
GERMANY

A. Kövér
Nuclear Research Institute of Hungary
Hungarian Academy of Science
P.O. Box 51
H-4001 Debrecen
HUNGARY

G. H. Kraft
c/o GSI Postbox 110541
Planck Str.
D-6100 Darmstadt
GERMANY

T. Kumatori
National Institute of Radiological Sciences
9-1, Anagawa-4-chome
Chiba-shi 260
JAPAN

H. P. Leenmouts
National Institute of Public Health & Environmental Hygiene
P.O. Box 1
NL-3720 BA Bilthoven
THE NETHERLANDS

Li De-Ping
Professor and Director of North China Institute of Radiation Protection, NMI
Tai-yuan, Shan-Xi
THE PEOPLE'S REPUBLIC OF CHINA

Librarian
Centre d'Etudes
Nucléaires de Saclay
P.O. Box 2, Saclay
Fig-sur-Yvette (S&O)
FRANCE

Librarian
CSIRO
314 Albert Street
P.O. Box 89
East Melbourne, Victoria
AUSTRALIA

Librarian
HCS/EHE
World Health Organization
CH-1211 Geneva 27
SWITZERLAND

Librarian
Kernforschungzentrum
Karlsruhe
Institut für Strahlenbiologie
Postfach 3640
D-75 Karlsruhe 1
GERMANY

Librarian
Max-Planck-Institut für
Biophysics
Forstkasstrasse
D-6000 Frankfurt/Main
GERMANY

Librarian
Ministry of Agriculture,
Fisheries & Food
Fisheries Laboratory
Lowestoft, Suffolk NR33
OHT
ENGLAND

Librarian
National Institute of
Radiological Sciences
9-1, Anagawa-4-chome
Chiba-shi 260
JAPAN

Librarian
Supervising Scientist for the
Alligator Rivers Region
Level 23, Bondi Junction Plaza
P.O. Box 387
Bondi Junction NSW 2022
AUSTRALIA

Library
Atomic Energy Commission of
Canada, Ltd.
Whiteshell Nuclear Research
Establishment
Pinawa, Manitoba ROE 1L0
CANADA

Library
Department of Meteorology
University of Stockholm
Arrhenius Laboratory
S-10691 Stockholm
SWEDEN

Library
Risφ National Laboratory
DK-4000 Roskilde
DENMARK

Ma Fubang, Director
Chief Engineer
Institute of Atomic Energy
P.O. Box 275
Beijing
THE PEOPLE'S REPUBLIC
OF CHINA

A. M. Marko
9 Huron Street
Deep River, Ontario KOJ 1PO
CANADA

H. Matsudaira, Director-General
National Institute of
Radiological Sciences
9-1, Anagawa-4-chome
Chiba-shi 260
JAPAN

R.G.C. McElroy
Atomic Energy Commission of
Canada, Ltd.
Dosimetric Research Branch
Chalk River, Ontario K0J 1J0
CANADA

M. L. Mendelsohn
Radiation Effects
Research Foundation
1-8-6 Nakagawa
Nagasaki 850
JAPAN

Meng Zi-Qiang
Department of Environmental
Science
Shanxi University
Tai-yuan, Shan-Xi
PEOPLE'S REPUBLIC
OF CHINA

J. C. Nénot, Deputy Director
Département de Protection
Centre d' Etudes Nucléaires
BP No. 6
F-92260 Fontenay-aux-Roses
FRANCE

R. V. Osborne
Atomic Energy of Canada Ltd.
Chalk River Nuclear
Laboratories
Chalk River, Ontario KOJ1 JO
CANADA

H. G. Paretzke
GSF Institut für Strahlenschutz
Ingolstadter Landstrasse 1
D-8042 Neuherberg
GERMANY

O. Pavlovski
Institute of Biophysics
Ministry of Public Health
Givopisnaya 46
Moscow D-182
RUSSIA

V. Prodi
Department of Physics
University of Bologna
Via Irnerio 46
I-40126 Bologna
ITALY

Reports Librarian
Harwell Laboratory, Bldg. 465
UKAEA
Harwell, Didcot
Oxon OX11 ORB
ENGLAND

P. J. A. Rombout
Inhalation Toxicology
Department
National Institute of Public
Health and Environmental
Protection
P.O. Box 1
NL-3720 BA Bilthoven
THE NETHERLANDS

M. Rzeklecki
Commissariat à l'Énergie Atomique
Centre d'Etudes Nucleaires de Cadarache
BP No. 13-St. Paul Les Durance
FRANCE

J. Sinnaeve
Radiobiology Department
Commission of the European Communities
200 Rue de la Loi
B-1049 Brussels
BELGIUM

H. Smith
International Commission on Radiological Protection
P.O. Box 35
Didcot
Oxon OX11 ORJ
ENGLAND

J. W. Stather
National Radiological Protection Board
Building 383
Chilton, Didcot
Oxon OX11 ORQ
ENGLAND

Sun Shi-quan, Head
Radiation-Medicine Department
North China Institute of Radiation Protection, MNI
P.O. Box 120
Tai-yuan, Shan-Xi
THE PEOPLE'S REPUBLIC OF CHINA

J. W. Thiessen
Radiation Effects Research Foundation
1-8-6 Nakagawa
Nagasaki 850
JAPAN

D. Van As
Atomic Energy Board
Private Bag X 256
Pretoria 0001
REPUBLIC OF SOUTH AFRICA

Vienna International Centre Library
Gifts and Exchange
P.O. Box 100
A-1400 Vienna
AUSTRIA

M. Waligorski
Institute of Nuclear Physics
Radzikowskiego 152
31-342 Urakow
POLAND

Wang Hengde
North China Institute of Radiation Protection
P.O. Box 120
Tai-yuan, Shan-Xi
THE PEOPLE'S REPUBLIC OF CHINA

Wang Renzhi
Institute of Radiation Medicine
11# Tai Ping Road
Beijing
THE PEOPLE'S REPUBLIC OF CHINA

Wang Ruifa, Associate Director
Laboratory of Industrial Hygiene
Ministry of Public Health
2 Xinkang Street
P.O. Box 8018
Deshengmenwai, Beijing 100088
THE PEOPLE'S REPUBLIC OF CHINA

Wei Lü-Xin
Laboratory of Industrial Hygiene
Ministry of Public Health
2 Xinkang Street
Deshengmenwai, Beijing 100088
THE PEOPLE'S REPUBLIC OF CHINA

B. C. Winkler, Director Licensing
Raad Op Atomic
Atoomkrag Energy Board
Privaatsk X 256
Pretoria 0001
REPUBLIC OF SOUTH AFRICA

Wu De-Chang
Institute of Radiation Medicine
27# Tai Ping Road
Beijing
THE PEOPLE'S REPUBLIC OF CHINA

ONSITE

DOE Richland Operations Office (3)

P. W. Kruger, A5-90
E. C. Norman, A5-16
R. D. Freeberg, A5-19

Tri-Cities University Center

H. Gover, Librarian, H2-52

Hanford Environmental Health Foundation (2)

L. J. Maas, B6-61
M. J. Swint, H1-02

Westinghouse Hanford Co.

D. E. Simpson, B3-55

Pacific Northwest Laboratory (96)

W. J. Apley, P7-46
S. T. Autrey, K2-38
R. W. Baalman, K1-50 (10)
W. J. Bair, K1-50
C. A. Baldwin, P7-58 (10)
N. E. Ballou, P7-07
R. M. Bean, P8-08
L. A. Braby, P8-47
T. D. Chikalla, P7-75
T. T. Claudson, K1-66
S. D. Colson, K2-14
W. C. Cosby, P8-08
D. W. Dragnich, BWO
R. D. DuBois, P8-47
C. G. Edmonds, P8-19
C. E. Elderkin, K6-11
J. W. Falco, K1-40
D. R. Fisher, K3-53
M. E. Geusic, K2-57
W. A. Glass, K3-53
R. H. Gray, K1-33
R. Harty, K3-55
L. A. Holmes, K1-29
J. R. Houston, A3-60
A. C. James, K3-51
J. R. Johnson, K3-53
R. A. Kennedy, P7-82
M. L. Knotek, K1-48
W. W. Laity, K2-50
E. A. Lepel, P8-08
J. A. Mahaffey, P7-82
N. F. Metting, P8-47
J. H. Miller, P8-47
R. J. Miller, K3-58
J. T. Munley, K3-58
J. M. Nelson, P8-47
J. F. Park, P7-52
R. W. Perkins, P7-35
G. F. Schiefelbein, P8-38
L. C. Schmid, K1-34
B. D. Shipp, K1-73
R. D. Smith, P8-19
D. L. Springer, P7-56
J. A. Stottlemyre, K6-75
T. S. Tenforde, K1-50 (15)
B. L. Thomas, P7-72
H. R. Udseth, P8-19
B. E. Vaughan, K1-66
R. E. Wildung, P7-54
W. R. Wiley, K1-46
J. R. Williams, K7-22
L. D. Williams, K1-41
W. E. Wilson, P8-47
N. A. Wogman, P7-35
J. D. Zimbrick, P7-58
Health Physics Department Library
Life Sciences Library (2)
Publishing Coordination
Technical Report Files (5)

END

DATE
FILMED
7/22/93